

ornl

AUG 28 1980
DATE ISSUED _____

ORNL/TM-7348

ORNL
MASTER COPY

OAK
RIDGE
NATIONAL
LABORATORY



ORNL Breeder Reactor Safety Quarterly Technical Progress Report for January—March 1980

M. H. Fontana

J. L. Wantland

OPERATED BY
UNION CARBIDE CORPORATION
FOR THE UNITED STATES
DEPARTMENT OF ENERGY

No longer AT.
David R Hammi
4/17/2008

~~TECHNOLOGY~~
~~data~~
~~rn-~~
~~ns~~
~~of~~

Printed in the United States of America. Available from
the Department of Energy
Technical Information Center
P.O. Box 62, Oak Ridge, Tennessee 37830
Printed Copy A07 ; Microfiche A01

This report was prepared as an account of work sponsored by an agency of the United States Government. Neither the United States Government nor any agency thereof, nor any of their employees, makes any warranty, express or implied, or assumes any legal liability or responsibility for the accuracy, completeness, or usefulness of any information, apparatus, product, or process disclosed, or represents that its use would not infringe privately owned rights. Reference herein to any specific commercial product, process, or service by trade name, trademark, manufacturer, or otherwise, does not necessarily constitute or imply its endorsement, recommendation, or favoring by the United States Government or any agency thereof. The views and opinions of authors expressed herein do not necessarily state or reflect those of the United States Government or any agency thereof.

ORNL/TM-7348
Dist. Category UC-79,
-79e, -79p

Contract No. W-7405-eng-26

800417

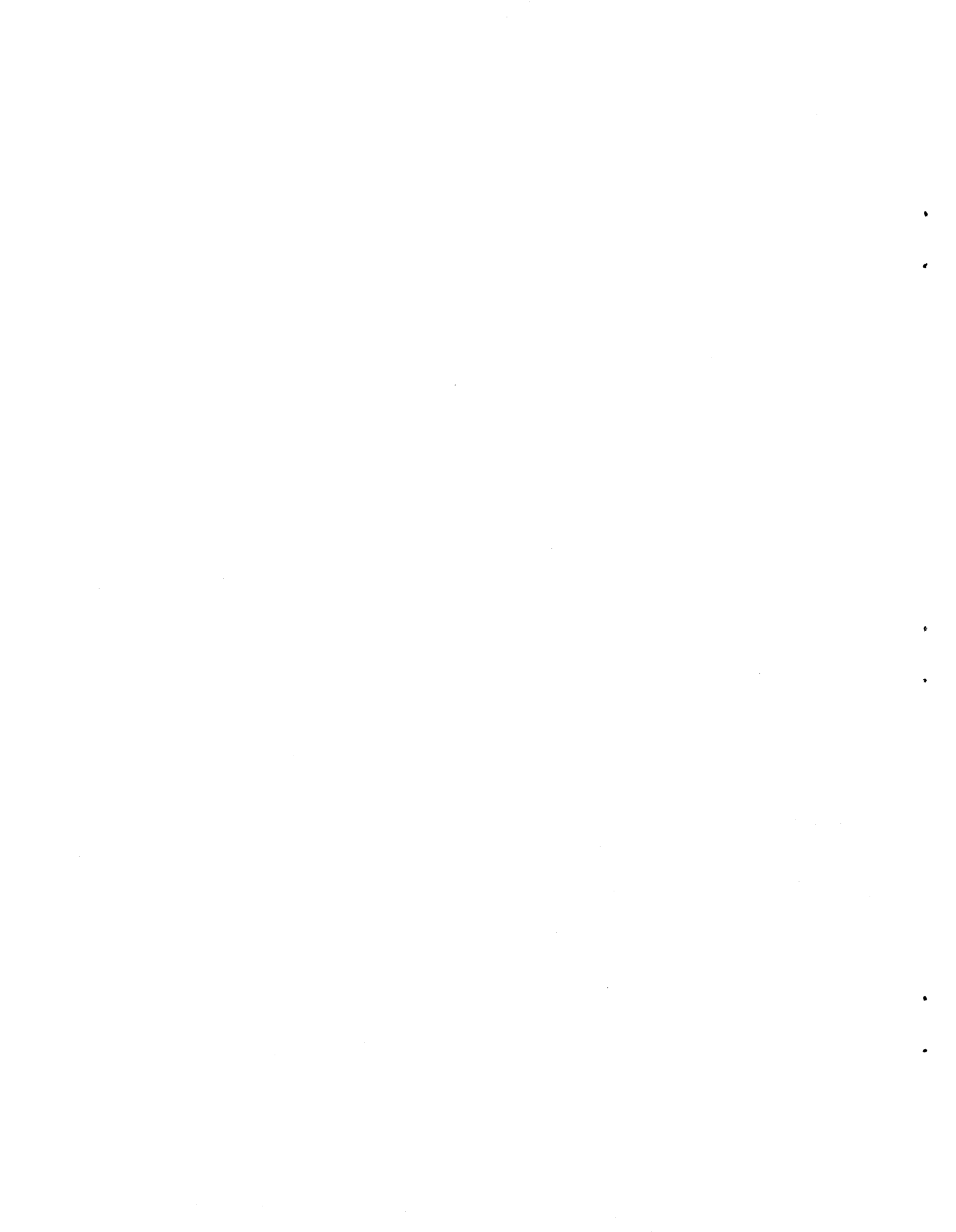
ORNL BREEDER REACTOR SAFETY QUARTERLY TECHNICAL
PROGRESS REPORT FOR JANUARY-MARCH 1980

M. H. Fontana J. L. Wantland

Date Published: August 1980

NOTICE This document contains information of a preliminary nature.
It is subject to revision or correction and therefore does not represent a
final report.

Prepared by the
OAK RIDGE NATIONAL LABORATORY
Oak Ridge, Tennessee 37830
operated by
UNION CARBIDE CORPORATION
for the
DEPARTMENT OF ENERGY



CONTENTS

	<u>Page</u>
PREVIOUS BREEDER REACTOR SAFETY PROGRESS REPORTS	v
SUMMARY	vii
GLOSSARY OF ACRONYMS	xi

PART 1

ABSTRACT	1-3
1. TASK 01 — ORNL LOA 2 TASKS: THORS PROGRAM	1-4
1.1 THORS Planning and Analysis	1-4
1.1.1 THORS Bundle 9 Phase 2 Two-Phase Transient Test Plan	1-4
1.1.2 Detection of dryout in Bundle 9 Phase 2 tests	1-33
1.1.3 SAS3D prediction of Bundle 9 intrasubassembly boiling incoherence	1-39
1.1.4 Pretest analysis for Bundle 9 Phase 2 Part A testing	1-45
1.1.5 Bundle 9 Phase 1 record of experimental data	1-56
1.1.6 Bundle 9 bypass flow split analysis	1-58
1.2 THORS Fabrication and Operation	1-72
1.2.1 Test facility operation	1-72
1.2.2 Test bundle	1-72
1.3 Reports and Major Correspondence Issued	1-76
1.4 Important Meetings	1-76
References	1-77

PART 2

ABSTRACT	2-1
2. TASK 02 — ORNL LOA 3 TASKS: ANALYTICAL MODELS FOR ENERGETICS ACCOMMODATION	2-3

PART 3

ABSTRACT	3-3
3. TASK 03 — ORNL LOA 4 TASKS: ENVIRONMENTAL ASSESSMENT OF ALTERNATE FBR FUELS	3-3

	<u>Page</u>
PART 4	
ABSTRACT	4-3
4. TASK 04 — ORNL LOA 4 TASKS: MODEL EVALUATION OF BREEDER REACTOR RADIOACTIVITY RELEASES	4-3
4.1 Comprehensive Testing of Selected Models	4-3
4.1.1 Particle-in-cell model	4-3
4.1.2 Hanford-67 data comparisons	4-4
4.1.3 Report ORNL-5573	4-5
4.2 Recommendations of Models and Parameters Best Suited to Breeder Reactor Assessments	4-5
4.3 Evaluation of Uncertainties Associated with Computational Models	4-5
4.3.1 Atmospheric dispersion parameters	4-5
4.3.2 Dose due to ¹³¹ I	4-6
4.4 Meetings	4-8
PART 5	
5. TASK 05 — ORNL LOA SUPPORT AND INTEGRATION: NUCLEAR SAFETY INFORMATION CENTER	5-3
5.1 Routine Services	5-4
5.2 ORNL-NSIC Reports	5-5
5.3 <i>Journal of Nuclear Safety</i>	5-6
PART 6	
ABSTRACT	6-3
6. TASK 06 — ORNL LOA SUPPORT AND INTEGRATION: BREEDER REACTOR RELIABILITY DATA ANALYSIS CENTER	6-3
6.1 Initial Data Collection and Evaluation	6-3
6.2 Development of the Data Base Management System	6-4
6.3 Interface and Coordination	6-4
6.4 Reports and Major Correspondence Issued	6-5
6.5 Important Meetings	6-5
PART 7	
ABSTRACT	7-3
7. TASK 07 — ORNL LOA SUPPORT AND INTEGRATION: CENTRAL DATA BASE FOR BREEDER REACTOR SAFETY CODES	7-3

PREVIOUS BREEDER REACTOR SAFETY PROGRESS REPORTS*

Prior information on these projects was presented in the following Breeder Reactor Safety and Core Systems Programs Progress Reports:†

<u>Period Covered</u>	<u>Report No.</u>
September–October 1972	ORNL/TM-4075
November–December 1972	ORNL/TM-4088
January–February 1973	ORNL/TM-4148
March–April 1973	ORNL/TM-4261
May–June 1973	ORNL/TM-4331
July–September 1973	ORNL/TM-4417
October–December 1973	ORNL/TM-4505
January–March 1974	ORNL/TM-4630
April–June 1974	ORNL/TM-4727
July–September 1974	ORNL/TM-4776
October–December 1974	ORNL/TM-4877
January–March 1975	ORNL/TM-4980
April–June 1975	ORNL/TM-5076
July–September 1975	ORNL/TM-5197
October–December 1975	ORNL/TM-5431
January–March 1976	ORNL/TM-5513
April–June 1976	ORNL/TM-5699
July–September 1976	ORNL/TM-5753
October–December 1976	ORNL/TM-5785
January–March 1977	ORNL/TM-5940
April–June 1977	ORNL/TM-6020
July–September 1977	ORNL/TM-6158
October–December 1977	ORNL/TM-6288
January–March 1978	ORNL/TM-6439
April–June 1978	ORNL/TM-6558
July–September 1978	ORNL/TM-6698
October–December 1978	ORNL/TM-6851
January–March 1979	ORNL/TM-6947
April–June 1979	ORNL/TM-7147
July–September 1979	ORNL/TM-7229
October–December 1979	ORNL/TM-7301

*Reported previously as LMFBR Safety and Core Systems Program Progress Reports.

†Information on the Breeder Reactor Project for 1968 through August 1972 is available in ORNL Nuclear Safety Research and Development Program Bimonthly Progress Reports.



SUMMARY

1. TASK 01 — ORNL LOA 2 TASKS: THORS PROGRAM

The THORS Bundle 9 Phase 2 Two-Phase Transient Test Plan has undergone internal and external review and has been approved for operation. It is documented in this report.

The loss of heater-internal thermocouples during Bundle 9 fabrication, assembly, and Phase 1 testing necessitated development of a method of determining dryout or near-dryout conditions in order to prevent bundle failure during Phase 2 (boiling) tests. This method is based on data from Bundle 6A boiling tests and relies on the response of wire-wrap thermocouples in the simulated fission-gas plenum to indicate when dryout is imminent.

Scoping calculations using SAS3D have indicated that the temperature-flow behavior of the central coolant channel in Bundle 9 is essentially independent of the influence of the duct wall inertial response, while coolant channel temperature-flow behavior in the outer regions of the subassembly are not independent of this effect. Thus, incorporation of a two-channel SAS model to represent intrasubassembly incoherence in two separate radial regions of Bundle 9 should be valid.

Significant modifications to the SABRE-2 transient subchannel analysis code have been made, and results from this modified version have been compared with data from the Bundle 9 Phase 1 Test Program. Pretest analyses of two natural-convection-to-boiling tests in the Bundle 9 Phase 2 Test Plan are included.

The Bundle 9 Phase 1 Record of Experimental Data report has been completed and has undergone coauthor and peer review.

Installation of the EM pump and expansion tank in the THORS facility has been completed. A preliminary shakedown, including the EM pump acceptance tests, has begun. Bundle 9 Phase 2 testing will be initiated following checkout.

2. TASK 02 — ORNL LOA 3 TASKS: ANALYTICAL
MODELS FOR ENERGETICS ACCOMMODATION

An adjoint code for the single-phase portion of MELT has been completed and validated. A supplementary code, SCG, is available to calculate sensitivity coefficients. Journal articles describing the work are soon to be published.

3. TASK 03 — ORNL LOA 4 TASKS: ENVIRONMENTAL
ASSESSMENT OF ALTERNATE FBR FUELS

Oxidation experiments with advanced alternate FBR fuels have determined that finely powdered (Th,U)C in quantities as small as 2 g will ignite spontaneously at room temperature on exposure to either air or a 21% O₂-Ar mixture. Uranium monocarbide samples, included for comparison, show a similar behavior. By contrast, ThC powder must be heated to ~250°C in either of these atmospheres before ignition occurs. Alpha-spectrometry measurements of the collector slides in a cascade impactor show that the entrainment of particles in the gaseous effluent during the oxidation of these fuels is insignificant under the conditions of these experiments. Graphic analysis of the time dependence of the amount of fuel sample oxidized indicates that the rate-controlling process is the nucleating and growth of the products of oxidation upon the original fuel particles. Components for a mass spectrometer were received in two shipments during the latter part of this quarter. After the manufacturer's representative has demonstrated that the instrument meets purchase specification requirements, it will be used to measure the composition of the gaseous effluent resulting from oxidation of FBR fuels. Several papers or reports were written and presented or published concerning the environmental impact attendant upon release of tritium. A progress report was received from Colorado State University describing their FY 1979 subcontract work on modeling the release of radioactivity from a thorium ore pile. A review of ORNL's work on LOA-4 topics was presented on January 16, 1980, to the Fast Breeder Reactor Safety Technology Management Center Staff meeting at ORNL. Several papers and reports were prepared describing primarily the environmental impact of tritium release. A paper entitled

"Environmental Impact of Radioactive Releases from Recycle of Thorium-Based Fuel Using Current Containment Technology" was presented March 17 at the second USDOE Environmental Symposium.

4. TASK 04 — ORNL LOA 4 TASKS: MODEL EVALUATION
OF BREEDER REACTOR RADIOACTIVITY RELEASES

A computer code is being developed to implement the particle-in-cell atmospheric dispersion model at ORNL. Work is continuing on a comparison between Hanford-67 atmospheric dispersion data for releases of fluorescein particles from a height of 56 m and values of the normalized, ground-level, centerline air concentration calculated by the computer code DWNWND. The computer program TEDPED has been used to perform a statistical analysis of values of the Gaussian plume dispersion parameters σ_y and σ_z based on short-term (≤ 30 min) air concentration measurements taken at Karlsruhe, Federal Republic of Germany. An evaluation of the variability of three biological factors in determining the dose per unit intake of ingested ^{131}I has been performed for several age categories using Monte Carlo techniques.

5. TASK 05 — ORNL LOA SUPPORT AND INTEGRATION:
NUCLEAR SAFETY INFORMATION CENTER

The NSIC serves the nuclear community through collection, analysis, and dissemination of relevant safety information. During the report period January–March 1980, NSIC processed 2821 documents, responded to 198 inquiries, serviced 396 SDI subscribers, and provided a variety of other services, as well as pursuing in-house work on several reports and on the technical progress review, *Nuclear Safety*. Two reports were issued during the quarter, and work is continuing or was initiated on several other reports. Work was also undertaken on material for several issues of *Nuclear Safety* as required by its publication schedule.

6. TASK 06 — ORNL LOA SUPPORT AND INTEGRATION: BREEDER
REACTOR RELIABILITY DATA ANALYSIS CENTER

Data collection efforts at EBR-II for this quarter include completing the "pedigreeing" of seven of its systems. In addition, EBR-II's cycling history through its fifth year of operation has been completed. The proposal to collect engineering and event data through HEDL's FFTF Plant Utilization Program has been approved, and initial data tape transfers have been made. The structure of the engineering, event, and operating files has been changed into the ADSEP form to make storage and searching more efficient. The failure rate program was modified to accept the new file structure.

7. TASK 07 — ORNL LOA SUPPORT AND INTEGRATION: CENTRAL
DATA BASE FOR BREEDER REACTOR SAFETY CODES

Update information from NSMH has been entered into the data base continuously. A new ANL evaluation of sodium properties data was received, and programs were written to allow entry of this data into SACRD. Several minor problems were encountered that will delay this work until contacts can be made with ANL personnel. The SACRD mailing list has been reviewed and updated. Software has been completed to allow remote display of plots. Several examples of uncertainty data have been prepared for entry into the data base.

GLOSSARY OF ACRONYMS

ACA	Active component assembly
ACRS	Advisory Committee on Reactor Safeguards
AI	Atomics International, Division of Rockwell Corporation
ANL	Argonne National Laboratory
ANS	American Nuclear Society
BN	Boron nitride
BNBF	Boron nitride backfilled
BNL	Brookhaven National Laboratory
BONA	Boiling Natrium
CCDAS	Computer-Controlled Data Acquisition System
CRCTA	Composite Reactor Components Test Activity (HEDL)
CREDO	Centralized Reliability Data Organization
CRBR	Clinch River Breeder Reactor
CRT	Cathode-ray tube
CSU	Colorado State University
DAS	Data Acquisition System
DBMS	Data Base Management System
DISSPLA	Display Integrated Software System and Plotting Language
DOE	Department of Energy
EBR-II	Experimental Breeder Reactor-II
EM	Electromagnetic
EOS	Equation of state
ETEC	Energy Technical Engineering Center (formerly LMEC)
FBR	Fast Breeder Reactor
FFTF	Fast-Flux Test Facility
FOP	First-order perturbation
FPS	Fuel pin simulator
FRSTMC	Fast Reactor Safety Technology Management Center
FTS	Federal Telecommunciation System
GA	General Atomic Company
GE	General Electric Corporation
GMI	Groth-Mazur Industries
HEDL	Hanford Engineering Development Laboratory

HPS	Health Physics Society
HTGR	High-Temperature Gas-Cooled Reactor
I&C	Instrumentation and Controls
ICE	Implicit Continuous Eulerian
INEL	Idaho National Engineering Laboratory
LASL	Los Alamos Scientific Laboratory
LMEC	Liquid-Metal Engineering Center (now ETEC)
LMFBR	Liquid-Metal Fast Breeder Reactor
LOA	Lines of Assurance
LOPI	Loss of Pipe Integrity
LWR	Light Water Reactor
MIT	Massachusetts Institute of Technology
MSAR	Mine Safety Appliance Research
NCSR	National Center of Systems Reliability (UK)
NOAA	National Oceanic and Atmospheric Administration
NPRDS	Nuclear Power Reliability Data Service
NRC	Nuclear Regulatory Commission
NSIC	Nuclear Safety Information Center
NSMH	<i>Nuclear Systems Materials Handbook</i>
OCI	Oxygen control and indicating system
ORCHIS	Oak Ridge Computerized Hierarchical Information System
ORNL	Oak Ridge National Laboratory
1-D	One-dimensional
PAL	Prototype Applications Loop (HEDL)
PG	Pasquill-Gifford
PIC	Particle-in-cell
PLSA	Properties for LMFBR Safety Analysis
PMD	Pressure measuring device
PNC	Power Reactor and Nuclear Fuel Development Corporation (Japan)
PO	Project office
QA	Quality assurance
RAS	Reactor Analysis and Safety (Division of ANL)
RECON	Remote Console Bibliographic Retrieval System (DOE)
RDMS	Reactor Data Management System (GE)

RRT	Reactor Research and Technology (Division of DOE)
RSR	Reactor Safety Research (Division of NRC)
RTD	Resistance temperature device
SACRD	Safety Analysis Computerized Reactor Data
SADCG	Safety Analysis Data Coordinating Group
SBT	Sodium Boiling Test
SCG	Sensitivity coefficient generation
SCTI	Sodium Component Test Installation
SDD	System Design Description
SDI	Selective Dissemination of Information
SFGP	Simulated fission-gas plenum
SHRS	Shutdown Heat Removal System
SRE	Sodium Reactor Experiment
SRL	Savannah River Laboratory
TGA/DTA	Thermogravimetric analysis/differential thermal analysis
THORS	Thermal-Hydraulic Out-of-Reactor Safety
3-D	Three-dimensional
TIC	Technical Information Center
TMC	Technology Management Center
TOP	Transient overpower
TREAT	Transient Reactor Test Facility
TSO	Time-sharing option
TTL	Transient Test Loop (HEDL)
TUC	Transient undercooling
TUCOP	Transient undercooling and overpower
2-D	Two-dimensional
UKAEA	United Kingdom Atomic Energy Authority
UOR	Unusual Occurrence Report
USAEC	United States Atomic Energy Commission
UT	The University of Tennessee
WARD	Westinghouse Advanced Reactor Division
WPAS	Work Package Proposal and Authorization System
ZPR	Zero-Power Reactor

Computer Codes

ADSEP	None
AIRDOS II	Air dose
ANISN	Anisotropic SN
COBRA	Coolant Boiling in Rod Arrays
DWNWND	None
KENO	None (Monte Carlo Code)
MELT	None (neutronic thermal-hydraulic code)
NEXUS	None (atmospheric dispersion of aerosols)
ORRIBLE/B6	None
SABRE	Subchannel Analysis of Blockages in Reactor Elements
SAS	Safety Analysis System
SPQR	Stochastic Program for Quasistatic Research
TEDPED	None
THERMIT	None (thermal-hydraulic code developed at MIT)

ORNL/TM-7348
Part 1
Dist. Category UC-79,
-79e, -79p

ORNL BREEDER REACTOR SAFETY — LOA 2
QUARTERLY TECHNICAL PROGRESS REPORT
FOR JANUARY—MARCH 1980

M. H. Fontana J. L. Wantland

AG 10 20 41 2

Task 01 — ORNL LOA 2 Tasks: THORS Program
[DRS 02.01]

OBJECTIVE

To provide products which will help make possible demonstration that the probability of failing to limit core damage (failing to assure no loss of in-pile coolability) following the failure of LOA 1 is less than one chance in one hundred.

[REDACTED] the data
[REDACTED] tern-
mer [REDACTED] ons
[REDACTED] of
Reactor Research and Technology

This document is an internal report of the Breeder Reactor
Program and contains preliminary and tentative information which
is subject to revision or correction and therefore does not represent a
final report.

Prepared by the
OAK RIDGE NATIONAL LABORATORY
Oak Ridge, Tennessee 37830
operated by
UNION CARBIDE CORPORATION
for the
DEPARTMENT OF ENERGY



ORNL BREEDER REACTOR SAFETY — LOA 2 QUARTERLY TECHNICAL
PROGRESS REPORT FOR JANUARY—MARCH 1980

M. H. Fontana J. L. Wantland

ABSTRACT

The THORS Bundle 9 Phase 2 Two-Phase Transient Test Plan has undergone internal and external review and has been approved for operation. The complete document is included in this report.

A method for determining dryout or near-dryout conditions during Bundle 9 Phase 2 tests has been developed, based on data from wire-wrap thermocouples in the simulated fission-gas plenum region of Bundle 6A; this procedure was necessitated by the severe attrition of heater-internal thermocouples experienced in Bundle 9.

Scoping calculations were made to determine the effectiveness of a two-channel SAS3D model to describe intrasubassembly boiling incoherence for Bundle 9.

Results from a modified version of SABRE-2 are compared with transient data from the THORS Bundle 9 Phase 1 Test Plan; then this code is used for pretest analysis of two natural-convection-to-boiling tests in the Phase 2 Test Plan.

The Bundle 9 Phase 1 Record of Experimental Data report has been completed and has undergone coauthor and peer review.

The preliminary checkout for the THORS facility following modifications to install the EM pump and expansion tank has been initiated prior to the Phase 2 testing for Bundle 9.

Four documents were issued and four meetings were attended during this quarter.

1. TASK 01 — ORNL LOA 2 TASKS: THORS PROGRAM

M. H. Fontana J. L. Wantland

1.1 THORS Planning and Analysis

J. L. Wantland K. Haga*
N. E. Clapp G. A. Klein
J. F. Dearing A. E. Levin
P. W. Garrison R. H. Morris
W. R. Nelson

1.1.1 THORS Bundle 9 Phase 2 Two-Phase Transient Test Plan
(J. F. Dearing, N. E. Clapp, B. H. Montgomery,
R. H. Morris)

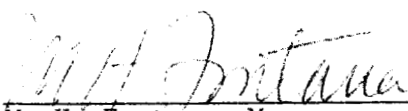
This section documents the THORS Bundle 9 Phase 2 Two-Phase Transient Test Plan, which has undergone internal and external review and has been approved for operation.

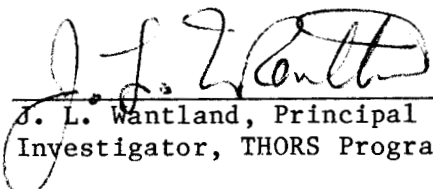
*Visiting engineer from PNC (Japan).

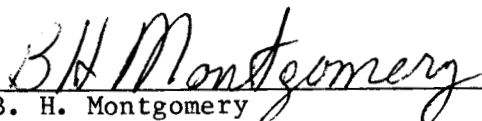
THORS BUNDLE 9 (TEST SERIES 11), PHASE 2
TWO-PHASE (TRANSIENT) TEST PLAN

Prepared by J. F. Dearing

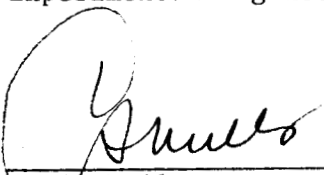
April 1, 1980

Approved:  4-2-80
M. H. Fontana, Manager
Breeder Reactor Safety Program
Date

Approved:  4-1-80
J. L. Wantland, Principal
Investigator, THORS Program
Date

Approved:  4-2-80
B. H. Montgomery
Project Engineer, THORS Facility
Date

Approved:  4/2/80
R. E. MacPherson, Head
Experimental Engineering Section
Date

Approved:  4/7/80
C. A. Mills
ETD Quality Assurance Coordinator
Date

INTRODUCTION

Sodium boiling tests have been carried out in four previous THORS bundles; in chronological order they were Bundles 5D, 3B, 6A and 3C. The most extensive testing was done with Bundle 6A,¹⁻³ a 19-pin bundle with half-size wire-wrap spacers between the 0.5-mm-thick (0.020-in.) duct wall and the edge pins. Bundle 6A was designed with half-size wire-wrap edge spacers and a thin duct wall in order to give a better thermal-hydraulic simulation of the interior of a 217-pin subassembly. The thermal insulation which backed the thin duct wall was soaked with sodium early in the test program, however, and the resulting radial heat transfer during the transient tests made the development of the boiling region decidedly not one-dimensional. This is probably the reason for the generally poor agreement (in terms of time between boiling initiation and dryout) between the one-dimensional SAS computer model and Bundle 6A experimental results.

Bundle 9 is a 61-pin bundle and as such has two more rows of fuel pin simulators (FPSs) than did the 19-pin Bundle 6A. Bundle 9 has full-size wire-wrap edge spacers and also a prototypic 3-mm-thick (0.120-in.) duct wall. Thus, rather than simulating the interior of a full subassembly, Bundle 9 simulates the correct edge geometry, but has fewer rings of subchannels in the bundle interior (Bundle 9 has four rings of interior subchannels while a 217-pin subassembly has eight). Approximately 35% of the flow area of Bundle 9 is made up by subchannels adjacent to the duct wall, while the corresponding number for a full subassembly is 20%. The steady-state power/flow area ratio for an edge subchannel (adjacent to the duct wall) is only 50% that of an interior subchannel, which means that the steady-state temperature in an edge subchannel is significantly less than in an interior subchannel. During a flow-reduction transient the temperature rise rate of the sodium in an edge subchannel is slowed by the heat capacity of the adjacent duct wall. Thus both steady-state and transient considerations indicate that the sodium in the edge subchannels of both a 217-pin subassembly and a 61-pin bundle would be significantly subcooled when boiling begins in the bundle interior — the difference being that boiling would occupy a greater number of interior subchannels in the 217-pin subassembly.

This comparison of the expected behavior of Bundle 9 with a 217-pin subassembly is compromised by the fact that, as in THORS Bundle 6A, the thermal insulation which backs the duct wall was also permeated with sodium before the beginning of the two-phase test program. This will not affect experimental results in Bundle 9 nearly as much as in Bundle 6A, however, because the thermal response of the sodium in a Bundle 9 edge subchannel is already slowed significantly by the heat capacity of the prototypic 3-mm-thick duct wall. Although the sodium-soaked insulation provides a thermal path to the much larger heat capacity of the bundle housing, this heat transfer will only become significant during long transients.

It is expected that boiling behavior in Bundle 9 will be much less affected by transverse (radial) heat transfer than in Bundle 6A, but it is not possible to predict beforehand how closely (or under what conditions) the boiling behavior will approach predictions of one-dimensional computer models. Two-phase tests in Bundle 6A were characterized by relatively long periods of stable boiling, during which the edge subchannels (cooled by heat transfer through the sodium-soaked insulation) slowly approached saturation conditions. One-dimensional models of these tests predicted much shorter time intervals between boiling inception and dryout than were seen experimentally. The fact that most of the interior subchannels in Bundle 9 will reach saturation conditions shortly after boiling inception (which has been predicted by single-phase, transient analysis with a modified version of COBRA III-C⁴) indicates a one-dimensional model may apply, whereas the fact that sodium in the edge subchannels will be highly subcooled at boiling inception indicates that a two-dimensional characterization may be necessary.

The attrition rate of heater-internal thermocouples before and during Phase 1 testing was, unfortunately, quite high (compare Figs. 1.5a and 1.5b).⁵ These thermocouples respond faster than wire-wrap thermocouples to dryout conditions on the cladding surface and are therefore important in protecting the bundle against FPS failure due to excessive temperatures. If dryout conditions were localized to a region with no heater internal thermocouples, bundle failure could occur before normal or automatic termination of the test.

This possible limit to the number of boiling transients, coupled with the presently unknown nature of boiling in Bundle 9, has resulted in a two-part strategy for test planning. Part A is designed to indicate the general character of sodium boiling in Bundle 9. Four tests will cover the range of pin heat flux covered in testing with Bundle 6A*, with initial and transient boundary conditions similar to specific runs in Bundle 6A. Part B will be written after a preliminary analysis of the results of Part A and will be issued as an addendum to this test plan. If boiling behavior in Bundle 9 does appear to be governed primarily by one-dimensional considerations, Part B will include tests to determine the effects of parameters to which one-dimensional models are highly sensitive, including bypass/test section flow split, superheat preconditioning, inlet valve pressure drop, and inlet subcooling. If boiling behavior does not appear to be one-dimensional, Part B will include tests with slower flow reduction ramp rates and/or higher initial outlet temperatures, in order to determine whether the two-dimensional behavior is due to transient conditions or the inherent power/flow area distribution in a 61-pin bundle. If the latter is the case (i.e., stable steady-state boiling is possible), the conditions of pin heat flux and forced inlet flow under which that is possible will be carefully mapped. Tests in Part A are ordered with the lower pin heat flux tests first, because these have a longer period of time between dryout and bundle failure during which manual or automatic shutdown can be effected. Tests in Part B will be ordered (based on the results of Part A) to maximize the information obtained.

Although there are presently no usable two- or three-dimensional code models of transient sodium boiling available, considerable use has been made of the COBRA III-C⁴ and SABRE-2⁶ transient, single-phase thermal-hydraulic subchannel analysis codes in the planning of this test program. These codes have been useful in determining (1) what combinations of initial and transient boundary conditions result in saturation conditions and (2) the shape of the axial and radial temperature profiles at boiling inception. Detailed one-dimensional heat conduction models of THORS boron nitride fuel pin simulators and the structure surrounding the pin bundle

*The complete Bundle 6A test plan is given in Ref. 1.

have been added to COBRA III-C. Cases simulating runs of Test 2 power-off transients in the Phase 1 testing* are in excellent agreement with experimental data. COBRA III-C utilizes a marching-type solution algorithm, however, and requires a (positive) inlet flow transient boundary condition, so it cannot be used on cases in which natural convection effects determine the flow. SABRE-2 (which presently has only a simple two-parameter subchannel structural thermal response model) can be used with either inlet flow or pressure drop transient boundary conditions. This code has been useful in planning Tests 202 and 203, in which the EM pump is turned off and a cold-leg static-head pressure-drop boundary condition determines the test section thermal-hydraulic response.

DESCRIPTION OF THORS FACILITY

The THORS Facility is an engineering-scale sodium loop for thermal-hydraulic testing of simulated LMFBR subassemblies. An isometric drawing of the facility is shown in Fig. 1.1. A flow diagram schematic of the THORS Facility is shown in Fig. 1.2. An electromagnetic pump has been added for the Phase 2 test program. This new pump should be capable of delivering $40 \text{ liters} \cdot \text{s}^{-1}$ (600 gpm) at a pressure of 1.38 MPa (200 psig). A transformer bank (not shown) can supply up to 2.0 MW electrical power to the test bundles (because of limitations in the current-carrying capability of the individual circuits, only 1.2 MW can be used by Bundle 9). Heat is removed by an air-cooled heat exchanger rated at 2 MW and shown at the right in the isometric drawing. The "old" test-section housing (used through Bundle 5) is shown on the left side. A portion of the circulating sodium is bypassed through an oxygen control and indicating (OCI) system which maintains system oxygen content at less than 10 ppm. For the transient boiling tests, a test section bypass line and expansion tank were installed to simulate (hydraulically) the other core assemblies. Valves in the piping system allow adjustment of flow resistances to simulate reactor conditions. Programmable pump control and heater-power control systems are available so that preprogrammed flow transients and bundle-power transients can be effected.

*The Bundle 9 Phase 1 test plan is given in Ref. 5.

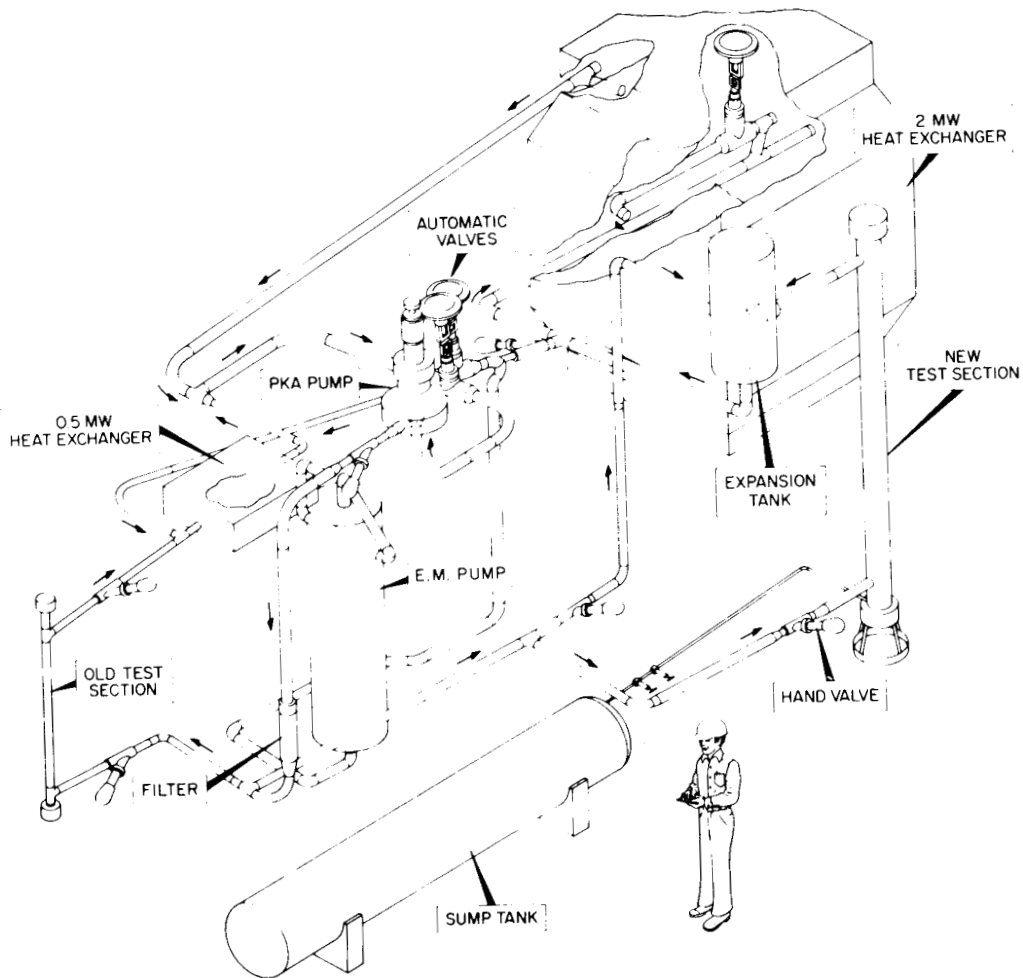


Fig. 1.1. Isometric drawing of THORS Facility for Phase 2 testing.

DESCRIPTION OF BUNDLE 9

Bundle 9 is a 61-pin bundle of CRBR dimensions: 5.84-mm-diam (0.230-in.) pins spaced by wire wraps of 1.42 mm diam (0.056-in.) on a 305-mm (12-in.) helical pitch. The bundle container is a hexagonal duct of 3.05-mm-thick (0.120-in.) stainless steel backed by (now sodium-soaked) thermal insulation. The duct thickness is typical of FFTF and CRBR fuel assemblies. The heated length is 914 mm (36.0 in.) with a 1.38 peak-to-mean chopped-cosine axial heat flux. The fuel pin simulators are rated at 40 kW/pin but are limited to 20 kW/pin by the allowable current-carrying capability of the electrical circuitry. Figure 1.3 is a cross-section

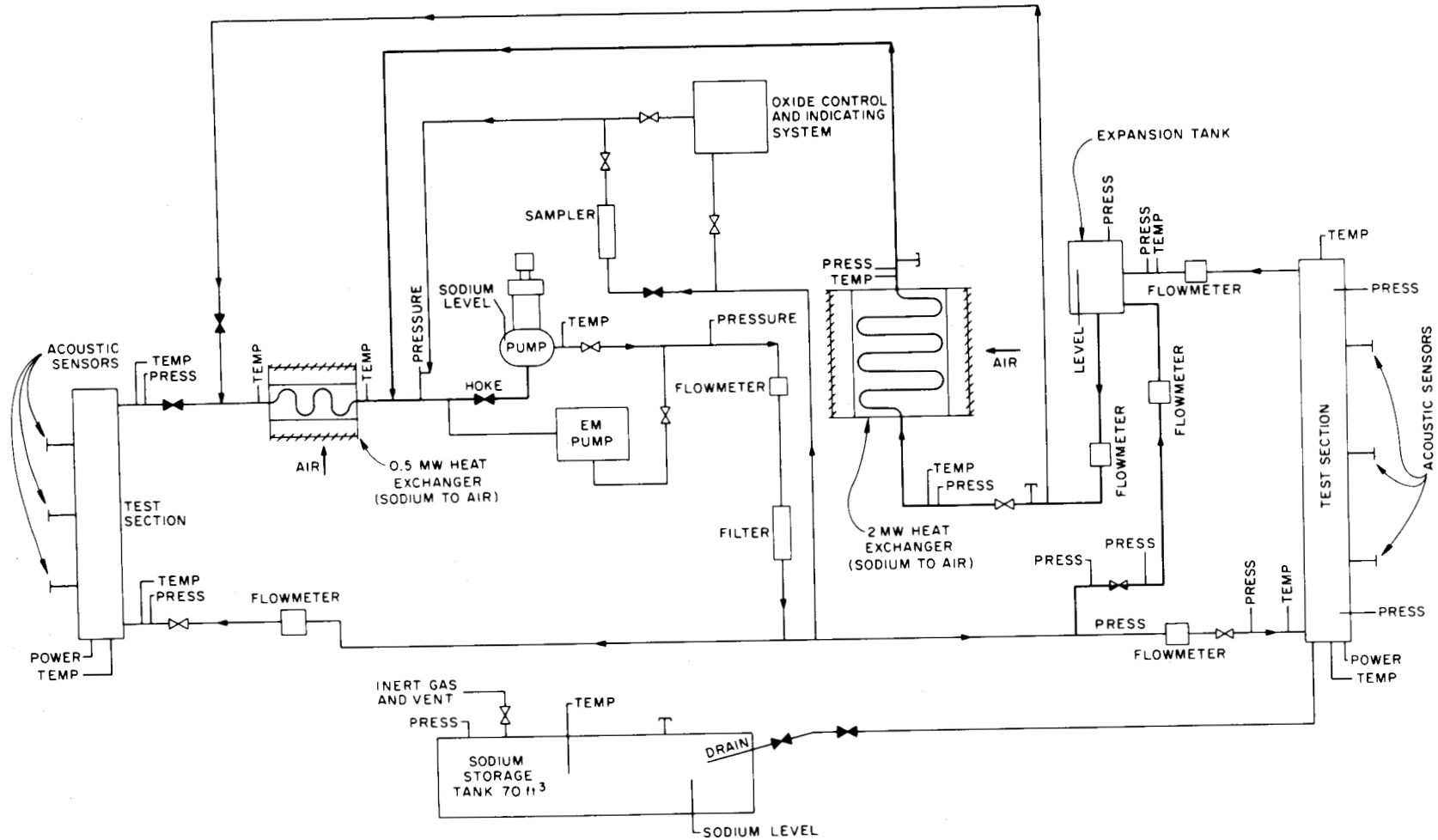


Fig. 1.2. Schematic of THORS Facility for Bundle 9 Phase 2 testing.

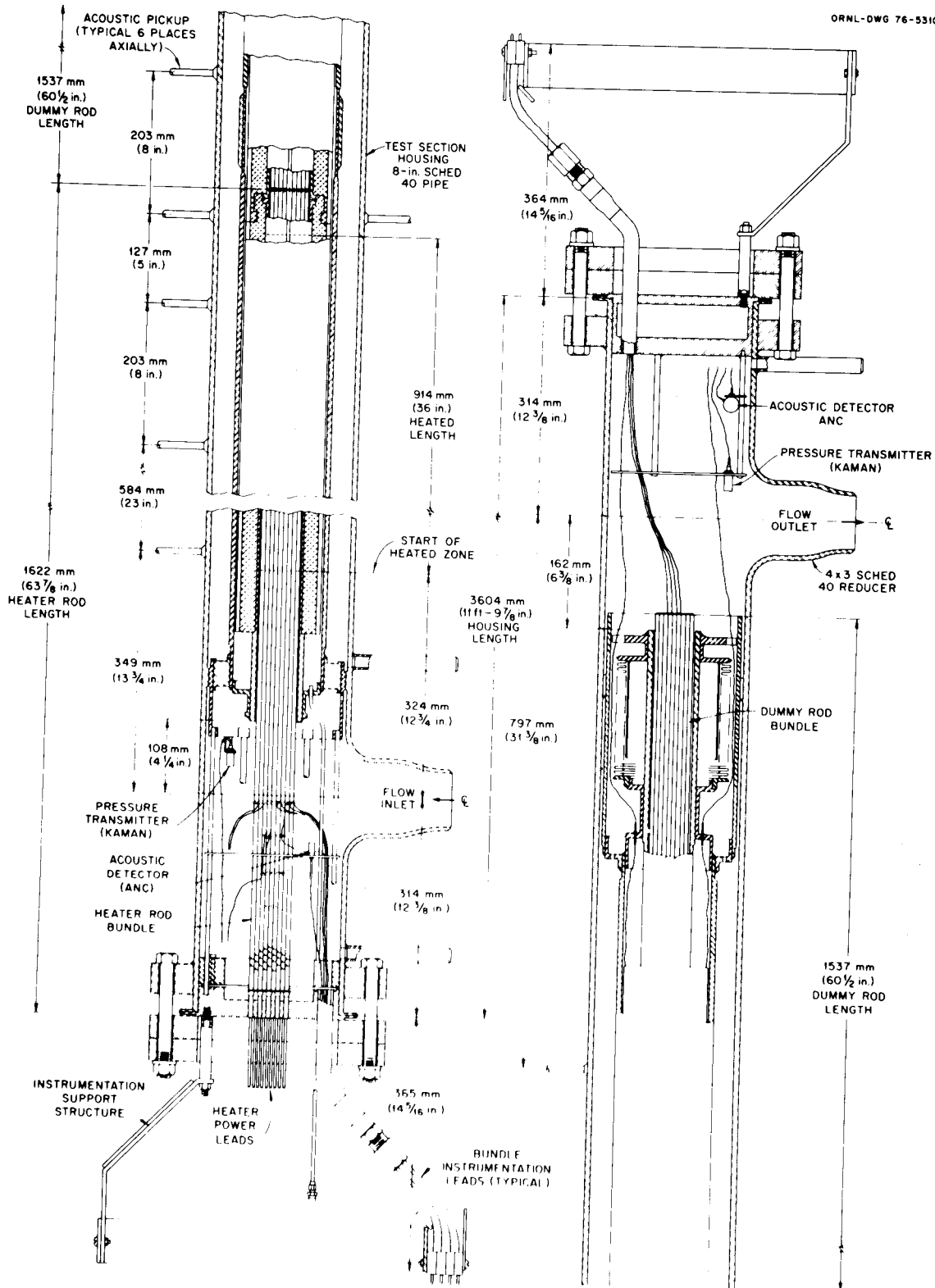


Fig. 1.3. THORS Bundle 9 (61-pin) installed in test section housing.

drawing of Bundle 9 in the test section housing. Figure 1.4 shows the construction of a fuel pin simulator.

Figure 1.5(a) shows the layout of operational thermocouple instrumentation in the heated section. Figure 1.5(b) shows the original planned heated section thermocouple layout. Twenty-seven heater-internal thermocouples, 13 wire-wrap thermocouples, and 23 duct-wall thermocouples failed during fabrication, assembly, and Phase 1 testing. Figure 1.6(a) shows the thermocouple layout for the simulated fission gas plenum region downstream of the heated section. Figure 1.6(b) shows the original planned layout in the fission-gas plenum.

DATA ACQUISITION SYSTEM

Data are recorded using a Data Acquisition System (DAS) controlled by a PDP-8E Computer. Data are logged at the rate of 10,000 points per second and stored on magnetic tape for subsequent processing and display. Data may be displayed on a high-speed character printer or on one of two cathode-ray tube (CRT) terminals (with graphic and hard copy capability) at the THORS operating console. An additional tape drive for copying magnetic data tape is also available.

Several flexible operating and logging programs are utilized.

1. Fast Scan Mode — Data in a prescribed sequence are continuously logged onto magnetic tape at 10,000 points per second for up to 12 min duration. A flexible system of high level—low level signal checking and test termination is available so that a test may be automatically terminated if selected signals exceed the prescribed limits. Simultaneously, every fifth data point is displayed on the console CRT for real-time monitoring during a test.
2. Operator's Log — Ten sets of data are taken, averaged, and converted to engineering units; and the standard deviation is computed. Eleven key parameters, standard deviation, and a test-bundle heat balance are printed at the console. Magnetic tape storage of these data is not utilized.

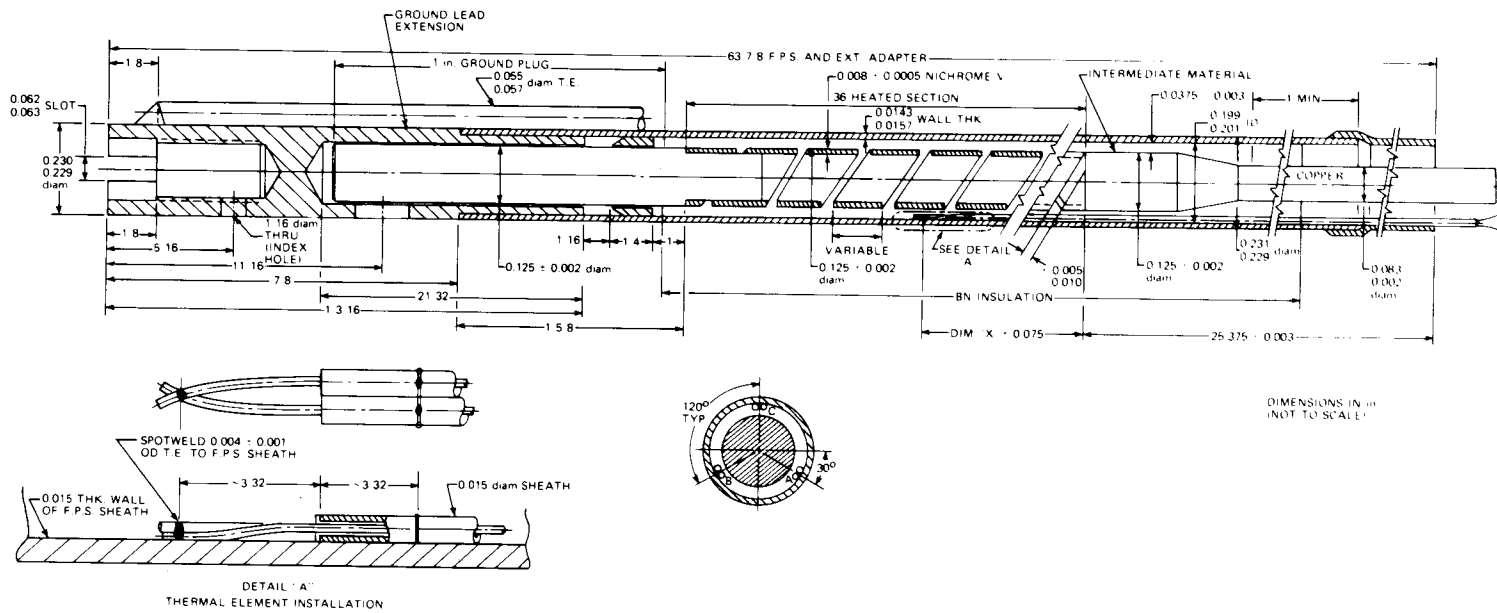


Fig. 1.4. Bundle 9 FPS.

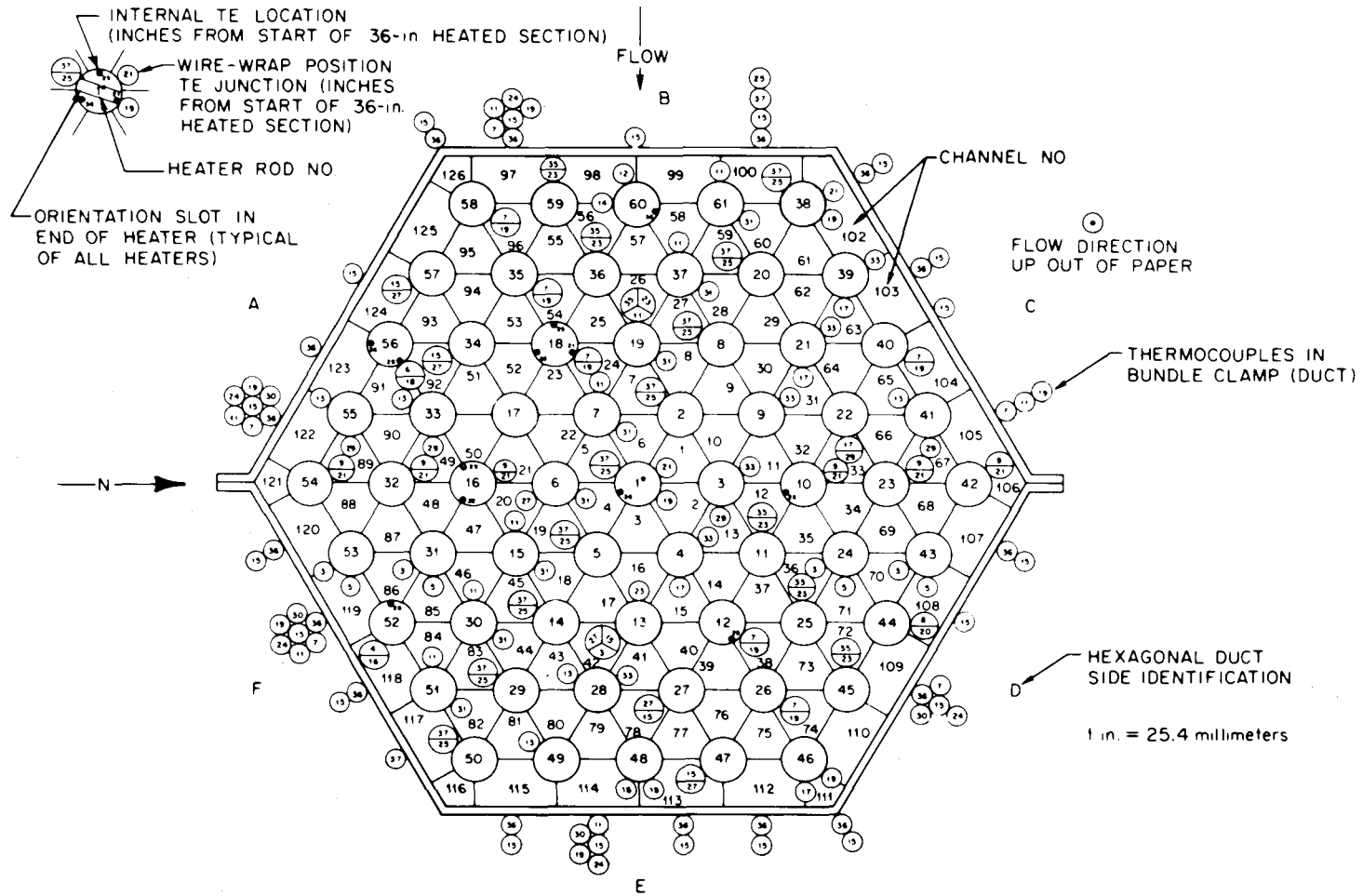


Fig. 1.5(a). Operational instrumentation in the heated section of THORS Bundle 9 after Phase 1 testing.

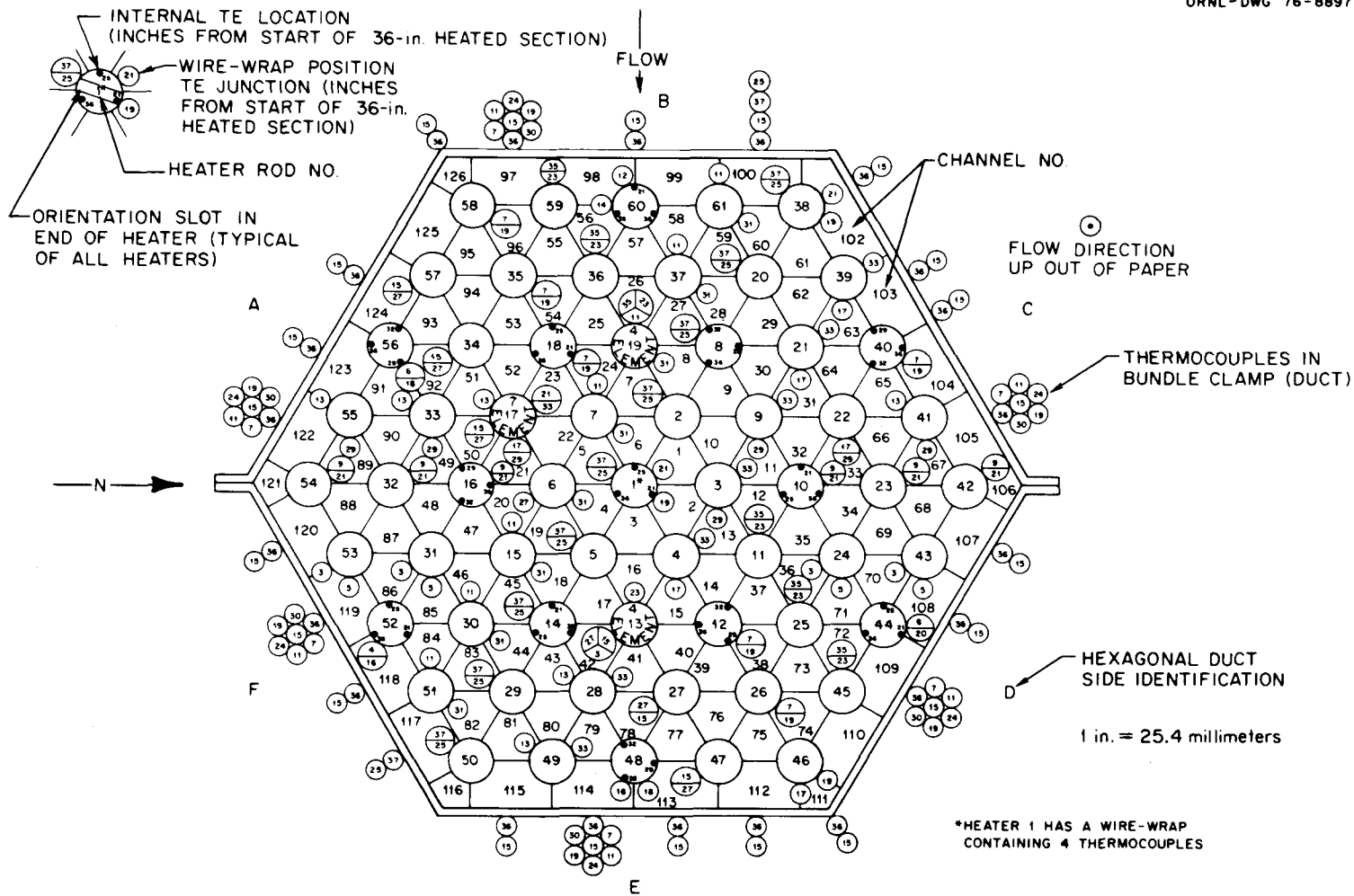


Fig. 1.5(b). THORS Bundle 9 planned heater rod bundle instrumentation.

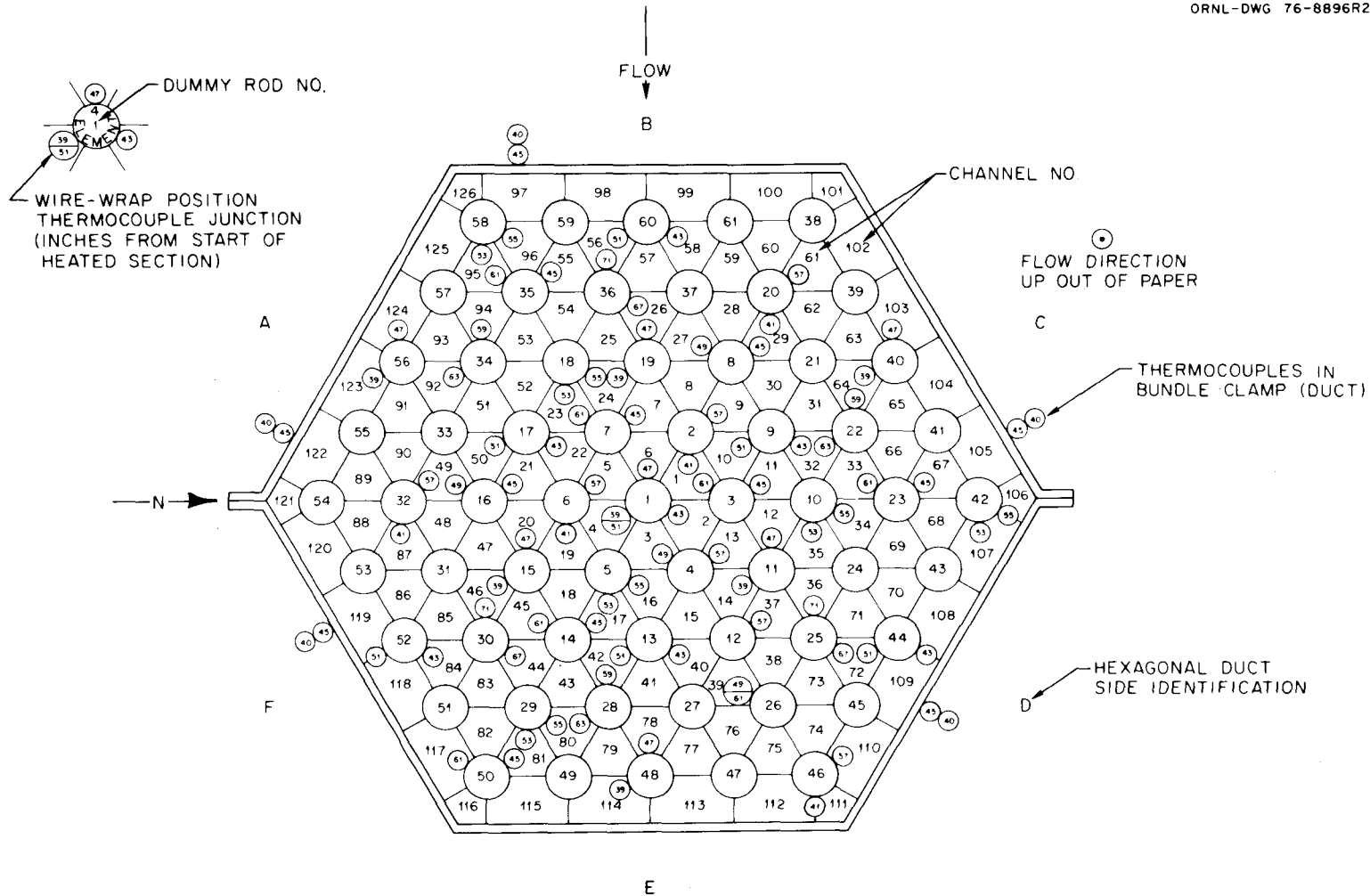


Fig. 1.6(a). Operational instrumentation in the simulated fission gas plenum of THORS Bundle 9 after Phase 1 testing.

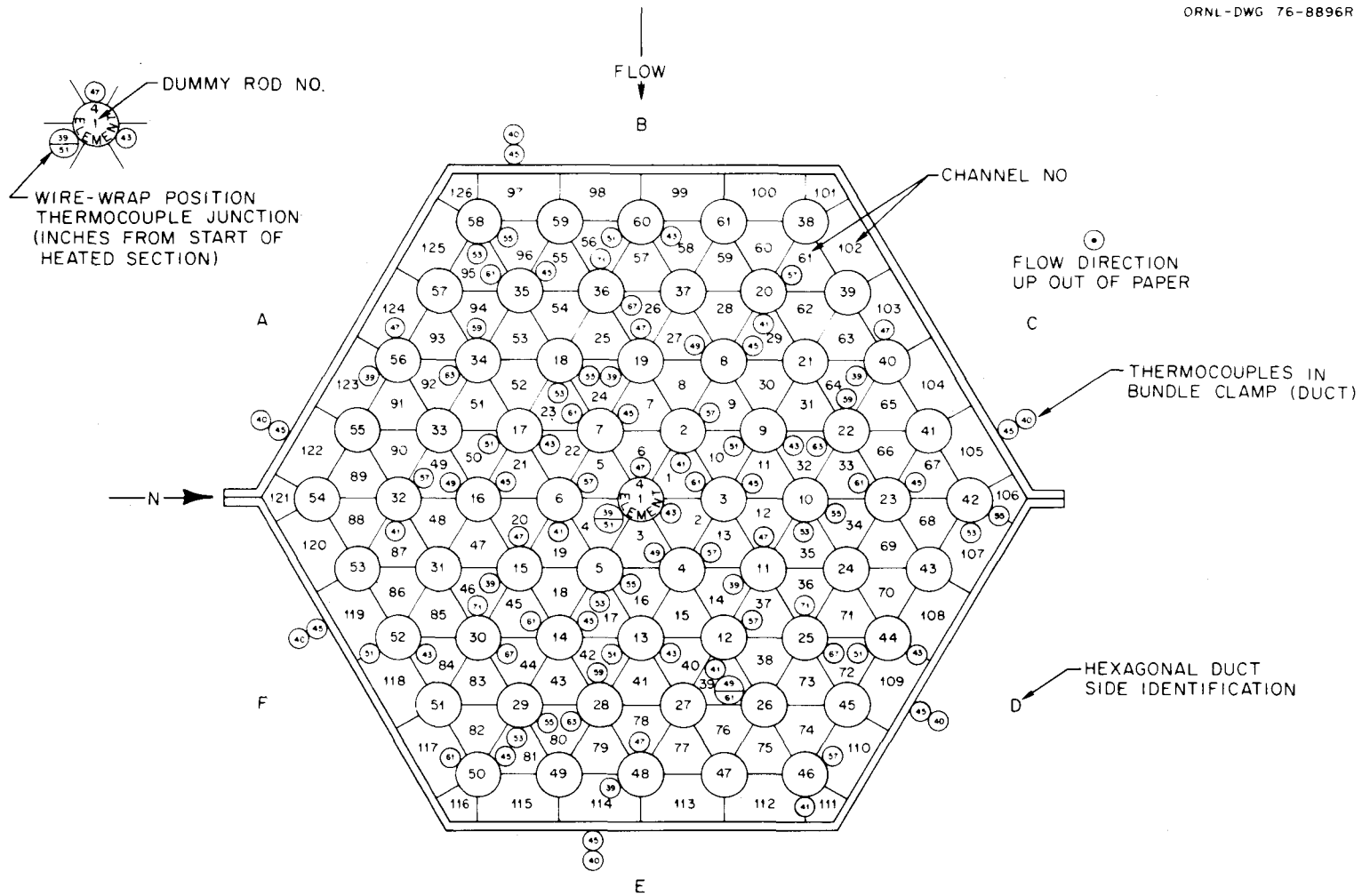


Fig. 1.6(b). Planned instrumentation in the simulated fission gas plenum of THORS Bundle 9.

3. Single-Scan Output - One set of all data signals is taken and converted to engineering units. The results and a test bundle heat balance are printed at the console. Magnetic tape storage is not utilized.
4. Isothermal Log - (Done with no power to the test bundle, but with the loop maintained at isothermal operating temperature at the beginning of each day.) Ten sets of data are taken, averaged, and converted to engineering units; and standard deviations are computed.
5. Slow Scan Mode - 1000 data points in a prescribed sequence are logged onto magnetic tape at a specified time interval. The time interval may be varied from 1.0 s to several minutes. This mode of operation proceeds in the "foreground" simultaneously with normal program operation.

The DAS-generated data tapes are copied to provide a second copy of the data. One of these tapes is used to generate data tapes which are compatible with the ORNL IBM-360 computers. Routines have been prepared to process these IBM-compatible tapes for further presentation of data in tables or plots. In addition, PDP-8 routines have been prepared for immediate posttest data presentations at the operating console. For example, using PDP-8 tapes generated in the fast scan mode (Item 1, above), ten consecutive sets of data are averaged, and standard deviations are computed. Output tables (similar to those described in Item 3, above) can be displayed on the high-speed character printer or on the CRTs at the operating console.

Peripheral routines have been prepared for rearranging the internal scan tables (which control the sequencing of data acquisition), changing calibration coefficients, etc.

SUMMARY OF PART A TESTING

Tests 1 and 2 are identical to their counterparts in the Phase 1 test program. Test 1 is run at steady-state conditions of 15 kW per pin, 7.4 liters·s⁻¹ inlet flow, and 370°C inlet temperature, as a benchmark comparison primarily for documentation of changes in pin distortion during testing. Test 2 is a power-off transient, with initial conditions of

1.0 kW per pin, $0.49 \text{ liter}\cdot\text{s}^{-1}$ inlet flow, and 370°C inlet temperature. Sodium leakage into the bundle insulation was discovered by comparison of Runs 7 and 8 of Test 2 during the Phase 1 test program. Tests 1 and 2 will be run at the start and again at the completion of the Part A testing.

Test 200 is designed to determine the maximum possible bypass/test section flow split as a function of test section flow. All two-phase testing in Part A will be run at the maximum bypass/test section flow split obtainable at the initial test section inlet flow conditions of Test 205 (determined in Run 101, Test 200), or 10:1, whichever is lower.

Test 201 is designed to give information on setting the EM pump controller so that the specified low flow of Tests 204 and 205 can be obtained in the presence of buoyancy-induced flow.

The conditions of Tests 202-205 are summarized in Table 1.1. The initial conditions of Tests 202 and 203 are such that the buoyancy-induced differential static head over the elevation difference between the beginning of the heated section and the inlet to the expansion tank is responsible for a large fraction of the test section flow. The two-phase transient is induced by cutting power to the EM pump. Test section flow will decrease rapidly to some minimum value (determined by the initial buoyancy-induced head) and then slowly increase as temperatures rise in the simulated fission-gas plenum.

The initial conditions of Tests 204 and 205 are such that the buoyancy-induced flow is a smaller fraction of the total test section flow. The two-phase transient is induced by a programmed reduction in the head provided by the EM pump. Referring to Fig. 1.7, the EM pump controller is set so that the initial test section inlet flow (F_1) is decreased at a specified ramp rate ($-0.41 \text{ liter}\cdot\text{s}^{-2}$) to a specified low flow (F_2). The head produced by the EM pump then remains constant until the transient is ended by a programmed flow increase or manual or automatic termination. The time interval between the beginning of the programmed flow decrease (or pump cut-off) and the transient-ending flow increase for each of Tests 202 through 205 is roughly inversely proportional to the pin power in the given test, so that structural components will achieve the same approximation to steady-state thermal conditions. The

Table 1.1. Summary of Part A Two-Phase Transient Testing^a

Test	Power		Initial flow (F_1)		Transient boundary conditions	Analogous run in Bundle 6A
	kW/pin	w/cm ²	Liters·s ⁻¹	gpm		
202	3.1	18.4	0.55	8.7	Cut power to EM pump, record data for 5 min	Test 55, Run 101 (no boiling in 20-s transient)
203	4.1	24.5	0.73	11.5	Cut power to EM pump, record data for 4 min	Test 55A, Run 101 (violent boiling)
204	6.8	40.5	1.21	19.1	Controlled flow reduction to specified minimum, record data for 2.5 min	Test 71H, Run 101 is similar to Run 107 of this test (dryout)
205	15.0	89.2	2.66	42.0	Controlled flow reduction to specified minimum, record data for 1.5 min	Test 73E, Run 102A is similar to Run 104 of this test (dryout)

^aInitial conditions common to all transient runs:

1. inlet temperature of 390°C (730°F);
2. outlet temperature of 700°C (1300°F);
3. test section inlet valve set to 115% of test section ΔP at a test section inlet flow of 8.77 liters·s⁻¹ (139 gpm) (this flow produces the same pin bundle sodium velocity at which the inlet valve was set in Bundle 6A);
4. bypass/test section flow split determined by Test 200, Run 101, or set to 10:1, whichever is lower.

ORNL DWG 79 17084 ETD

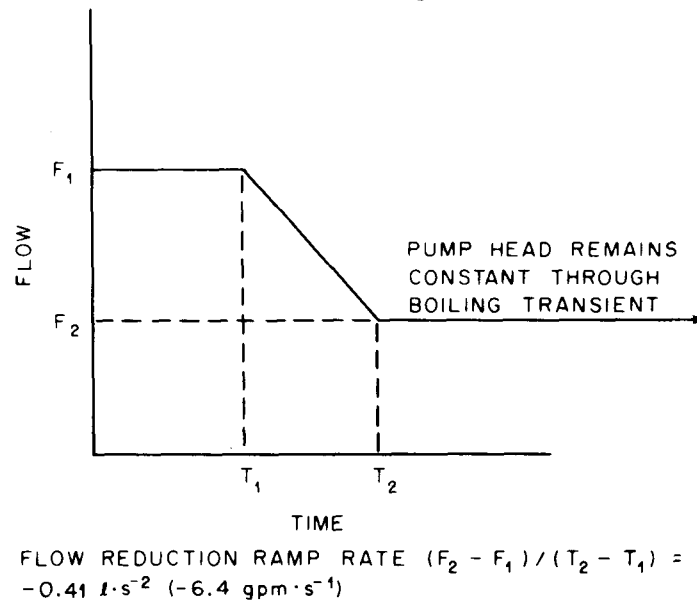


Fig. 1.7. Controlled flow reduction for Phase 2 transient testing.

test will be terminated if temperatures exceed the following limitations:

heater-internal thermocouples	1010°C (1850°F)
wire-wrap thermocouples	982°C (1800°F)
duct wall thermocouples	927°C (1700°F)

Test termination consists of an immediate cut in the power to all fuel pin simulators and, in the case of Tests 202 and 203, a restart of the pump to its initial forced flow.

At any point in this test plan the testing may be terminated or modified, and the sequence of runs in any test may be altered by the Project Engineer and the Program Coordinator.

Test 1

Purpose: To determine the reproducibility of bundle temperature profiles throughout the test program. The steady-state temperature distribution in the bundle is documented at various times during the test program by recording the bundle temperatures for 60 s while the bundle is being operated at the following conditions.

Procedure:

1. Open test section inlet valve.
2. Close bypass line valve.
3. Adjust inlet temperature to 370°C (700°F), test-section inlet flow to 7.38 liters·s⁻¹ (117 gpm), and heater power to 15 kW/pin.
4. Establish steady-state conditions.
5. Establish a heat balance.
6. Record 60 s of instrument responses on magnetic tape in fast scan mode.

Test 2

Purpose: To determine the condition of the thermal insulation which insulates the pin bundle from the test section housing. Results of this test during the Phase 1 test program showed that sodium had leaked into the insulation. Any further deterioration will be evident by comparing results of this test run before and after Phase 2 Part A.

Procedure:

1. Open test section inlet valve.
2. Close bypass line valve.
3. Adjust heater power to 1.0 kW/pin, test section inlet flow to $0.49 \text{ liter}\cdot\text{s}^{-1}$ (7.8 gpm), and test section inlet temperature to 370°C (700°F).
4. Establish steady-state conditions.
5. Start recording instrument responses on magnetic tape in fast scan mode. After 30 s at steady-state conditions, shut off heater power (continue recording data in fast scan mode).
6. Two minutes after shutting off heater power, discontinue data acquisition.

Test 200

Purpose: In order to simulate a constant pressure-drop boundary condition between test section inlet and outlet, transient tests are run with a parallel bypass line. This test will determine the maximum bypass/test section flow split possible with the new EM pump for the initial flow conditions of Tests 202 through 205.

Procedure:

1. Set the test section inlet valve to 115% of the test section Δp at a test section inlet flow of $8.77 \text{ liters}\cdot\text{s}^{-1}$ (139 gpm) (this flow produces the same pin bundle sodium velocity at which the inlet valve was set in Bundle 6A), isothermal conditions (390°C or 730°F).
2. Establish steady-state, isothermal conditions at 390°C (730°F).
3. Find the maximum bypass/test section flow split possible at each of the test section flow conditions listed below.
4. Record data.

Run	Test section inlet flow [$\text{liters}\cdot\text{s}^{-1}$ (gpm)]
101	2.66 (42.0)
102	1.21 (19.1)
103	0.73 (11.5)
104	0.55 (8.7)

Test 201

Purpose: The EM pump controller is set to achieve a specified low flow in order to obtain saturation conditions in the test section in Tests 204 and 205. Previously the pump controller has been set at isothermal (test section inlet temperature) conditions. For runs in which natural convection effects were responsible for a significant fraction of the test section flow, this method was not very accurate. This test will provide data which will be helpful in determining the low-flow setting of the pump controller which will give a specified low flow, with natural convection effects taken into account.

Procedure:

1. Set the test section inlet valve to 115% of the test section Δp at a test section inlet flow of $8.77 \text{ liters}\cdot\text{s}^{-1}$ (139 gpm) (this flow produces the same pin bundle sodium velocity at which the inlet valve was set in Bundle 6A), isothermal conditions (390°C or 730°F).
2. Set the valve on the bypass line to obtain the bypass/test section flow split determined in Test 200, Run 101, or 10:1, whichever is lower.
3. With a common test section inlet temperature of 390°C (730°F), obtain steady-state conditions at each set of power/flow conditions listed below.
4. Record the setting of the pump controller and the resulting test section inlet flow.

Run	Test section inlet flow [$\text{liters}\cdot\text{s}^{-1}$ (gpm)]	Bundle power	
		kW	kW/pin
101	2.09 (33.2)	721	11.8
102	1.52 (24.1)	523	8.6
103	0.95 (15.0)	326	5.3
104	0.69 (10.9)	237	3.9
105	0.54 (8.6)	187	3.1
106	0.38 (6.0)	130	2.1

Test 202

Discussion: The EM pump will be turned off after steady-state conditions are established at a test section inlet flow of 0.55 liter \cdot s $^{-1}$ and a pin power of 3.1 kW. This test is similar to Test 55, Run 101, run in Bundle 6A, in which sodium did not boil in the 30 s before forced flow was reestablished. Analysis with SABRE-2 indicates that boiling may not occur here, either, but that natural convection effects will increase the test section flow as the fission-gas plenum heats up, reaching a maximum temperature very close to saturation conditions.

Procedure:

1. Set test section inlet valve to 115% of the test section Δp at a test section inlet flow of 8.77 liters \cdot s $^{-1}$ (139 gpm) (this flow produces the same pin bundle sodium velocity at which the inlet valve was set in Bundle 6A), isothermal conditions (390°C or 730°F).
2. Set valve on bypass line to obtain the bypass/test section flow split determined in Test 200, run 101, or 10:1, whichever is lower.
3. Obtain steady-state conditions of test section inlet temperature, outlet temperature, and test section flow at the following conditions for a period of at least 1 h:

test section inlet temperature	390°C (730°F)
test section inlet flow	0.55 liter \cdot s $^{-1}$ (8.7 gpm)
total bundle power	189 kW
4. Record data in fast scan mode for 5 min, beginning 10 s before cutting power to the EM pump.
5. Cut power to EM pump.
6. If dryout conditions do not prematurely terminate the test, end test by returning to initial flow conditions 4.5 min after cutting power to EM pump.

Test 203

Discussion: The EM pump will be turned off after steady-state conditions are established at a test section inlet flow of $0.73 \text{ liter}\cdot\text{s}^{-1}$ and a pin power of 4.1 kW. This test is similar to Test 55A, Run 101, run in bundle 6A,² in which saturation conditions were obtained $\sim 30 \text{ s}$ after the pump run-down. Superheat conditions existed for $\sim 15 \text{ s}$ until violent boiling began, with no dryout observed. Analysis with SABRE-2 indicates that saturation conditions will be reached in Test 203 $\sim 10 \text{ s}$ after power to the EM pump is cut.

Procedure:

1. Set test section inlet valve to 115% of the test section Δp at a test section inlet flow of $8.77 \text{ liters}\cdot\text{s}^{-1}$ (139 gpm) (this flow produces the same pin bundle sodium velocity at which the inlet valve was set in Bundle 6A), isothermal (390°C or 730°F) conditions.
2. Set valve on bypass line to obtain the bypass/test section flow split determined in Test 200, Run 101, or 10:1, whichever is lower.
3. Obtain steady-state conditions of test section inlet temperature, outlet temperature, and test section flow at the following conditions for a period of at least 1 h:

test section inlet temperature	390°C (730°F)
test section inlet flow	$0.73 \text{ liter}\cdot\text{s}^{-1}$ (11.5 gpm)
total bundle power	250 kW
4. Record data in fast scan mode for 4 min, beginning 10 s before cutting power to EM pump.
5. Cut power to EM pump.
6. If dryout conditions do not prematurely terminate the test, end test by returning to initial flow conditions 3.5 min after cutting power to EM pump.

Test 204

Discussion: The EM pump controller is set to ramp down the initial test section inlet flow (F_1) at a rate of $-0.41 \text{ liter}\cdot\text{s}^{-2}$ ($-6.4 \text{ gpm}\cdot\text{s}^{-1}$) to a low flow (F_2) which is lower in subsequent runs of this test. The low flow in run 101 should produce temperatures close to but not reaching saturation conditions, while the low flow in Run 102 should produce saturation conditions in the bundle interior. If dryout conditions are not reached (it is expected that they will be) in prior runs, the results of Run 107 may be compared directly with Test 71H, Run 101, run in Bundle 6A.² Analysis with a modified version of COBRA III-C indicates that saturation conditions will be reached ~ 5 s after the beginning of the Run 107 flow transient and that the entire bundle cross-section interior to the edge pins will be involved in boiling several seconds thereafter.

Procedure:

1. Set the test section inlet valve to 115% of the test section Δp at a test section inlet flow of $8.77 \text{ liters}\cdot\text{s}^{-1}$ (139 gpm) (this flow produces the same pin bundle sodium velocity at which the inlet valve was set in Bundle 6A), isothermal conditions (390°C or 730°F).
2. Set the valve on the bypass line to obtain bypass/test section flow split determined in Test 200, Run 101, or 10:1, whichever is lower.
3. Obtain steady-state conditions of test section inlet temperature, outlet temperature, and test section flow at the following conditions for a period of at least 1/2 h.

test section inlet temperature	390°C (730°F)
test section inlet flow	$1.21 \text{ liters}\cdot\text{s}^{-1}$ (19.1 gpm)
total bundle power	415 kW

4. Record data in fast scan mode for 2.5 min, beginning 10 s before the programmed flow reduction begins.
5. Begin the two-phase transient by starting the programmed flow reduction to the low flow (F_2) given below for each run (pump setting determined in Test 201).
6. If dryout conditions do not prematurely terminate the test, end test by returning to initial flow conditions 2 min after the beginning of the programmed flow reductions.

Run	Inlet low flow (F_2) [liters·s ⁻¹ (gpm)]	Average steady-state two-phase quality at exit*
101	0.95 (15.0)	-0.05
102	0.79 (12.6)	-0.025
103	0.69 (10.9)	0.0
104	0.61 (9.6)	0.025
105	0.54 (8.6)	0.05
106	0.44 (7.1)	0.10
107	0.38 (6.0)	0.15

*Useful in planning conditions so as to run tests systematically further into the boiling regime. However, it should be noted that boiling will not occur under steady-state conditions, nor is it well described by bundle average parameters. A saturation temperature of 943°C (1730°F) has been assumed. If the actual saturation temperature is found to differ by more than 20°C, the low flows will be changed.

Test 205

Discussion: As in Test 204, the EM pump controller is set to ramp down the initial test section inlet flow (F_1) at a rate of $-0.41 \text{ liter}\cdot\text{s}^{-1}$ ($-6.4 \text{ gpm}\cdot\text{s}^{-1}$) to a low flow (F_2) which is lower in subsequent runs of this test. The low flow in Run 101 should produce temperatures close to but not reaching saturation conditions, while the low flow in Run 102 should produce saturation conditions in the bundle interior. If dryout conditions are not reached (it is expected that they will be) in prior runs, the results of Run 104 may be compared directly with Test 73E, Run 102A, run in Bundle 6A,² in which dryout was observed 14 s after boiling initiation. Dryout should be expected to occur even sooner in Run 104.

Procedure:

1. Set the test section inlet valve to 115% of the test section Δp at a test section inlet flow of $8.77 \text{ liters}\cdot\text{s}^{-1}$ (139 gpm) (this flow produces the same pin bundle sodium velocity at which the inlet valve was set in Bundle 6A), isothermal conditions (390°C or 730°F).
2. Set the valve on the bypass line to obtain bypass/test section flow split determined in Test 200, Run 101, or 10:1, whichever is lower.
3. Obtain steady-state conditions of test section inlet temperature, outlet temperature, and test section flow at the following conditions for a period of at least 1/2 h.

test section inlet temperature	390°C (730°F)
test section inlet flow	$2.66 \text{ liters}\cdot\text{s}^{-1}$ (42.0 gpm)
total bundle power	915 kW

4. Record data for 1.5 min, beginning 10 s before the programmed flow reduction begins.

5. Begin the two-phase transient by starting the programmed flow reduction to the low flow (F_2) given below for each run (pump setting determined in Test 201).
6. If dryout conditions do not prematurely terminate the test, end test by returning to initial flow conditions 1 min after the beginning of the programmed flow reduction.

Run	Inlet low flow (F_2) [liters·s ⁻¹ (gpm)]	Average steady-state two-phase quality at exit*
101	2.09 (33.2)	-0.050
102	1.76 (27.9)	-0.025
103	1.52 (24.1)	0.0
104	1.34 (21.2)	0.025
105	1.19 (18.9)	0.050

*Useful in planning conditions so as to run tests systematically further into the boiling regime. However, it should be noted that boiling will not occur under steady-state conditions, nor is it well described by bundle average parameters. A saturation temperature of 943°C (1730°F) is assumed. If the actual saturation temperature is found to differ by more than 20°C, the low flows will be changed.

1.1.2 Detection of dryout in Bundle 9 Phase 2 tests
(A. E. Levin)

During the fabrication, assembly, and Phase 1 tests on THORS Bundle 9, a significant number of heater-internal thermocouples were lost. These thermocouples are important because they indicate most clearly the conditions on the FPS surface. The Bundle 9 Phase 2 Test Plan includes a number of tests in which the bundle is to be run to dryout. However, without heater-internal thermometry, it may be difficult to detect dryout in time to prevent bundle failure. Therefore, a study was undertaken using data from Bundle 6A tests to determine whether any other instrumentation still available on Bundle 9 might be helpful in detecting dryout.

The configuration of an LMFBR bundle, with a long, unheated fission-gas plenum region above the core, helps to provide the means by which dryout may be detected indirectly. Boiling is initiated in THORS by reducing the inlet flow at constant power. The coolant above the heated section of the bundle, in the SFGP, thus remains subcooled at boiling inception. In turn, a substantial heat sink occurs and promotes condensation, which, along with the pumping action of flow oscillations, shown in Fig. 1.8, causes the coolant to heat up gradually. At some point, the fluid in the SFGP becomes saturated. When this occurs, condensation can no longer take place, and the voided region caused by boiling in the heated section grows long enough to allow the FPSs to dry out. The SFGP is heavily instrumented with wire-wrap thermocouples in Bundle 9, as it was in Bundle 6A. Detection of this saturation front in the SFGP by these wire-wrap thermocouples provides an indirect means of determining when dryout is about to occur.

Several traces of thermocouples from Bundle 6A boiling tests are shown in Figs. 1.9 through 1.12. The four tests, all described as either dryout or violent boiling runs, are Test 71F, Run 101; Test 71G, Run 101; Test 71H, Run 101; and Test 72B, Run 101. Details of these tests can be found in Ref. 2. In all of the tests, the SFGP wire-wrap thermocouples exhibited steep temperature ramps prior to the onset of dryout. The rapid temperature oscillations of the heater-internal thermocouples indicate dryout. The timing of these ramps in the SFGP region is dependent on the axial position of the wire-wrap thermocouples: the thermocouple at

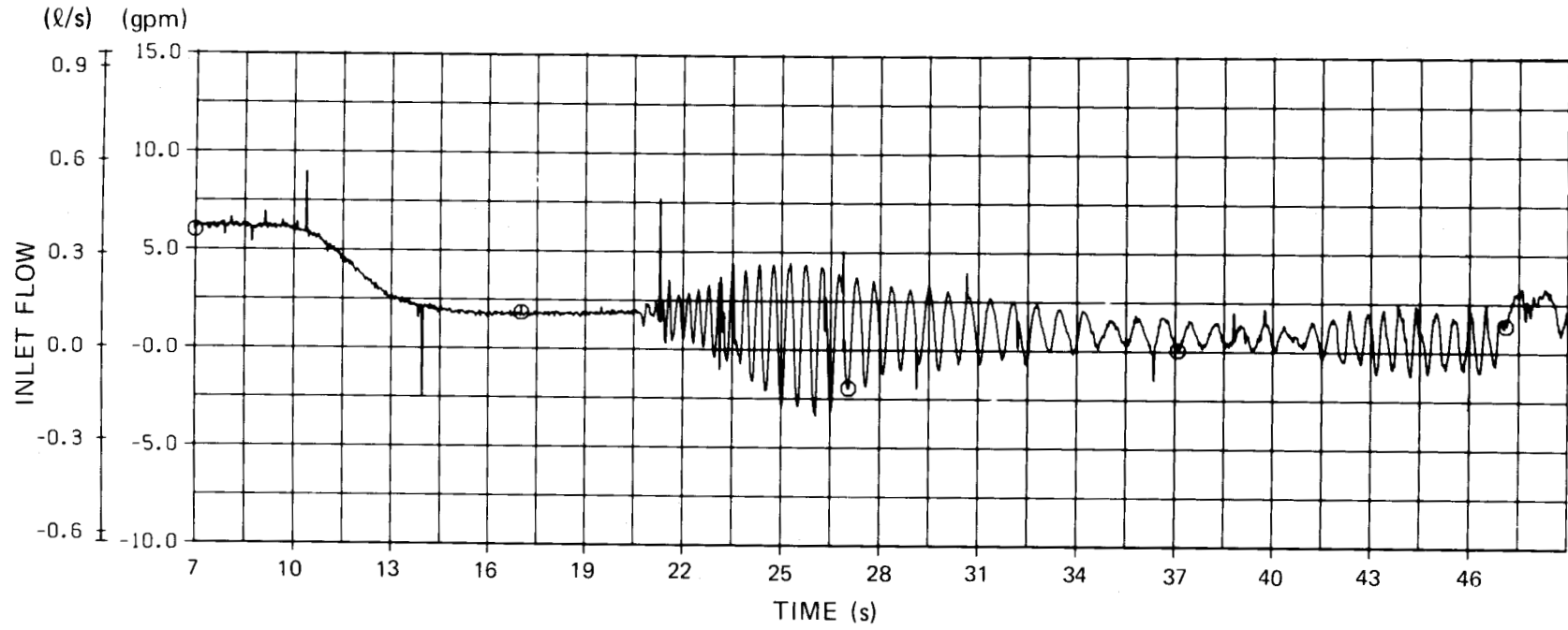


Fig. 1.8. Test section inlet flow during Test 71H, Run 101, THORS Bundle 6A.

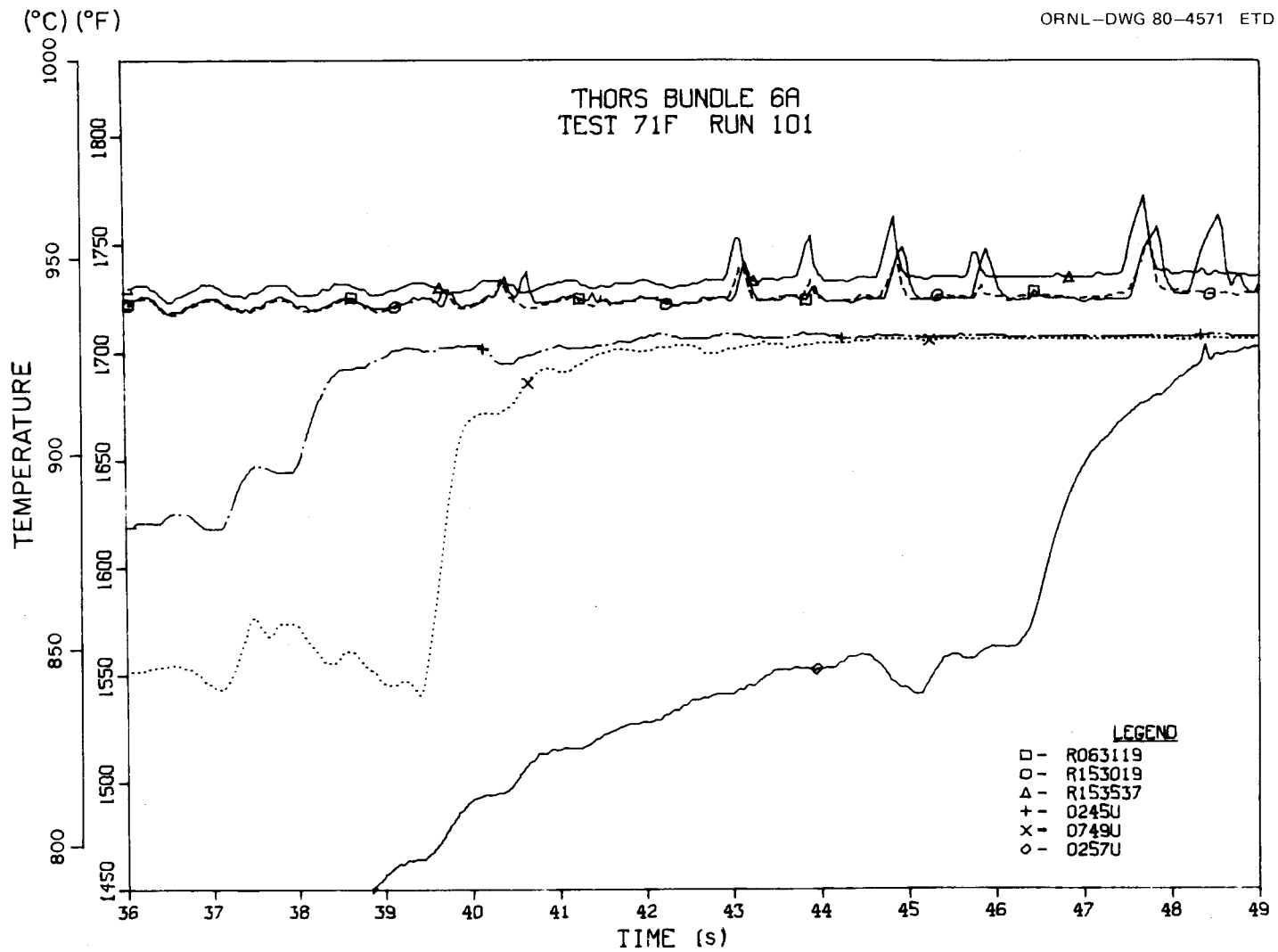


Fig. 1.9. Heater-internal and SFGP wire-wrap thermocouple temperatures during Test 71F, Run 101, THORS Bundle 6A.

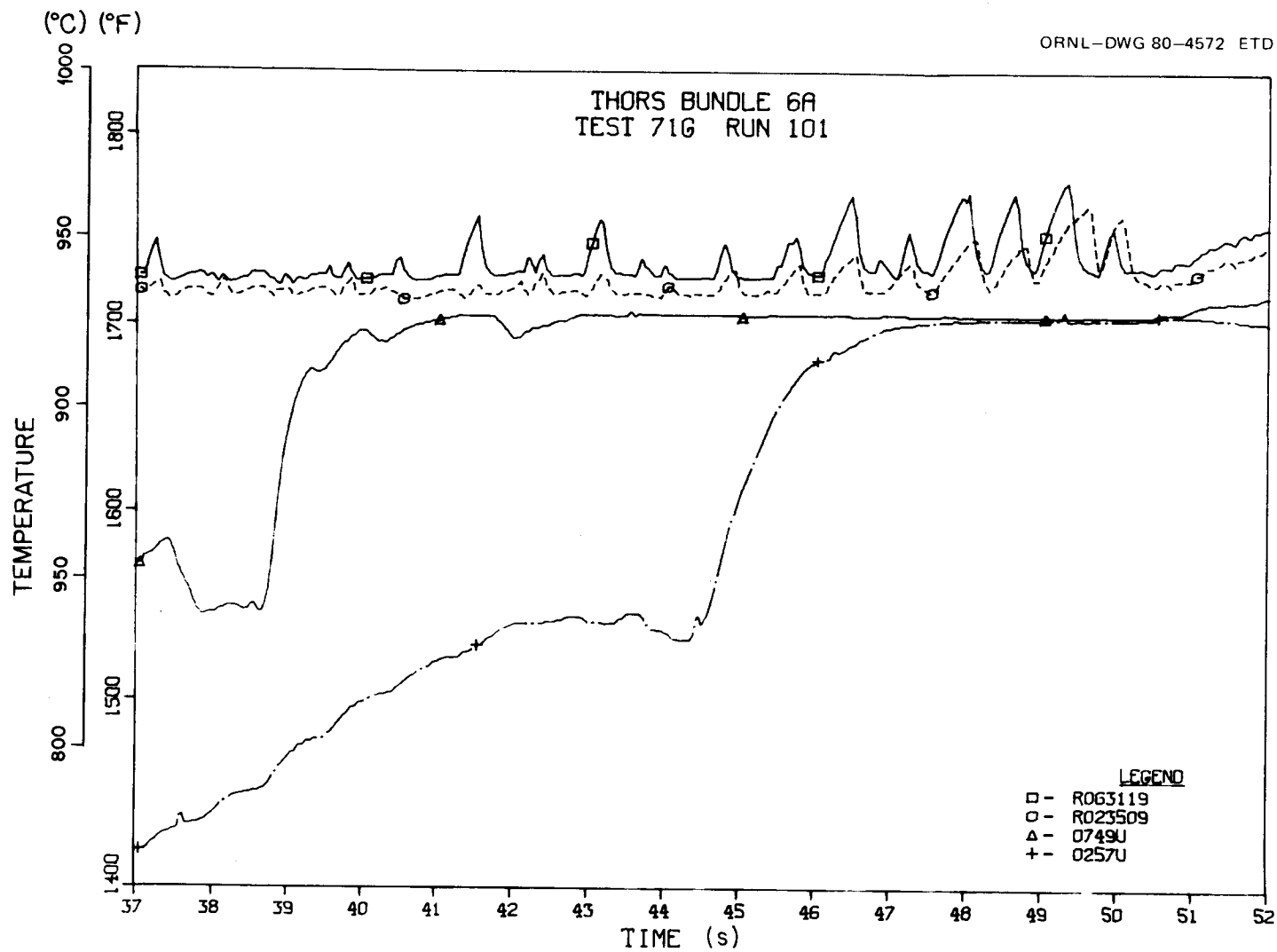


Fig. 1.10. Heater-internal and SFGP wire-wrap thermocouple temperatures during Test 71G, Run 101, THORS Bundle 6A.

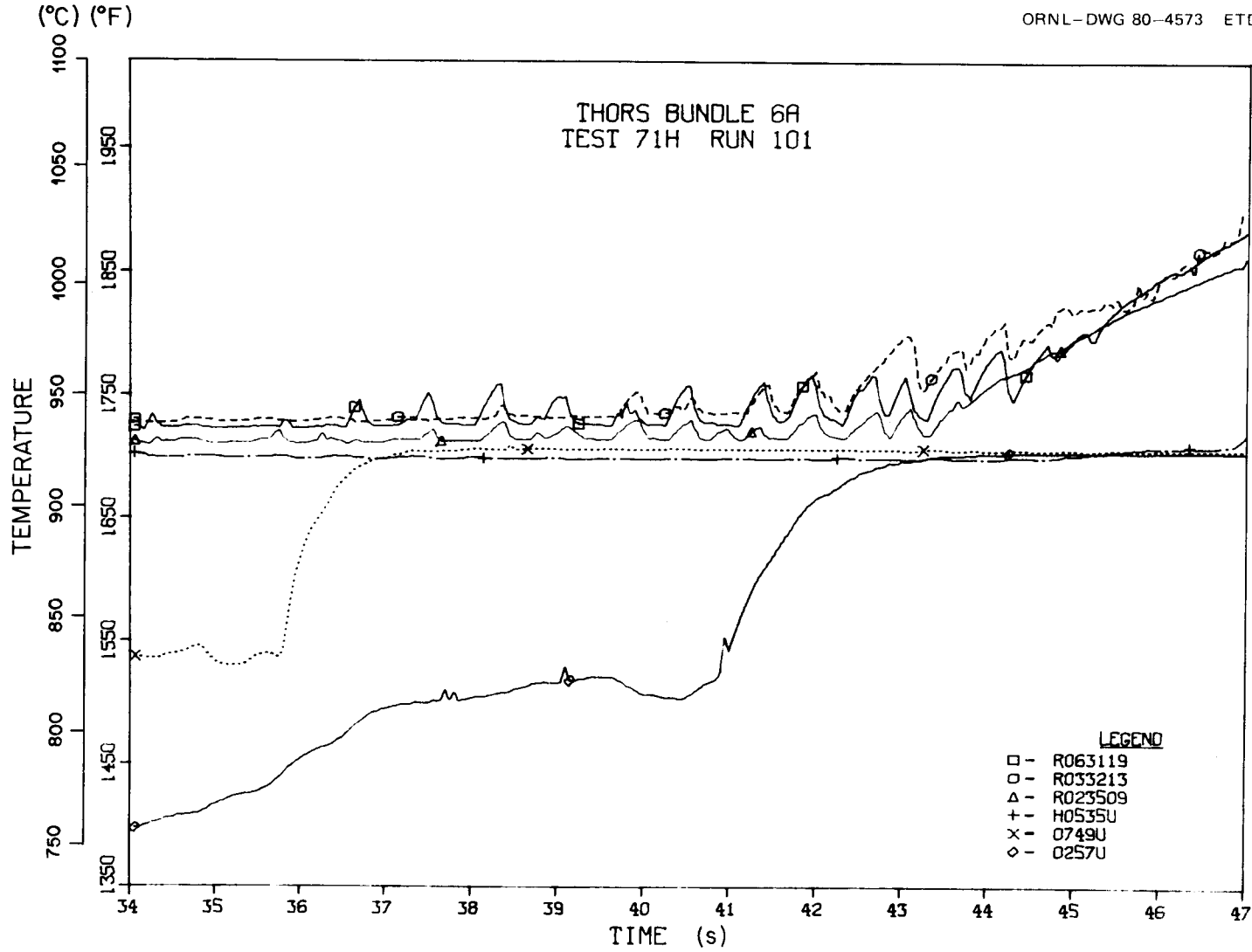


Fig. 1.11. Heater-internal, heater wire-wrap, and SFGP wire-wrap thermocouple temperatures during Test 71H, Run 101, THORS Bundle 6A.

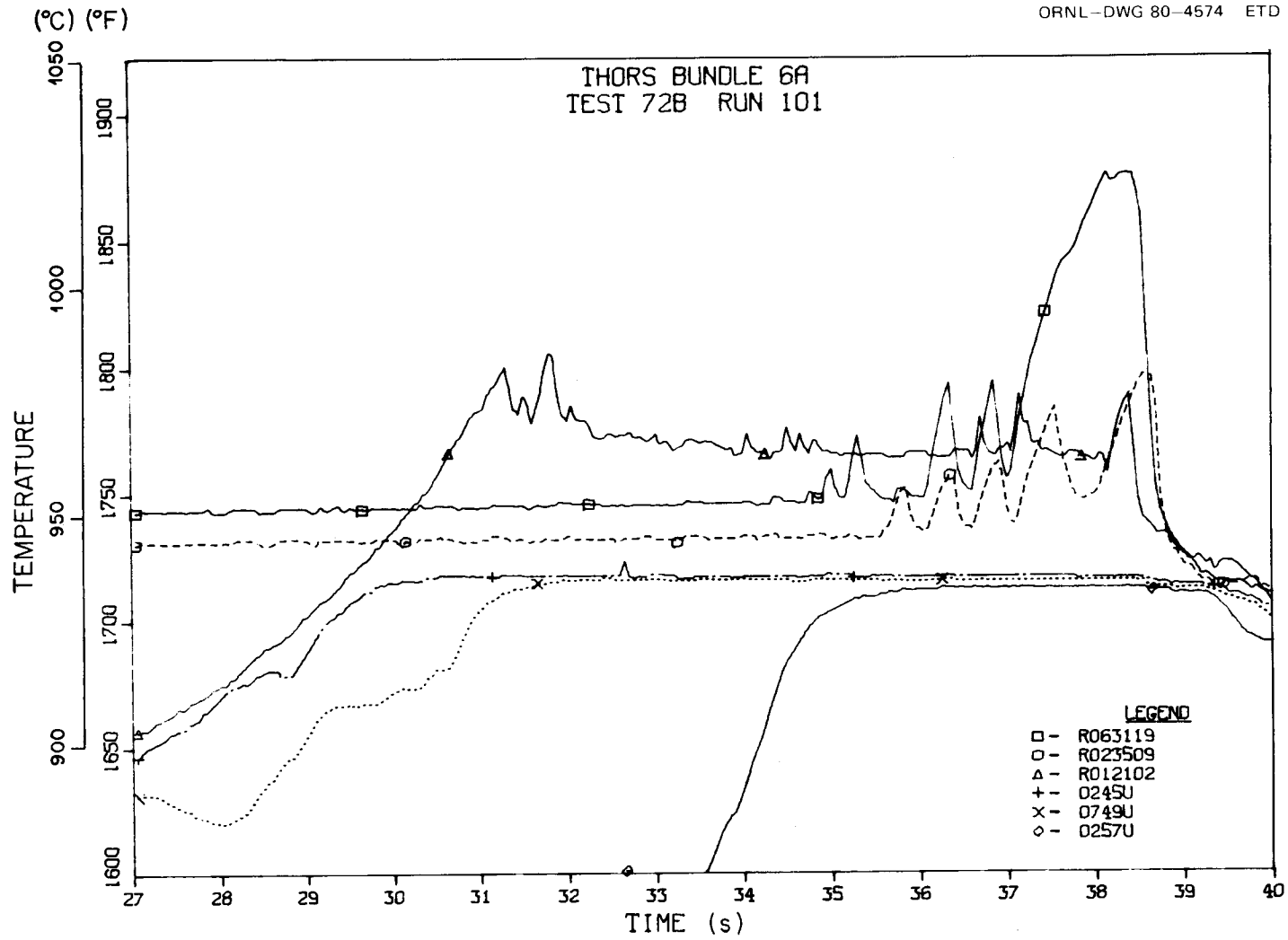


Fig. 1.12. Heater-internal and SFGP wire-wrap thermocouple temperatures during Test 72B, Run 101, THORS Bundle 6A.

station 45, 1.143 m (45 in.) above the bottom of the heated section increases first, followed by the thermocouple at station 49 (1.245 m); the thermocouple at station 57 (1.448 m) is the last to exhibit such behavior and does so shortly before detection of incipient dryout in the heated portion of the bundle.

Based on these data, the following recommendations have been made.

1. *Strip chart recorders should be used to monitor several wire-wrap thermocouples near the inner ring of FPSs in the SFGP, at axial levels ranging from ~1.143 to 1.448 m (45 to 57 in.). This will facilitate real-time processing of thermocouple outputs.*
2. *When behavior similar to that noted in Bundle 6A boiling tests is seen on these SFGP thermocouples, the operator should wait several seconds to see if the remaining heater-internal thermocouples will detect dryout. The data acquisition system will shut off FPS power when a specified high temperature limit is exceeded. The waiting period is dependent on the power of the bundle during the test — the higher the power, the shorter the waiting time.*
3. *If the bundle power is not cut by the DAS within this waiting period, the test should be terminated manually.*

This procedure will be implemented during Bundle 9 Phase 2 testing with the aid of the I&C Division. It should provide a means by which to perform boiling and dryout tests without causing the bundle to fail prematurely because of excessively high FPS temperatures following dryout.

1.1.3 SAS3D prediction of Bundle 9 intrasubassembly boiling incoherence (K. Haga and G. A. Klein)

Analysis. A preliminary analysis of the temperature-flow distribution in Bundle 9 was made using the SAS3D code. The purpose of this study was to investigate the importance of radial incoherence of boiling within a subassembly in order to determine whether the experimental boiling results are inconsistent with single-pin boiling calculations using a multinode, radial conduction model to predict the temperature distribution through the housing structure which has become degraded by sodium soaking of the insulation.

A SAS channel contains a fuel pin and its associated coolant and structure. This channel normally represents an average pin in a subassembly or group of subassemblies; thus, radial coherence of important behavior within a subassembly is suggested. Ideally, a multiple-pin, multiple-coolant subchannel model should provide for heat, coolant mass, and momentum transfer between SAS channels at all axial locations, but these cannot all be provided for by the SAS3D code. However, F. E. Dunn of ANL developed an intermediate SAS3D model to describe intrasubassembly boiling incoherence which includes many of the most important channel-to-channel coupling effects.⁷ The existing SAS code can be used by employing a very simple multipin model that neglects all radial communication within a subassembly and uses isolated, uncoupled SAS channels to represent various parts of the subassembly. The applicability of this type of model to represent the temperature flow distribution in two separate radial regions of the pin bundle was examined for Bundle 9. Ideally, this model can be represented by concentric rings of coolant subchannels and fuel pins, starting with channel 1 on the outside and working inward, as shown in Fig. 1.13. Because the SAS inlet plenum treatment allows cross-flow between channels, this model allows liquid cross-flow at the bottom of the pins but not in the pin section itself. Also, in the SAS boiling model, vapor flow is equivalent to heat flow in a voided region, and channel-to-channel heat flow between voided channels is equivalent to channel-to-channel vapor flow. The structure in channel 1 represents the subassembly duct wall, with a small addition for spacer wires. In the central channel or channels, the structure represents only the spacer wires. In channel 1, heat added to the clad will make its way to the coolant more rapidly than heat added to the structure, because the channel 1 structure represents a thick duct wall. In the central channels, the structure is thin, and any heat added to the structure will quickly make its way to the coolant.

As a first approximation to determine the validity of this type of model for representing Bundle 9, the central channel structure was assumed to have a thickness of 1×10^{-5} cm, which essentially approximates an adiabatic condition for the structure or no heat flow between the two adjacent radial channels. That is, the SAS channel representing the central

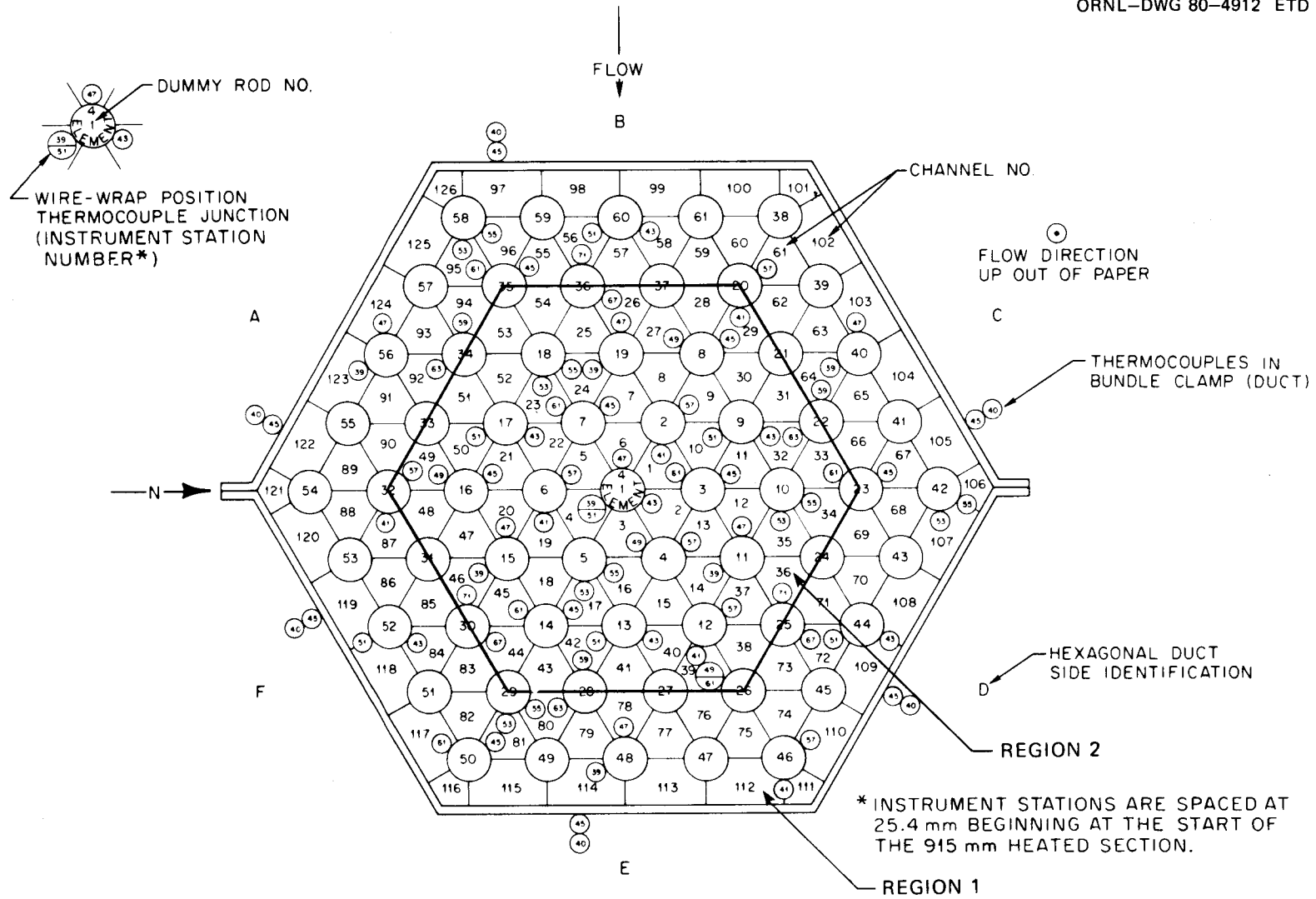


Fig. 1.13. THORS Bundle 9 divided into two regions for SAS3D analysis.

channel region was modeled to behave as if it were not influenced by the radial temperature distribution present along the bundle outer channels. This assumption will be examined further.

In addition, a detailed representation for the inertial response of the structure was included in the SAS representation for channel 1. This was accomplished by coupling the SAS3D model of an equivalent fuel pin and its associated coolant (representing the concentric ring of outer coolant subchannels and fuel pins) to the multinode radial conduction model developed by J. F. Dearing to describe the structure's inertial response to local coolant temperature changes within the channel at each axial location.⁸

Very crude "scoping" calculations were made with the basic single-channel SAS fuel pin model to determine if the type of multichannel approximation mentioned above can prove valid as a first-approach representation for Bundle 9. The effectiveness of a two-channel model was determined by comparing the program's single-channel predictions with the Bundle 9 Phase 1 Test 2, Run 8 experimental data associated with the two regions mentioned above. For this test, the bundle inlet flow was maintained constant at 0.41 m/s while the heater pin power was cut from an initial pin power of 1.0 kW/pin to a zero power condition.

Results. The measured temperature changes for two regions of the bundle were compared with the SAS3A code predictions for an equivalent representation of a typical Bundle 9 coolant channel, and a preliminary assessment was made of the influence of the structure's thermal inertia on the coolant response of each region. As a first approach, the structure for a SAS channel that would normally reside within region 2 can be represented by the wrapper wire's inertial response plus an arbitrarily small addition to this structure to represent that portion of the housing's inertial response which would ultimately influence the flow of heat transported from this central region by the coolant from the region bordering the duct wall. The influence of this additional negative heat flow will ultimately have to be included as depicted in the multiregion model of Dunn.

The coolant flow area for the coolant channel associated with an equivalent channel fuel pin would roughly represent 1/61 of the total

flow area for Bundle 9. Likewise, the degraded structure associated with this fuel pin should represent 1/61 of the total structure for Bundle 9. For the reasons outlined, the fraction of this structure's inertial response for equivalent SAS channels assumed to reside within the central and the outer channel regions of the bundle will be varied to determine its influence on the predicted temperature distribution associated with an equivalent flow channel located within the central, rather than outer, region of the bundle.

Coolant temperatures for Bundle 9 Test 2, Run 8 were measured by wire-wrap thermocouples located in the third-ring subchannels and duct wall as shown in Fig. 1.14. Figure 1.14(a and b) shows the experimental data and calculational results obtained from the SAS3A code for both steady-state conditions and conditions corresponding to 20 s after reduction of the pin power to 0 kW/pin.

As shown in Fig. 1.14(a), the results of this study verify the hypothesis that the temperature-flow behavior of the central coolant channel is essentially independent of any influence of the inertial response of the duct wall. In Fig. 1.14(b), the predicted duct wall temperature results from the identical SAS single-channel fuel pin model mentioned previously were compared with the measured Bundle 9 Test 2, Run 8 duct wall temperatures. Again, the fraction of the housing wall structure's inertial response was varied to determine its influence on the predicted duct wall temperature distribution. At 20 s beyond the start of the transient, the predicted results appear to agree best with the measured data if one assumes the sodium had soaked ~50% of the housing wall insulation's available pores.

Conclusions. A two-pin, two-region coolant subchannel model similar to the one proposed by Dunn apparently can be used to describe the intra-subassembly boiling incoherence that would be present in the two-phase tests to be conducted in THORS Bundle 9. Preliminary scoping calculations have indicated that the temperature-flow behavior of the central coolant channel is essentially independent of the influence of the duct wall inertial response. On the other hand, within the outer region of the bundle, the predicted duct wall temperature results agree best with the measured

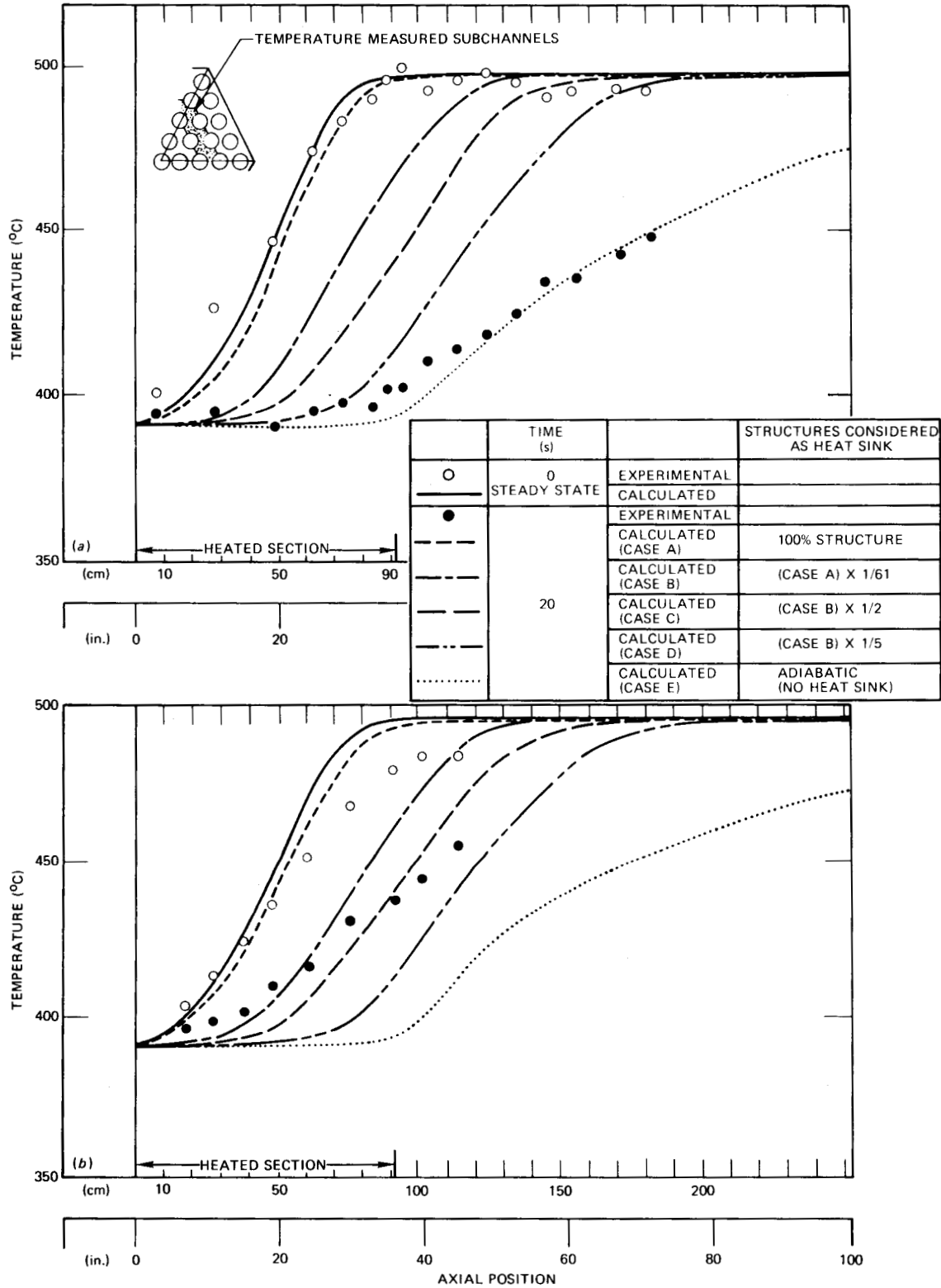


Fig. 1.14. Comparison between experimental data and calculations using SAS3D for (a) axial fluid and (b) duct-wall temperature distributions in Bundle 9 during Phase 1 Test 2, Run 8.

data if one assumes that the sodium had soaked ~50% of the housing wall insulation's available pores.

Future calculations will include coupling these two isolated channels through the SAS inlet plenum, while still assuming no heat and fluid cross-flow between channel one and channel two. These calculations will be followed by incorporation of a model similar to Dunn's to include channel-to-channel heat flow between the two voided regions.

1.1.4 Pretest analysis for Bundle 9 Phase 2, Part A testing
(J. F. Dearing)

Modifications to SABRE-2 (version dated June 1, 1978) for modeling THORS Bundle 9 Transient Tests. The following changes have been made to the SABRE-2 (Ref. 6) coding to allow accurate representation of THORS Bundle 9 transient testing:

1. A $K\rho V^2$ -type representation of frictional loss in the test section inlet valve has been included in the first axial node [V is the inlet subchannel sodium axial velocity and a value of $K = 12$ simulates the valve setting described in the Phase 2, Part A Test Plan (Sect. 1.1.1)]. Inclusion of this term is necessary to give proper system response for natural convection transients with constant cold-leg static-head pressure-drop boundary conditions.
2. Subroutine B9SRC (Bundle 9 Structural Radial Conduction) has been coupled to SABRE-2 to represent transient heat transfer from the edge subchannels to the duct wall and surrounding structure. A volume-averaged temperature of the edge subchannels is used as a boundary condition for the one-dimensional (radial) implicit finite-difference representation of conduction heat transfer in the structure. The B9SRC routine uses the tridiagonal form of Gauss elimination-back-substitution to solve for new structural temperatures and then calculates the linear heat transfer (W/m) from the structure to the edge subchannels, which receive equal volumetric power density.
3. The total subchannel heat source term S_I (W/m^3) is formed as the sum of the heat source from the internal structure (still calculated by

the original two-parameter model) and the heat source from the external structure (provided by B9SRC for edge subchannels, zero elsewhere). The expression for $\partial X/\partial t$ (Eq. 4.3.1, Ref. 6) is no longer valid — $\partial X/\partial t$ is now calculated as a finite difference.

4. Transverse thermal conduction through the boron nitride FPSs is modeled using the results of the analysis presented in Ref. 9. Specifically, the laminar component of Γ (Eq. 7.10, Ref. 10) is multiplied by an appropriate "shape conduction factor" (2.3 for the heated section, 1.5 in the SFGP). This correction is important for the low-flow tests analyzed here, because thermal conduction dominates transverse (radial) heat transfer.

Comparison of SABRE-2 results with Bundle 9 Phase 1 data. The one-twelfth-section model of Bundle 9 used in the SABRE-2 analysis is shown in Fig. 1.15. The SABRE-2 code calculates the transient three-dimensional pin bundle thermal hydraulics, while subroutine B9SRC calculates radial conduction heat transfer in the structure surrounding the pin bundle (radial nodes 9–16). Node 9 represents the 3.0-mm-thick stainless steel duct

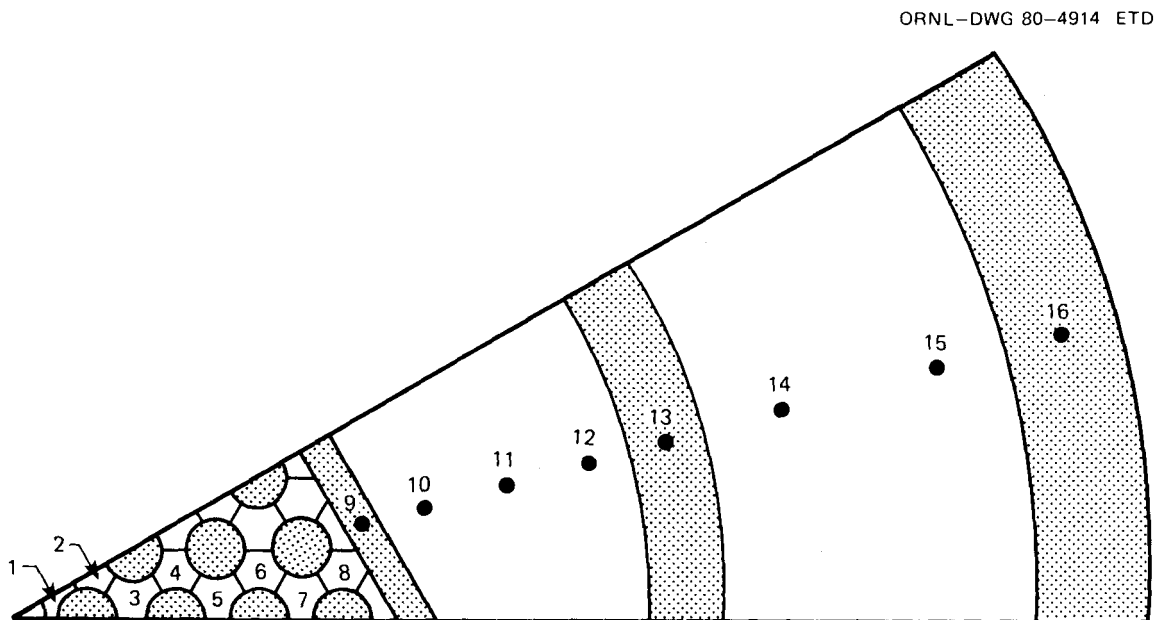


Fig. 1.15. One-twelfth-section model of THORS Bundle 9 showing radial nodalization used for radial temperature profiles.

wall; nodes 10, 11, 12, the thermal insulation (possibly sodium-soaked); node 13, the stainless steel containment; nodes 14 and 15, the sodium-filled annulus; and node 16, the Hastelloy outer housing.

The effects of wire wraps are modeled by making average corrections to subchannel areas and wetted perimeters and by using a value of 10 (as explained subsequently) for the SABRE turbulent mixing multiplier "FMIX." Default values of all other correlation parameters are used.

Figure 1.16 is a cross section of the heated section of Bundle 9 showing the location of two diametral traverses along which data are plotted. THORS wire-wrap thermocouple data and SABRE-2 results are plotted in Fig. 1.17 along these traverses at three axial locations, for the steady-state portion of Test 2, Run 8 (pin power = 1.0 kW, inlet velocity = 0.41 ms^{-1} , inlet temperature = 390°C).⁵ The SABRE results are symmetric about the bundle center, of course, because a one-twelfth section was used. The excellent comparison between code and data at these low flow conditions (~5% nominal) was made possible by including the transverse thermal conduction shape factors discussed in the previous section.

Figure 1.18 is similar to Fig. 1.17 except for the nominal flow conditions of Test 12 Run 101 (pin power = 20 kW, inlet velocity = 7.6 ms^{-1} , inlet temperature = 361°C).⁵ A value of 10 for the turbulent thermal mixing parameter FMIX was determined by comparison of code results and wire-wrap thermocouple data for this run. The radial and axial temperature profiles calculated by SABRE-2 are relatively insensitive to large variations in FMIX, probably because the coded correlation for turbulent thermal mixing gives results which are much too small for a wire-wrapped pin bundle. The value of FMIX used here is a "best estimate," which could be decreased or increased by a factor of 5 without significant deterioration of the comparison shown in Fig. 1.18.

After steady-state conditions were established in Test 2, Run 8, the power to the FPSs was cut and data were taken for ~70 s. Test 2 was designed to indicate the presence of sodium in the thermal insulation backing the duct wall by recording the change in response of pin bundle thermocouple instrumentation during a power-cut transient. This change was first noted in Run 8. In the SABRE-2 model the power was ramped to zero

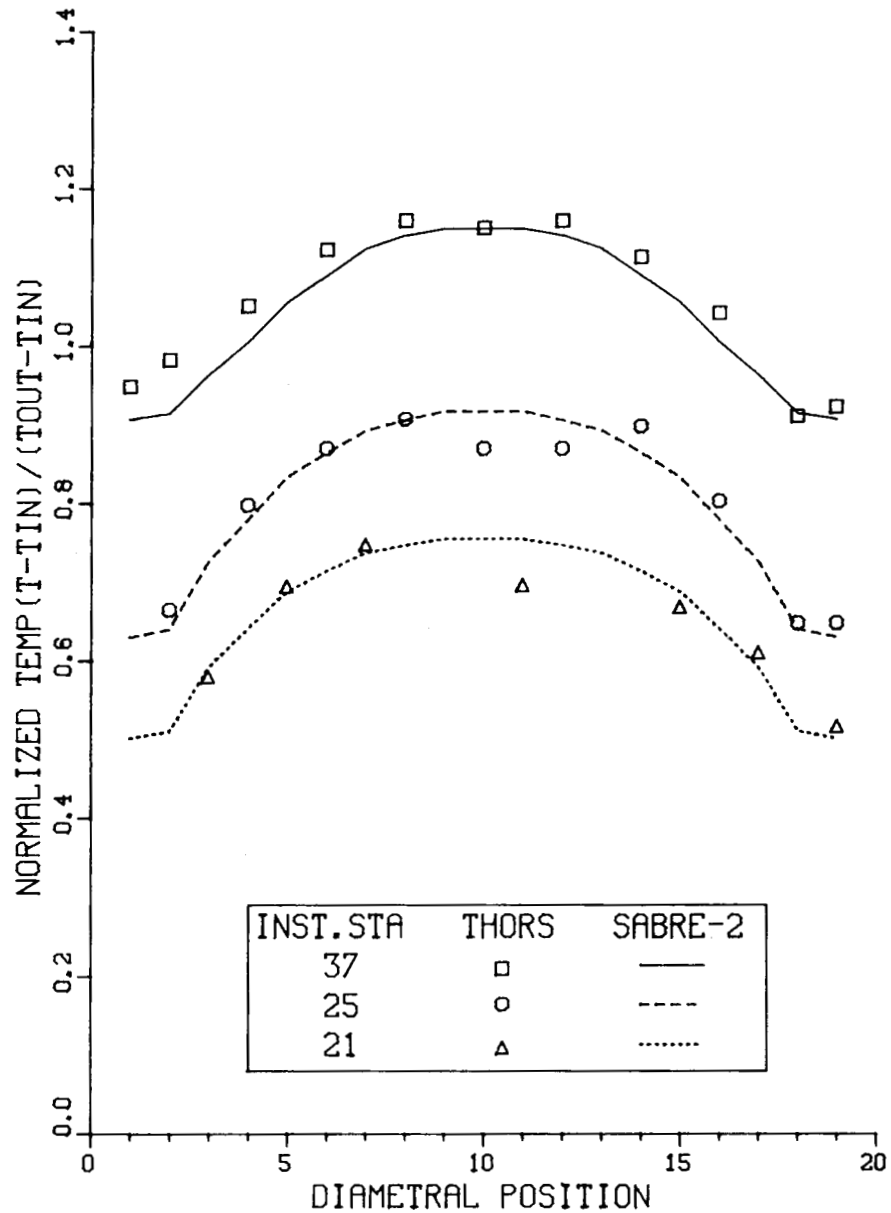


Fig. 1.17. Comparison of wire-wrap thermocouple data and SABRE-2 results at three diametral traverses for Test 2, Run 8 (pin power = 1.0 kW, test section inlet velocity = $0.41 \text{ m}\cdot\text{s}^{-1}$, test section inlet temperature = 390°C), THORS Bundle 9 Phase 1 Test Plan.

in the first second, and a constant pressure-drop boundary condition of 25.2 kPa was applied. Initially, natural convection is responsible for a significant fraction (~10%) of the test section flow; as the test section cools off, this fraction decreases, as shown by both inlet flowmeter data and SABRE-2 in Fig. 1.19 (power to FPSs cut at 28.5 s).

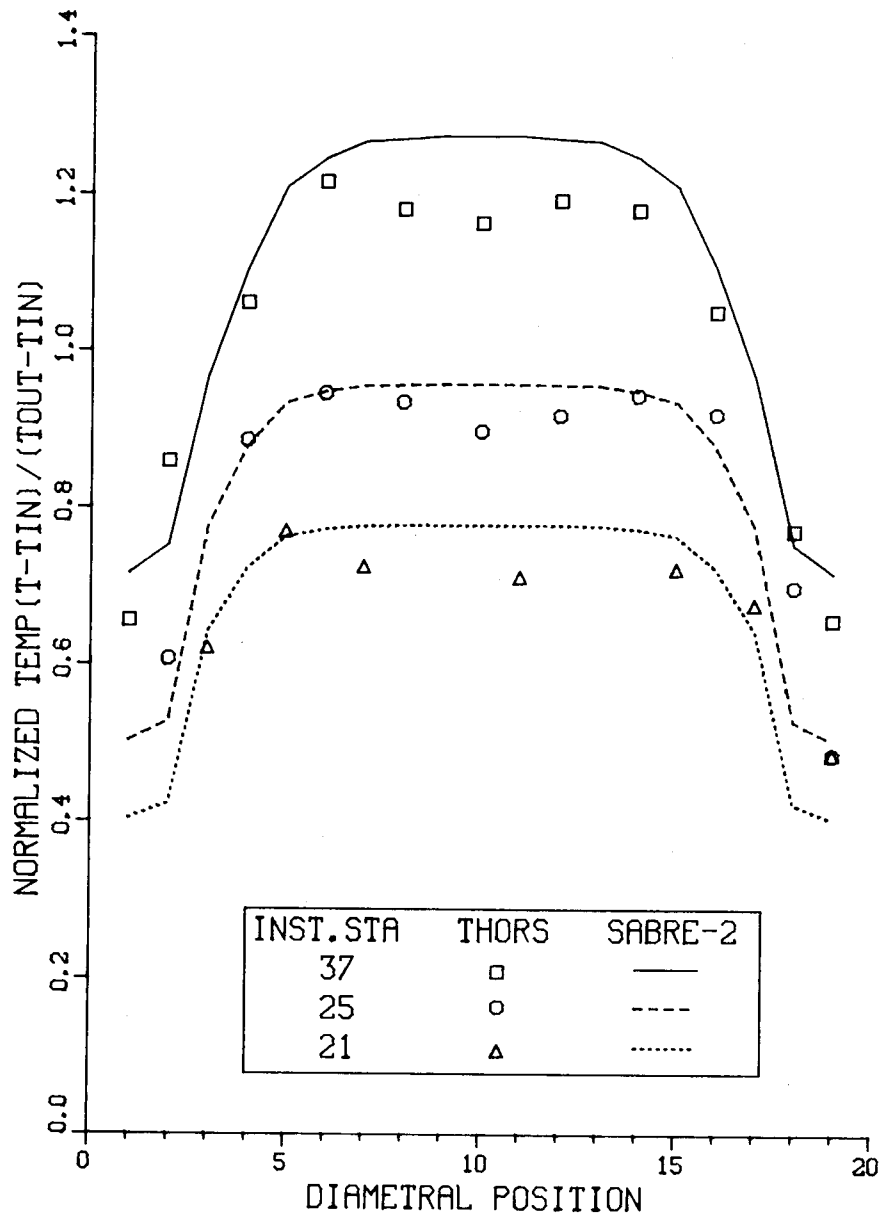


Fig. 1.18. Comparison of wire-wrap thermocouple data and SABRE-2 results at three diametral traverses for Test 12, Run 101 (pin power = 20 kW, test section inlet velocity = $7.6 \text{ m}\cdot\text{s}^{-1}$), test section inlet temperature = 361°C), THORS Bundle 9 Phase 1 Test Plan.

Axial temperature profiles at time zero (steady-state) and 20 s into the Test 2, Run 8 power-cut transient are shown in Fig. 1.20. Wire-wrap thermocouple data from the third subchannel ring are compared with SABRE-2 results in radial node 4 (see Fig. 1.15). The effective thermal conductivity of the sodium-soaked insulation was adjusted to 40% that of pure

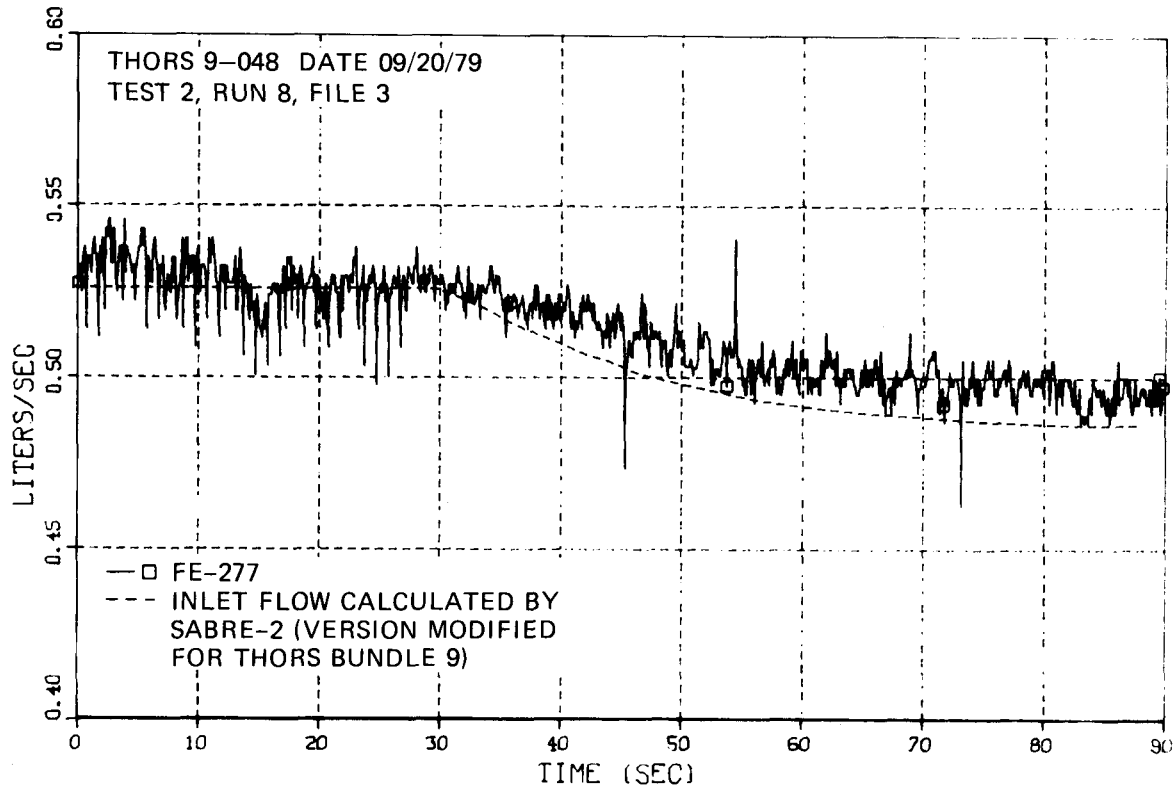


Fig. 1.19. Comparison of measured and computed test section inlet flow for Test 2, Run 8 (power-cut transient), THORS Bundle 9 Phase 1 Test Plan.

sodium to give the agreement shown here. (The value of 40% was also determined using the B92D two-dimensional model described in Ref. 11.)

Pretest analysis of natural convection Tests 202 and 203, THORS Bundle 9 Phase 2 Test Plan. Test 202, with a pin power of 3.1 kW, is the lowest-power test to be run in Phase 2 Part A. The sodium-soaked insulation is expected to have its largest effect here. Initial conditions are as follows: inlet temperature, 388°C; bulk outlet temperature, 704°C; and inlet flow, 0.55 liter·s⁻¹. At t = 0 s the EM pump is turned off. In the SABRE-2 model a constant cold-leg (elevation 2.63 m) static-head pressure drop of 22.16 kPa is then applied for the transient.

Figure 1.21 shows the SABRE-calculated inlet flow transient for cases of dry and sodium-soaked insulation. The flow rapidly falls to ~50% of its initial value in ~1 s, then slowly increases as the test section heats up. Note the change in time scale at 10 s.

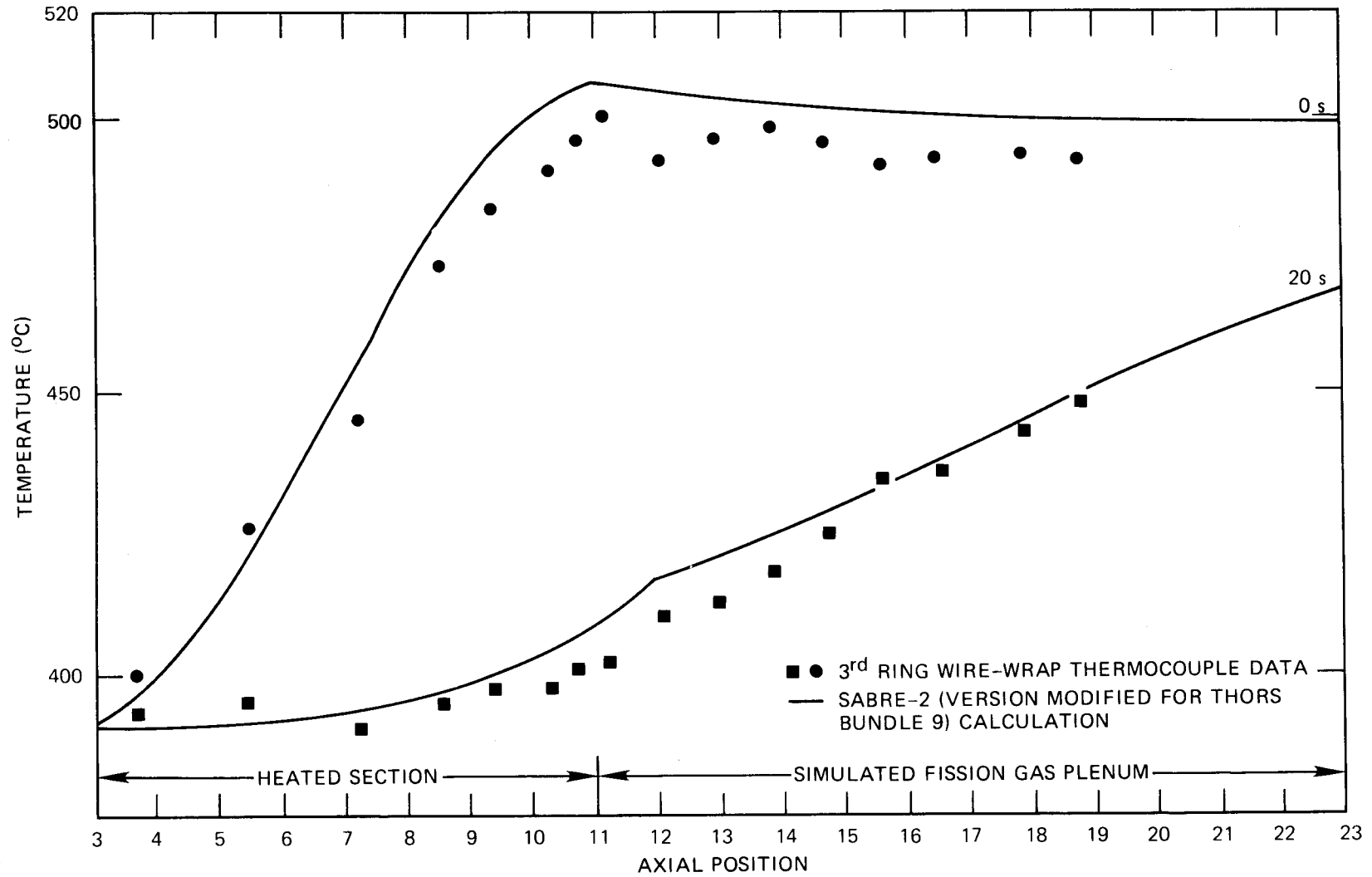


Fig. 1.20. Comparison of third-subchannel-ring wire-wrap thermocouple data with SABRE-2 results (radial node 4) at 0 and 20 s, Test 2, Run 8 (power-cut transient), THORS Bundle 9 Phase 1 Test Plan.

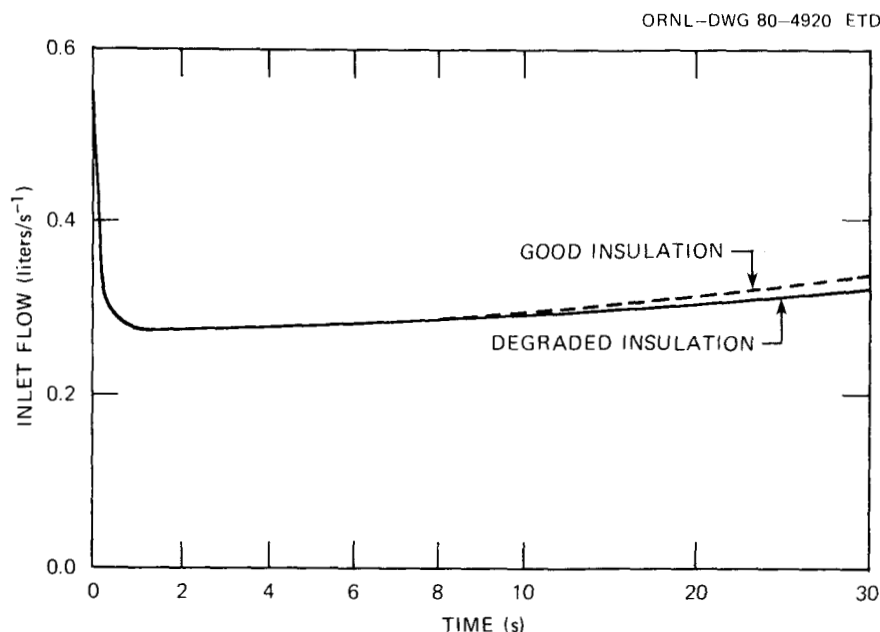


Fig. 1.21. Test section inlet flow computed by SABRE-2 for Test 202, THORS Bundle 9 Phase 2 Test Plan.

Figure 1.22 shows radial temperature profiles at 40 s at the end of the heated section. Both the "good" and "degraded" insulation cases slightly exceed expected saturation conditions near the center of the pin bundle.

Figure 1.23 (see Fig. 1.15 for location of radial nodes) shows the transient response of node 1 (bundle center) at the end of the heated section, again for both insulation cases. Both reach a maximum temperature at ~30 s, then fall off slowly as the inlet flow increases.

Figure 1.24 shows axial temperature profiles of node 1 at 0 s and 40 s; the degraded insulation case is lagging by ~50°C at the end of the fission-gas plenum.

Figure 1.25 shows subchannel axial flow redistribution caused by natural convection at 20 s at the end of the heated section. The flow in the central subchannels has decreased by only 70% of the decrease in the edge subchannels.

These figures indicate that the pin power in Test 202 (3.1 kW/pin) is close to the lower limit that will produce boiling under natural convection conditions in Bundle 9 (for the given initial conditions of test

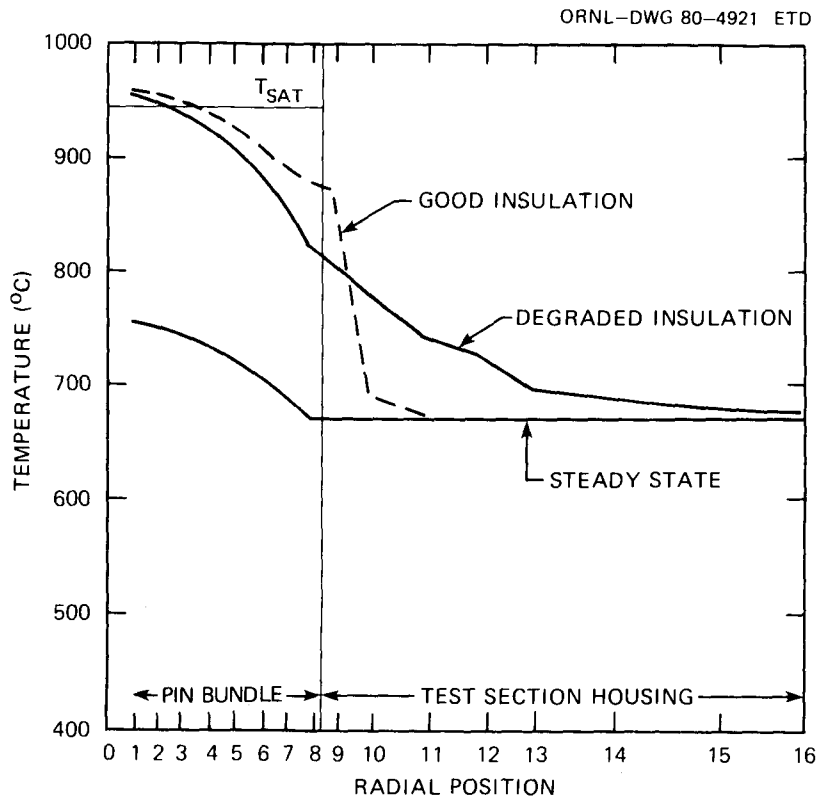


Fig. 1.22. Radial temperature profiles at end of heated section at 0 and 40 s in Test 202, THORS Bundle 9 Phase 2 Test Plan (calculated by SABRE-2).

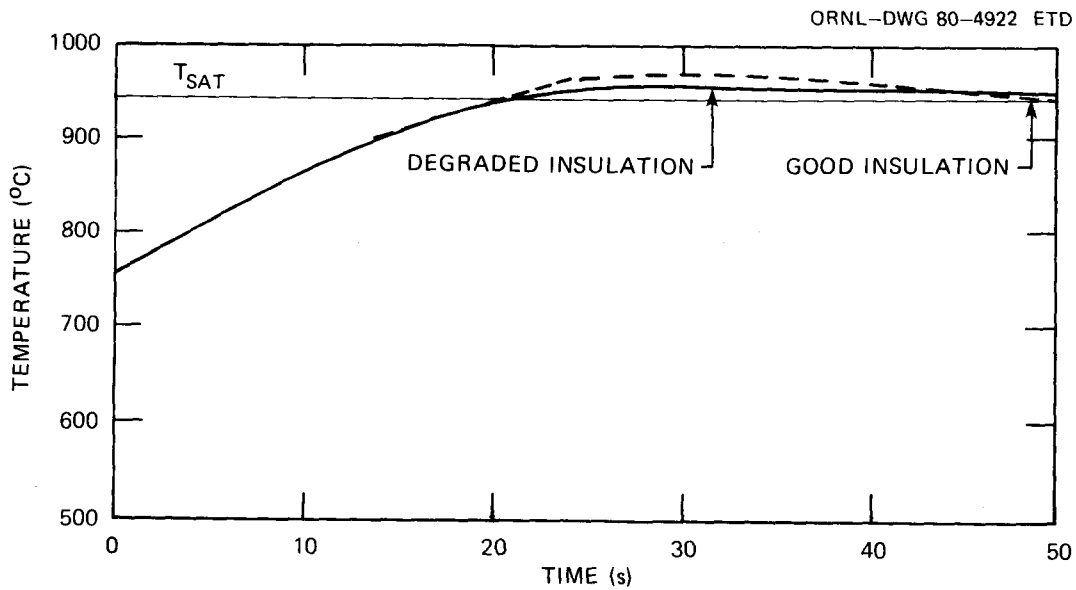


Fig. 1.23. Temperature transient in central channel at end of heated section for Test 202, THORS Bundle 9 Phase 2 Test Plan (calculated by SABRE-2).

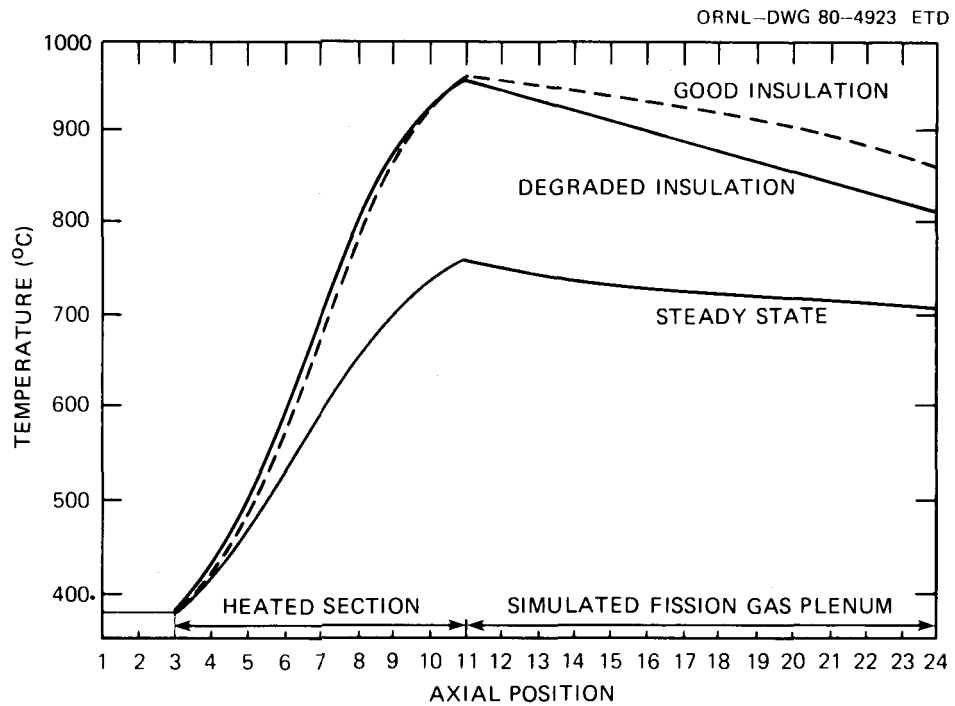


Fig. 1.24. Axial temperature profiles at 0 and 40 s in a central subchannel for Test 202, THORS Bundle 9 Phase 2 Test Plan (calculated by SABRE-2).

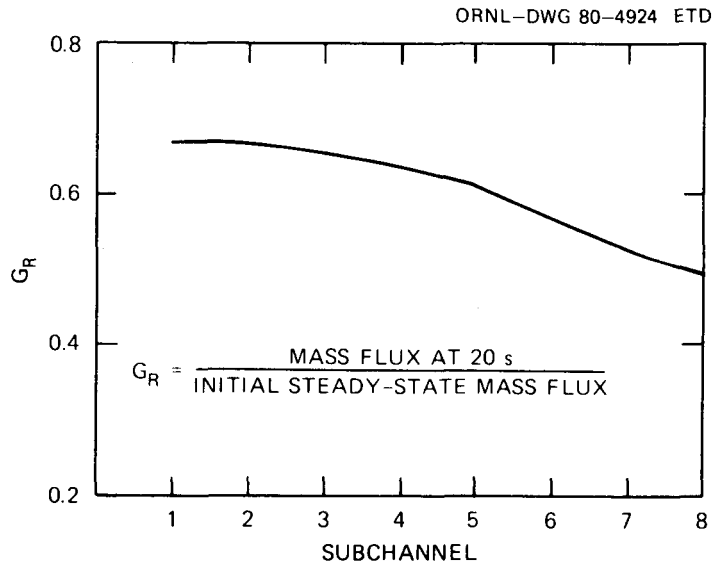


Fig. 1.25. Subchannel axial flow redistribution at end of heated section 20 s into Test 202, THORS Bundle 9 Phase 2 Test Plan (calculated by SABRE 2).

section inlet valve setting, test section inlet temperature, and bulk test section temperature rise.) Depending on superheat and local saturation conditions, boiling may not occur in Test 202. If it does, the boiling will probably be limited to a small region near the center of the bundle. The condition of the thermal insulation does not affect conditions near the expected boiling region very much, but it does affect the degree of subcooling in the edge subchannels and in the fission-gas plenum. The dynamic behavior of the boiling region is, of course, affected by this degree of subcooling.

Test 203 is the other natural convection transient to be run in Phase 2 Part A. Initial conditions are similar to Test 202, except that the pin power of 4.1 kW requires a test section inlet flow of $0.73 \text{ liter}\cdot\text{s}^{-1}$ to obtain the same bulk outlet temperature (704°C).

Test section outlet flow and temperature at the end of the heated section (at the bundle center and edge) are shown in Fig. 1.26 as a function of time from the power cut to the EM pump. SABRE-2 predicts that the flow will drop rapidly to $\sim 40\%$ of its initial value and then slowly recover as the test section heats. Saturation conditions should be reached near the center of the pin bundle at $\sim 10 \text{ s}$. The condition of the bundle insulation makes only a small difference in the temperature of the edge subchannels at that time.

Figure 1.27 shows radial temperature profiles at the end of the heated section at 0, 10, and 20 s after the power cut to the EM pump in Test 203. By 20 s, boiling should be occurring in most of the interior subchannels and should be much more violent than boiling in Test 202. Results from this single-phase model become less meaningful as the voiding dynamics alter the subchannel flow distribution, as they certainly will between 10 and 20 s.

1.1.5 Bundle 9 Phase 1 record of experimental data (R. H. Morris and W. R. Nelson)

The Bundle 9 Phase 1 Record of Experimental Data report has undergone coauthor and peer review and is in the final stages of preparation.

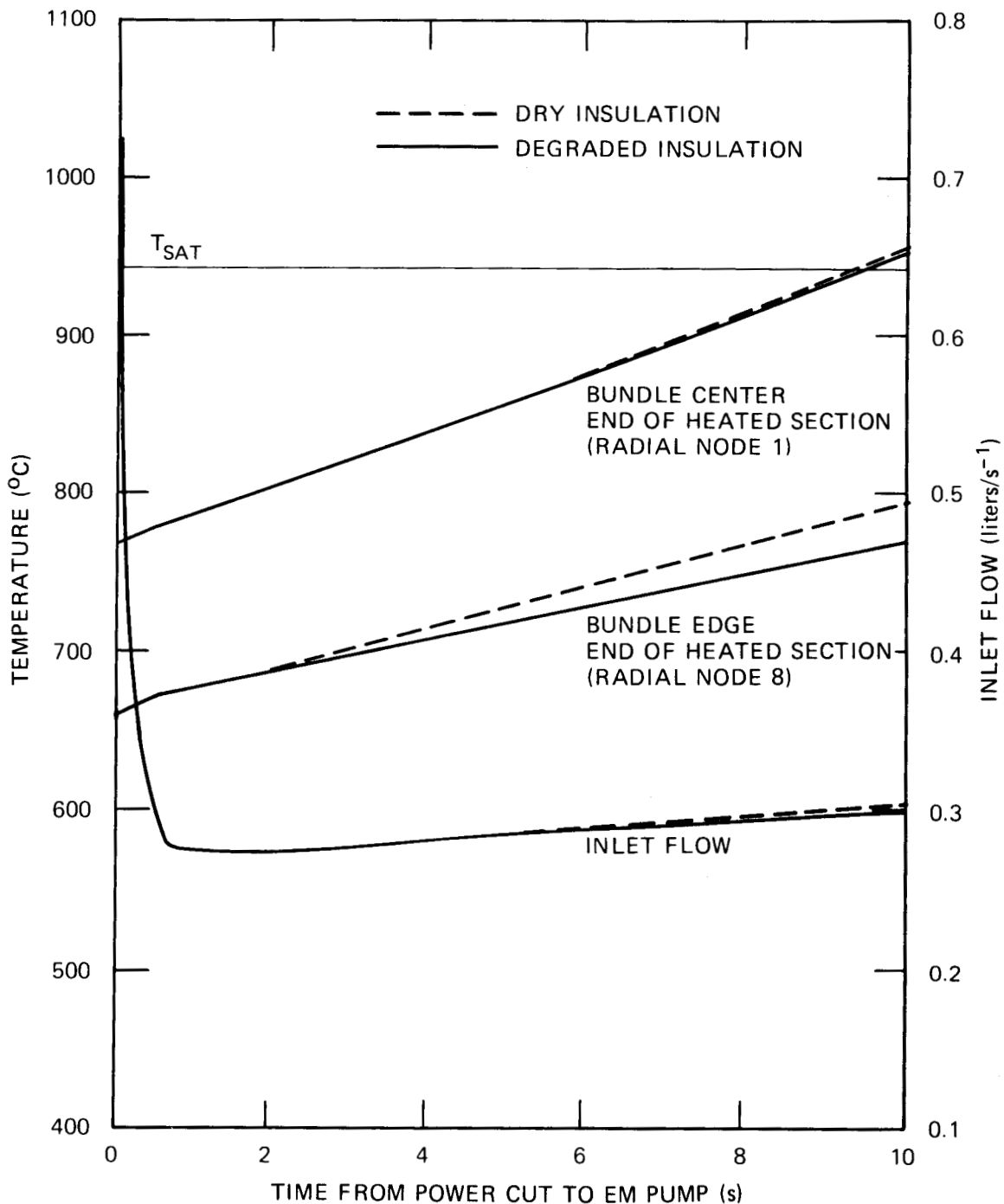


Fig. 1.26. Test section inlet flow and temperatures in a central and an edge subchannel at end of heated section as a function of time for Test 203, THORS Bundle 9 Phase 2 Test Plan (calculated by SABRE-2).

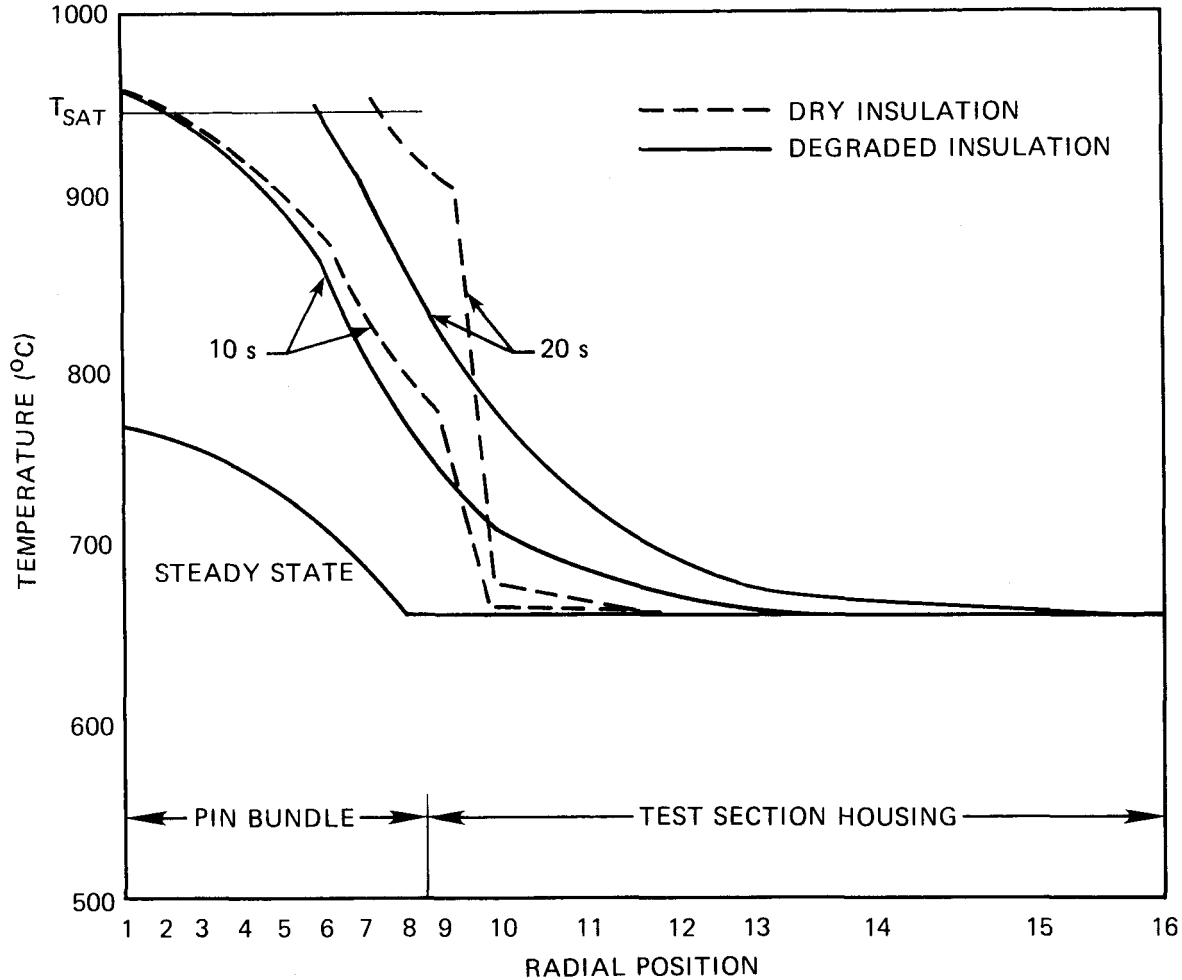


Fig. 1.27. Radial temperature profiles at 0, 10, and 20 s at end of heated section for Test 203, THORS Bundle 9 Phase 2 Test Plan (calculated by SABRE-2).

1.1.6 Bundle 9 bypass flow split analysis (G. A. Klein, K. Haga, and P. W. Garrison)

Because the LMFBR coolant inlet plena are closed, voiding in the core can lead to counteracting pressure buildup in the inlet plenum, which retards the rate at which voiding progresses downward through the core. Another result of this pressure buildup in one group of subassemblies is an increase in coolant flows through the nonvoiding subassemblies, or through the bypass assemblies. The PRIMAR-2 module has been written for the SAS3A and SAS3D LMFBR accident analysis code to treat these inlet plenum hydraulic coupling effects.

The model used in PRIMAR-2 is illustrated in Fig. 1.28. A single equivalent loop is treated. The loop contains pipes, a pump, and an intermediate heat exchanger (IHX). The test section and bypass have a common inlet plenum and a common outlet plenum. The initial exit pressure, $p_x(t = 0)$ is specified by the user, who also specifies the initial coolant flows $G_c(t = 0)$ for the heated core channel and the fraction f_c of the total flow that goes through the core channels. The rest of the flow goes through the bypass channel:

$$A_{bp} G_{bp}(t = 0) = \left(\frac{1 - f_c}{f_c} \right) \sum_i A_c(i) G_c(i, 1, t = 0) .$$

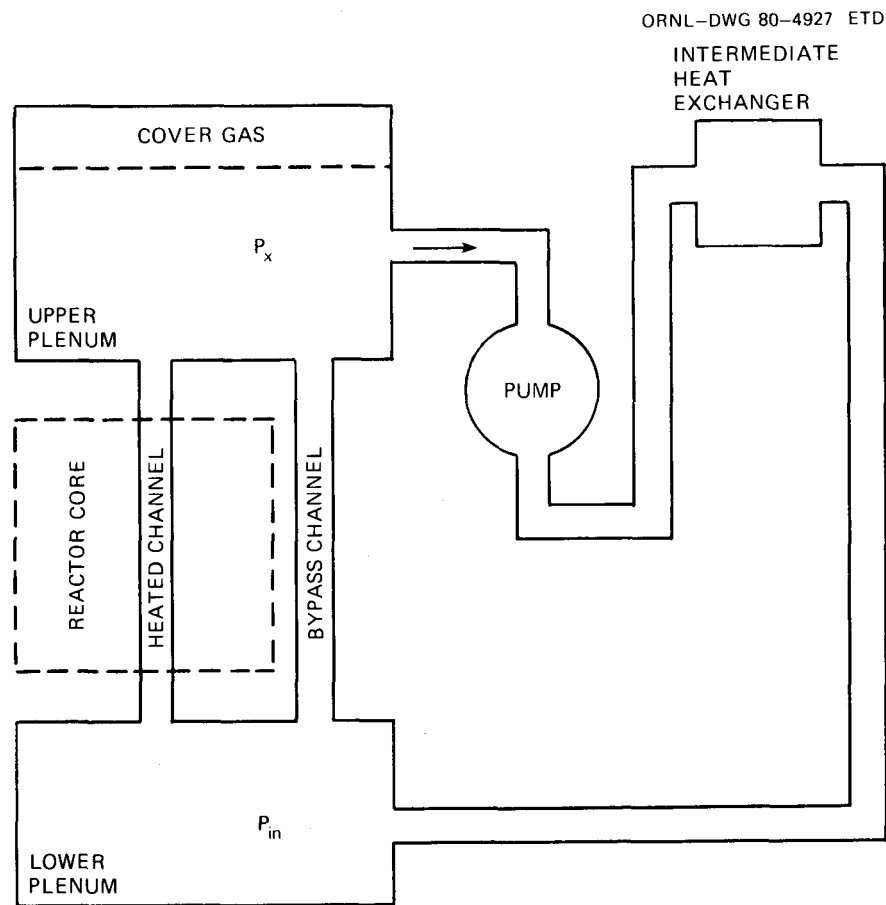


Fig. 1.28. Primary coolant loop model used in the PRIMAR-2 module (written for the SAS LMFBR accident code).

With the simple pump treatment used in PRIMAR-2, the relative location of the pump in the loop is irrelevant, and the only relevant aspect of the location of the IHX is the height Z_{IHX} of its thermal center. The steady-state coolant dynamics module calculates the inlet plenum pressure $p_{in}(t = 0)$ from the exit pressure and core channel flows. The bypass orifice coefficient k_{bp} is adjusted to make the steady-state bypass channel pressure drop equal to the core channel pressure drop. The loop flow is set to the sum of the core flow plus bypass flow. The pump head term is calculated at steady state from a balance between the loop and test section pressure-drop terms. The time-dependence of this term, $\Delta P_p(t) = \Delta P_{po} f_p(t)$, varies approximately as the square of the normalized coolant flows $[f_p(t) \propto \{\dot{m}(t)/\dot{m}(t = 0)\}_{TS}^2]$, and the function $f_p(t)$ is obtained from a user-supplied table.

Using the above SAS coolant-dynamics model, the influences of variations in the bypass-to-test-section flow ratios were examined. In anticipation of the results of this study, a large bypass in parallel with the test section would be expected to behave hydrodynamically as if a fixed pressure-drop boundary condition were imposed across the heated test section. As the bypass-to-test-section flow ratio decreases, this situation would correspond to a flow-vs-time boundary condition across the test section, with an expected corresponding decrease in the predicted amplitude of the flow oscillations. This type of behavior was observed experimentally in a comparison of 5:1 and 10:1 flow-split tests performed for Bundle 6A.² Test 71H, Run 101 corresponds to a 5:1 flow split. The operating conditions for these two tests are shown in Table 1.2. Table 1.3 shows a comparison of the amplitude and period of the flow oscillations for each of these two test cases. In agreement with these expected trends, the amplitude of the flow oscillations appears to decrease with a decrease in the bypass-to-test-section flow ratio, while the period remains unchanged.

A reduction in the amplitude of the flow oscillations is physically significant. Following the onset of voiding, a thin liquid film is assumed to be left covering the vertical surfaces. For large voids in an annular flow regime, the film is assumed to move in an axial direction;

Table 1.2. Comparison of 5:1 and 10:1 flow-split tests

Condition	Results		Comparison
	61A-101 5:1	71H-101 10:1	
Power, kW	129	129	} Same
Flow at boiling inception, liter/s	0.11	0.11	
Test section inlet temperature, °C	383	387	
Time at start of transient, s	0.0	0.0	} Same
Time at boiling inception, s	11.0	11.0	
Time at partial dryout, s	34.8	26.8	
Time at power-flow scram, s		36.8	
Time at normal flow increase, s	38.0		

Table 1.3. 5:1 vs 10:1 results

	5:1	10:1	Comparison
<u>Test section flow oscillations</u>			
Frequency, c/s			
11-16 s	2.8 ^a	2.6 ^a	Note: Frequencies approximately same at boiling inception and at partial dryout.
16-21 s	1.9	1.8	
21-26 s	1.4	1.3 _b	
26-31 s	1.2 _b	1.3 ^b	
31-36 s	1.2 ^b	1.9	
Amplitude (peak-to-peak), gpm			
11-16 s	4.0 ^a	7.6 ^a	Note: Amplitude for 10:1 is consistently higher at boiling inception and at partial dryout.
16-21 s	4.8	6.8	
21-26 s	3.2	4.3 _b	
26-31 s	2.5 _b	1.9 ^b	
31-36 s	1.5 ^b	3.4	
<u>Bypass flow oscillations</u>			
Frequency: Same as for test section flow			
Amplitude, gpm			
11-16 s	3.7 ^a	6.0 ^a	Note: Bypass flow oscillation amplitudes have consistently lower magnitudes than test section flow amplitudes.
16-21 s	3.7	5.1	
21-26 s	3.7	2.0 _b	
26-31 s	2.0 _b	1.3 ^b	
31-36 s	0.8 ^b	2.5	

^aBoiling inception.^bPartial dryout.

thus, the liquid film can be removed both by evaporation and by film motion dominated by the shear stress generated at the liquid vapor interface. As the slug returns, its liquid mass is deposited as film on the pin surface with which it comes in contact. Upon further film motion, this newly deposited liquid film can then replenish the liquid film in the neighboring downstream region. The deeper the penetration of the re-entering upper and lower liquid slugs into the voided region, the greater will be the deposition of liquid film on the pin surface, and this is expected to result in a delay in the time to dryout. Thus, as the amplitude of the flow oscillations increases, with an increase in the bypass flow ratio between Test 71H, Run 101 and Test 61A, Run 101, a delay in the time to dryout would be expected. This trend is not exhibited in the measured dryout times of the two tests, indicated in Table 1.2. The reason for this discrepancy appears to be that identical steady-state conditions were not achieved throughout the entire radial extent of the sodium-soaked insulation surrounding the duct wall. Thus, the inertial responses of the duct walls were different for the two tests. Test 71H, Run 101 exhibited a much more rapid duct wall response than did Test 61A, Run 101, as shown in Figs. 1.29(a and b). The result was an increase in the measured time to dryout for Test 71H, Run 101 and an inconsistency in the expected results.

In performing the flow-split tests outlined in Table 1.2, the bypass valve was set to achieve the desired flow split prior to coastdown of the prescribed initial flow. An examination of the isothermal and heated-test data for both the 5:1 and 10:1 flow-split tests indicates that the flow split does not remain constant throughout the transient, but tends to redistribute itself in the following manner. For the isothermal flow tests, the bypass-to-test-section flow ratio increases substantially as shown in Table 1.4; however, for the heated tests, this ratio remains fairly constant, increasing slightly for Test 61A, Run 101, while decreasing slightly for Test 71H, Run 101. Because the magnitude of this flow split may be different in the Bundle 6A and Bundle 9 test results, the SAS3A program was used to examine the nature of this flow split for the Bundle 9 test flow conditions. Two isothermal runs representing a 5:1 and a 10:1 flow split were made with the SAS3A program. The results of the study for the

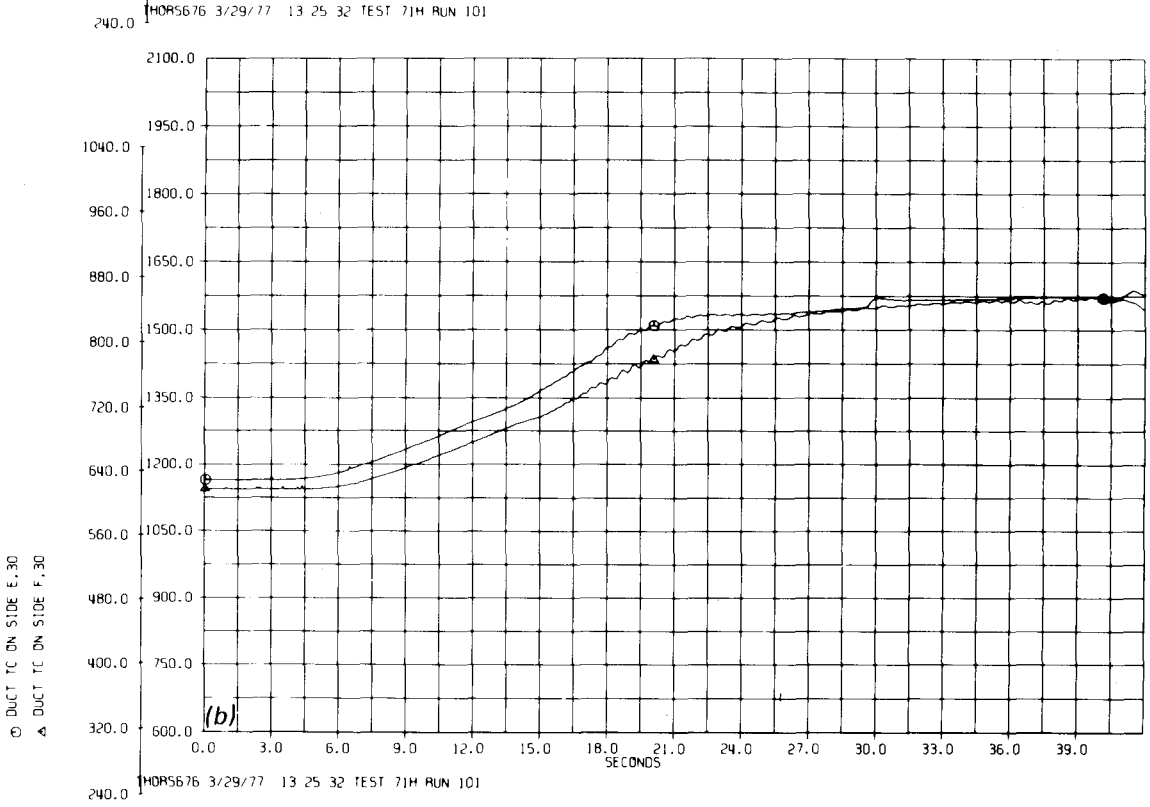
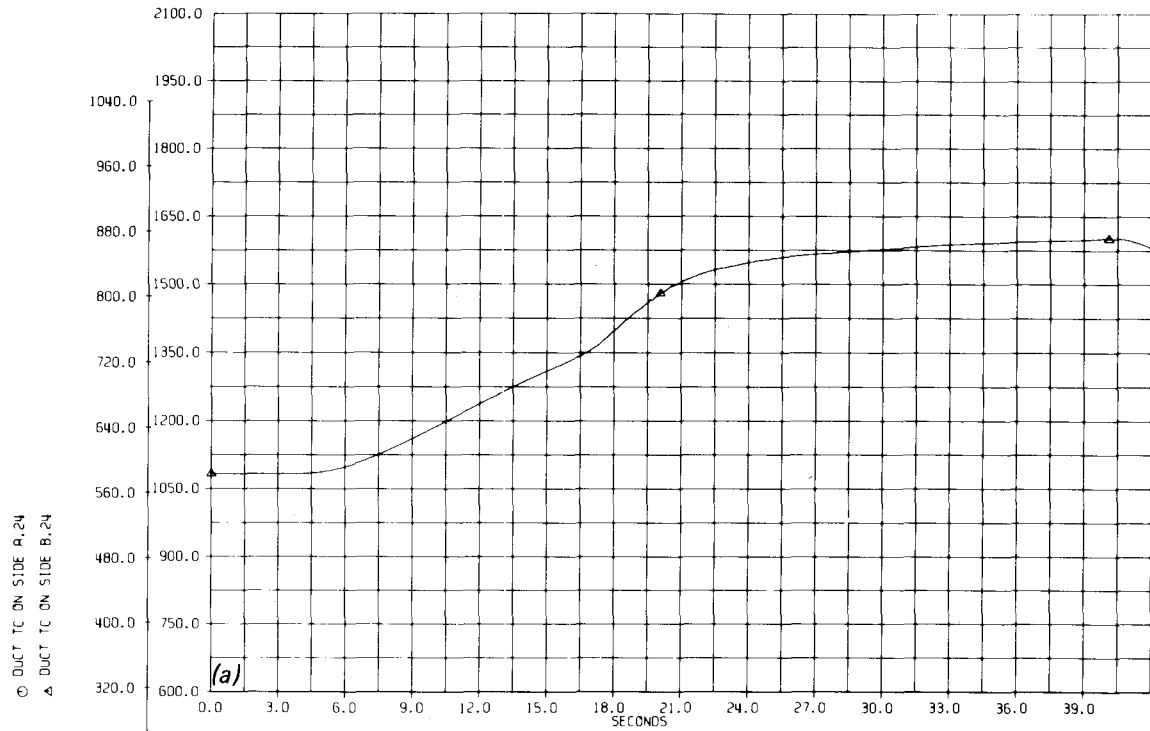


Fig. 1.29. Thermocouple temperature traces for thermocouples located (a) on side B.24 and (b) on sides E.30 and F.30, THORS Test 71H, Run 101.

Table 1.4. Flow-split data as measured in THORS

Test	Power (kW)	\dot{w}_{TS} (liters·s ⁻¹)	\dot{w}_{bypass} (liters·s ⁻¹)	R_1^a	\dot{w}_{TS} (liters·s ⁻¹ minimum)	\dot{w}_{bypass} (liters·s ⁻¹ minimum)	R_2^b
61A-100	0	0.36	2.21	6.2	0.07	0.69	10
61A-101	130	0.38	2.13	5.6	0.11	0.68	6.4
71-100	0	0.32	3.34	10.6	0.06	1.02	16
71H-101	130	0.39	4.04	10.4	0.11	0.96	8.9
71-100A	0	0.28	3.12	11.0	0.07	1.01	14.6

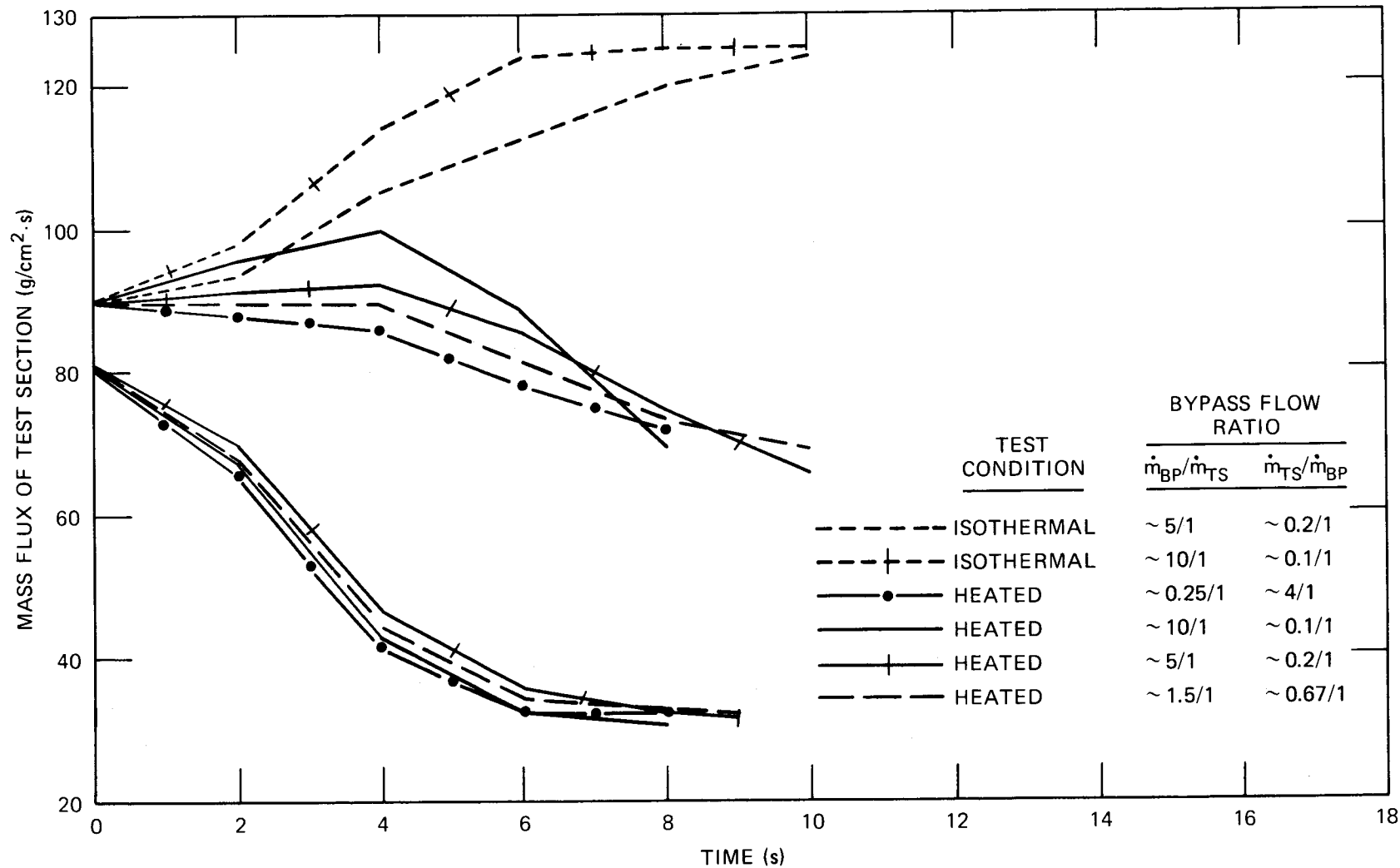
$$\alpha_{R_1} = \frac{\dot{w}_{bypass}}{\dot{w}_{TS}} \Bigg|_{\text{maximum flow value}}$$

$$b_{R_2} = \frac{\dot{w}_{bypass}}{\dot{w}_{TS}} \Bigg|_{\text{minimum flow value}}$$

isothermal case indicate a 16.5% increase in the bypass flow ratio at boiling inception for the 5:1 initial bypass/test section test case and a 17.5% increase in the bypass flow ratio at boiling inception for the 10:1 initial bypass/test section test case. These results are in agreement with the measured trends for the Bundle 6A data. The above analysis was repeated for the heated test conditions outlined in the Bundle 9 test plan for Test 204 (analogous to Bundle 6A Test 71H, Run 101 power flow conditions) for four different bypass flow ratios: 10:1, 5:1, 1.5:1, 0.25:1. In all cases, the ratio of bypass-to-test-section flow decreased by ~10%. The results of this analysis are shown in Fig. 1.30(a). Because the magnitude of the flow split just prior to boiling inception is expected to have a definite influence on the amplitude of the flow oscillations and measured time to dryout, in modeling the Bundle 9 two-phase flow transients the flow split must be properly satisfied at the low-flow test condition just prior to boiling inception.

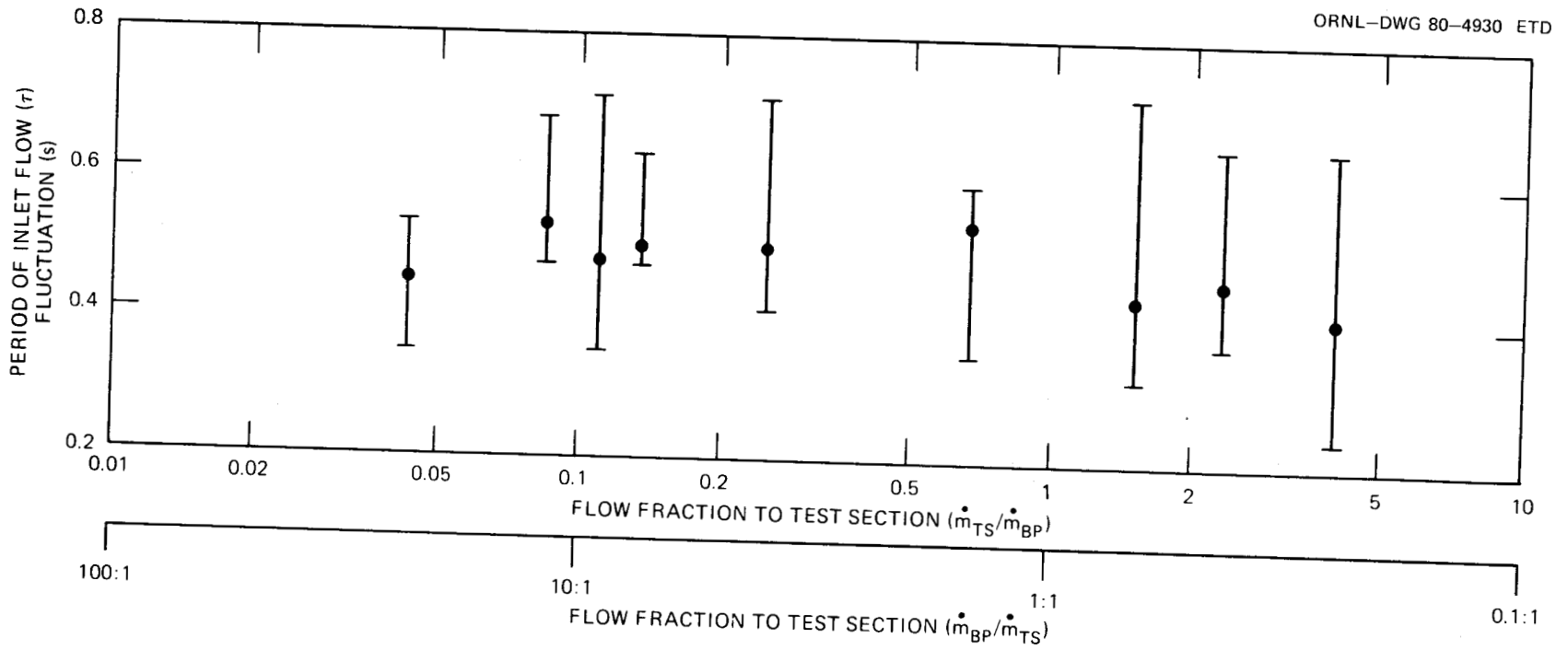
The influence of these variations in the bypass-to-test-section flow ratios were examined further using the SAS coolant dynamics model. To ensure that only the influence of the magnitude of the bypass flow ratio on the time to dryout was being examined in this study, the flow transient prior to boiling, which was predicted to occur at the inlet to the test section, was required to be approximately the same for all cases examined, as shown in Fig. 1.30(b). This was consistent with the requirement that the time to boiling inception be identical upon change in the bypass flow ratio. When these conditions are present, the interaction between the bypass and the voided test section, leading to changes in the pressure buildup in the inlet plenum with resultant enhancement or delay in the voiding process, can be examined. As shown in Fig. 1.31, no detectable trend appears in the predicted period of the flow oscillations; thus, the period of the flow oscillations essentially seems to remain unchanged, in agreement with the measured results from the Bundle 6A flow-split tests. Figure 1.32, however, indicates a decrease in the predicted amplitude of the flow oscillations with a decrease in the bypass flow ratio. This decrease becomes significant for flow ratios less than ~4.5:1.

As previously indicated, the greater the amplitude of the flow oscillations, the deeper the penetration of the reentering upper and lower



1-66

Fig. 1.30. (a) Change in normalized bypass flow ratio: $\{R^* = [\dot{m}_{BP}/\dot{m}_{TS}(t)]/[\dot{m}_{BP}/\dot{m}_{TS}(t=0)]\}$ with time during transient, (b) inlet mass flux vs time prior to boiling inception.



1-67

Fig. 1.31. Effect of flow-split ratio on period of inlet flow fluctuation.

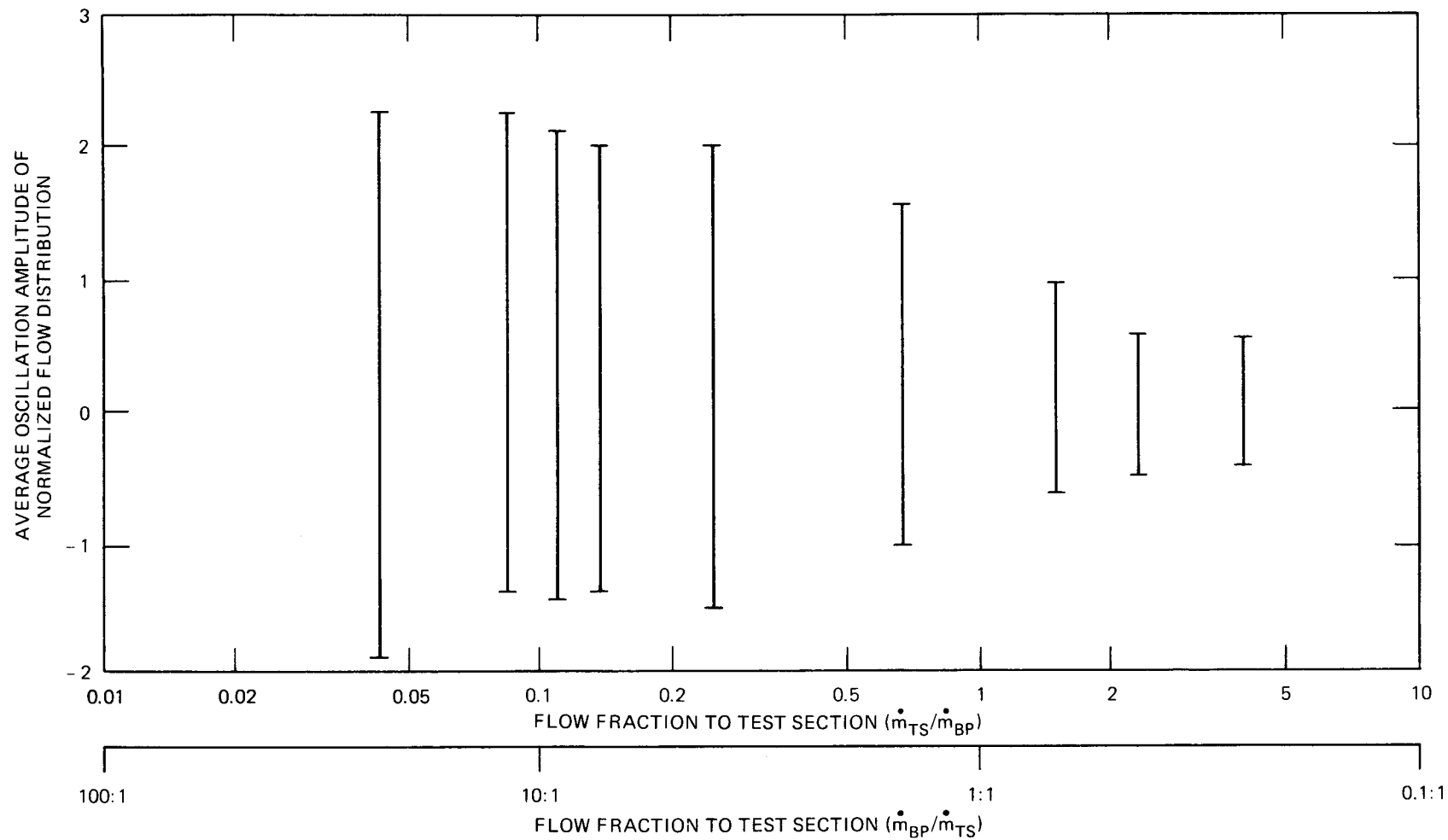


Fig. 1.32. Effect of flow-split ratio on inlet flow fraction amplitude.

liquid slugs into the voided region. This correlation can be seen in Figs. 1.33 and Fig. 1.34, which show the bubble axial interface locations with time since the start of vapor formation for bypass/test section flow ratios of 10.0/1.0 and 0.25/1.0 respectively. The liquid film will thus be replenished further into the voided zone, in accordance with the bypass flow ratio, with a resulting delay in time to dryout. Figure 1.35 shows both the time to boiling and time to dryout minus time to boiling for each of the bypass flow ratios examined. The plotted results on this figure are consistent with the trends outlined above. As the bypass flow ratio decreases beyond a value of $\sim 4.5:1$, the time to dryout consistently decreases. Thus, ensuring flow ratios greater than this value in the Bundle 9 test series would be preferable. For part A of the two-phase flow test series, this bypass ratio limit apparently cannot be attained. To

ORNL-DWG 80-4932 ETD

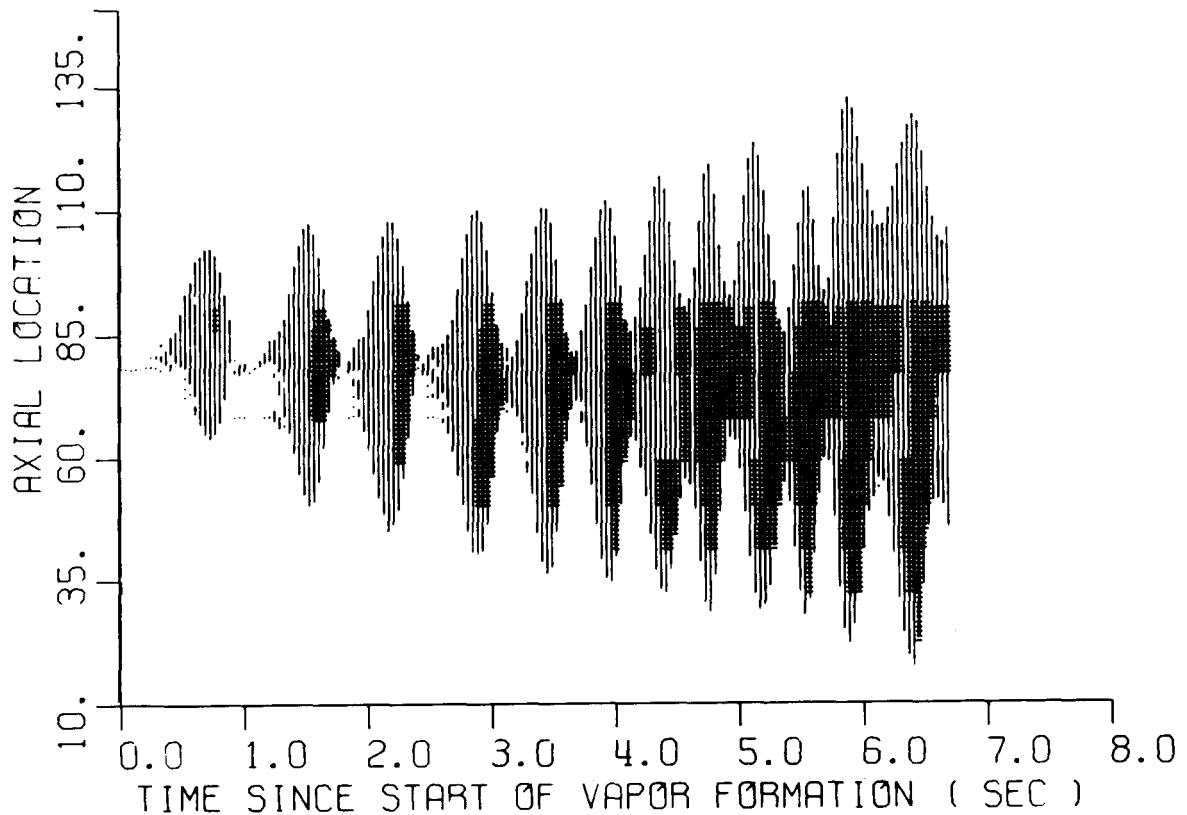


Fig. 1.33. Bubble axial interface locations with time since start of vapor formation for bypass-to-test-section flow ratio of 10:1.

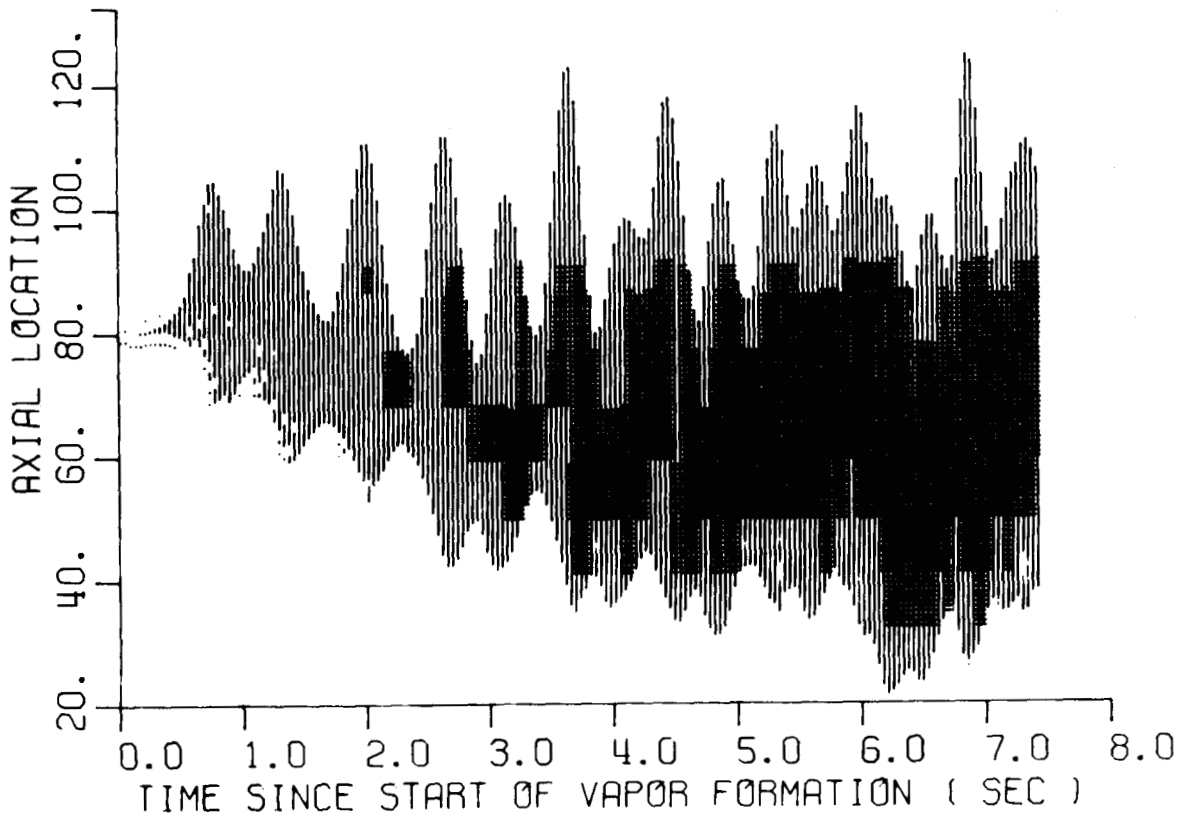
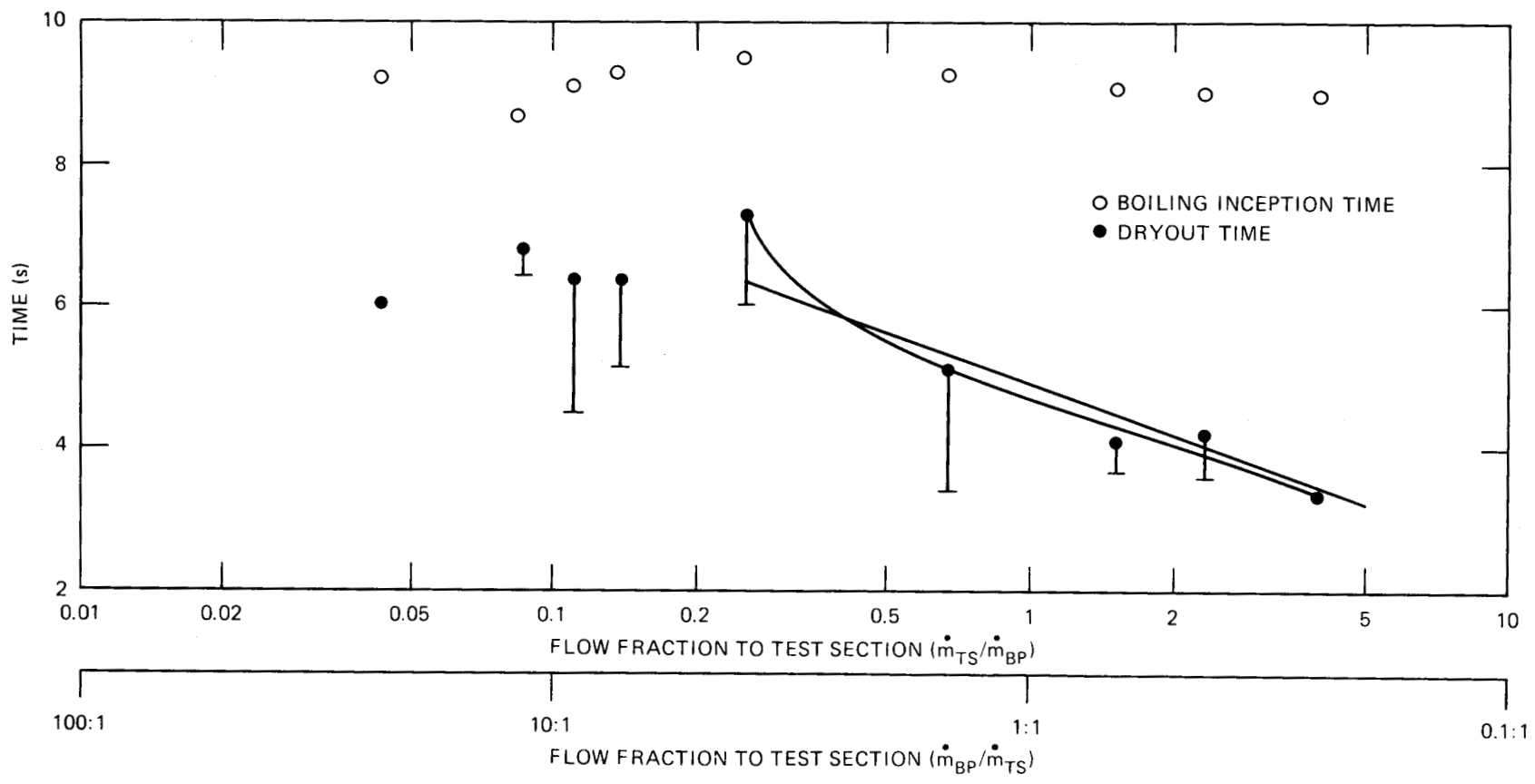


Fig. 1.34. Bubble axial interface locations with time since start of vapor formation for bypass-to-test-section flow ratio of 0.25:1.

determine what impact this has on the measured data, a bypass flow ratio of 3:1 will be examined. The results of Fig. 1.35 indicate that this reduction in the flow split will increase the time to dryout anywhere from 0.4 to 1.2 s. As the bypass flow ratio drops to 1.5:1, an increase of over 2 s in the predicted time to dryout occurs.

With an increase in bypass flow ratio, the period of the flow oscillations remains unchanged, but the amplitude of the flow oscillations decreases sharply with a decreasing ratio, for values of the test-section-to-bypass flow ratio less than $\sim 4.5:1$. In keeping with this trend, the time to dryout minus the time to boiling decreases rapidly for bypass flow ratios less than the above value, for the Bundle 9 geometry. Thus, it would have been preferable for the THORS loop to maintain a bypass ratio greater than 5:1, which corresponds to the low flow portion of a heated transient, to produce measured results consistent with an infinite bypass



1-71

Fig. 1.35. Effect of flow-split ratio on boiling inception and dryout times.

in parallel with the heated test section. However, the only result of a flow split of 3:1 appears to be an increase in the time to dryout ranging from 0.4 to 1.2 s.

1.2 THORS Fabrication and Operation

B. H. Montgomery

1.2.1 Test facility operation

The THORS facility was shut down following completion of the Bundle 9 Phase 1 Test Program for installation of the EM pump and expansion tank. This modification has been completed, and initial checkout has begun. The facility has operated for a total of 29,359 h, with 2,423 h at varying levels of power up to 1.2 MW. The operating history of the THORS facility is summarized in Table 1.5.

1.2.2 Test bundle

Bundle 9, a 61-pin full CRBR-length bundle, is now installed in the facility. This is the largest bundle tested to date in the THORS facility; its design is discussed in Ref. 12, and pictures of the bundle assembly are shown in Refs. 13 and 14.

The test program for this bundle has been divided into two parts: Phase 1, single-phase thermal-hydraulic tests, and Phase 2, boiling tests with transient flow and power. The Phase 1 Test Program has been completed. In preparation for Phase 2 testing, modifications to the facility were required.

A new expansion tank has been installed in the system to simulate the upper reactor plenum during the boiling tests. Because of operating problems that would be caused by the presence of two liquid-gas interfaces in the Phase 2 THORS piping configuration, an EM pump capable of supplying $40 \text{ liters} \cdot \text{s}^{-1}$ (600 gpm) at 1.4 MPa (200 psi) head has been installed in parallel with the centrifugal sodium pump, which will be valved out of the system when the EM pump is in use. Figure 1.36 is a schematic diagram of the facility, and Fig. 1.37 is an isometric drawing of the facility for the Phase 2 boiling tests.

Table 1.5. THORS operating experience

Bundle identification	Duct configuration	Number of heated pins	Blockage configuration	Heated length (mm)	Fission gas simulators	Isothermal operation (h)	Operation with power (h)
1A	Scalloped (bare edge rod)	19	None	610	No	1,300	200
2A	Hex (full-size edge gaps)	19	None	533	No	3,010	470
2B	Hex (full-size edge gaps)	19	13 and 24 channel inlet				
1B	Scalloped (bare edge rod)	19	None	610	No	894	350
3A	Scalloped (wrapped edge rods)	19	6 channel in heated zone	533	No	3,039	151
3B ^{a, b}	Scalloped (wrapped edge rods)	19	6 channel in heated zone	533	No	537	51
5A, 5B, 5C	Hex (half-size edge gaps)	19	12 channel ^c edge gap	457	No	3,252	391
5D ^a	Hex (half-size edge gaps)	19	None	457	No	2,827	97
6A ^d	Hex (half-size edge gaps)	19	None	914	FFTF length	7,864	380
3C ^e	Scalloped (wrapped edge rods)	31 ^f	6 channel in heated zone	533	FFTF length	3,666	190
9	Hex (full-size edge gaps)	61	None	914	CRBR length	2,970	143
						29,359	2,423

^aBoiling tests (with and without gas injection).

^bBoiling tests included 45 s with full bundle (heater 7 opened during boiling test with gas injection) and 11 min, 15 s with rod 7 inoperative; 10 min, 16 s of this time was continuous (without gas injection).

^cA 12-channel edge blockage flush with duct for Bundle 5A, flush followed by 0.36-mm displacement for 5B, removed for 5C.

^dThirty-eight tests were run in which boiling occurred; five of these runs were to dryout (unstable) conditions; total boiling time for the bundle was ~11.5 min.

^eTwenty-four tests were run in which boiling occurred; total boiling time for the bundle was ~10 min.

^fA major modification of Bundle 3B, this was a 19-pin bundle surrounded by 12 heated edge pins replacing the scalloped duct configuration of Bundle 3B.

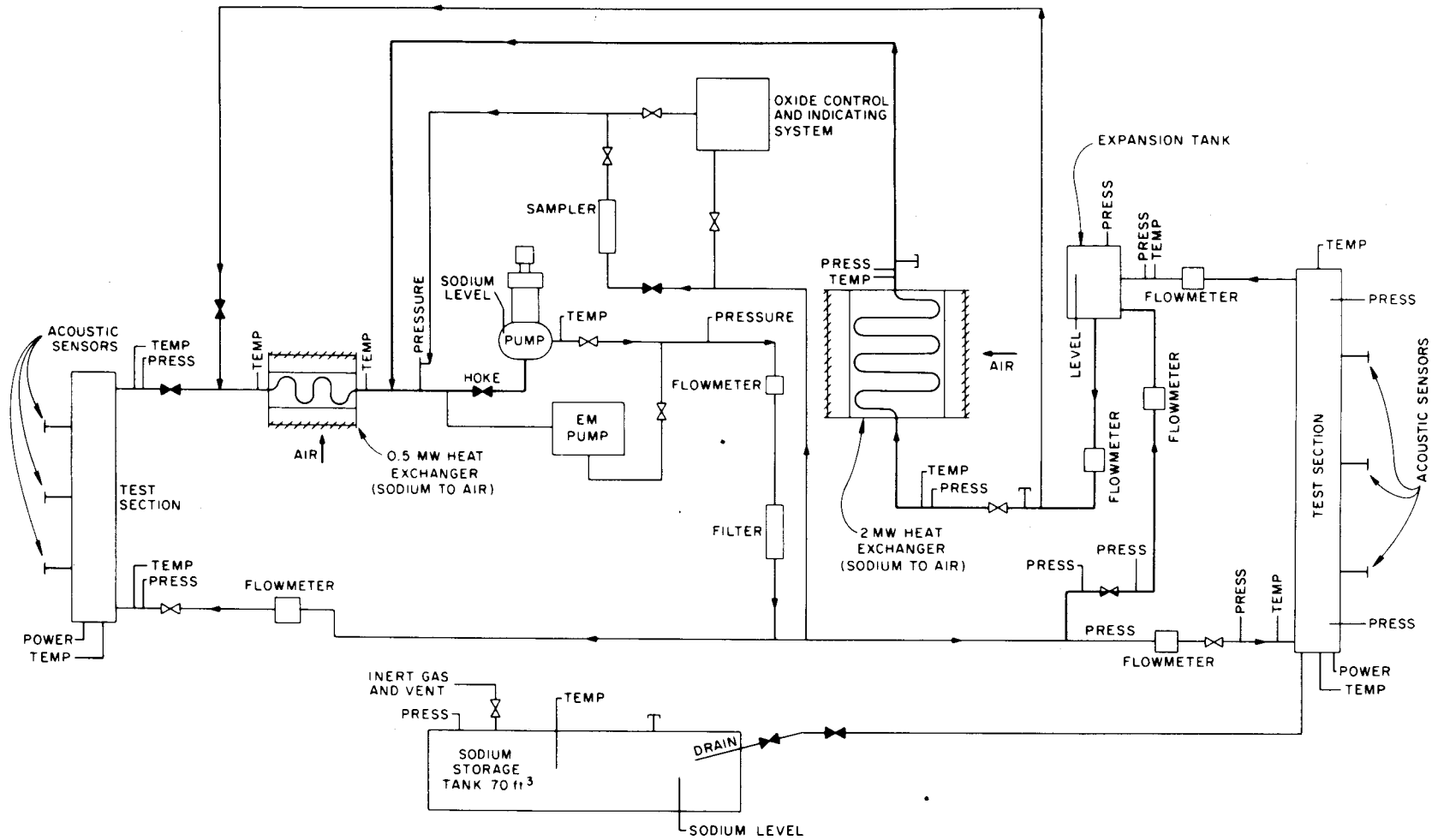


Fig. 1.36. Schematic diagram of THORS facility for Bundle 9 flow transient and boiling tests.

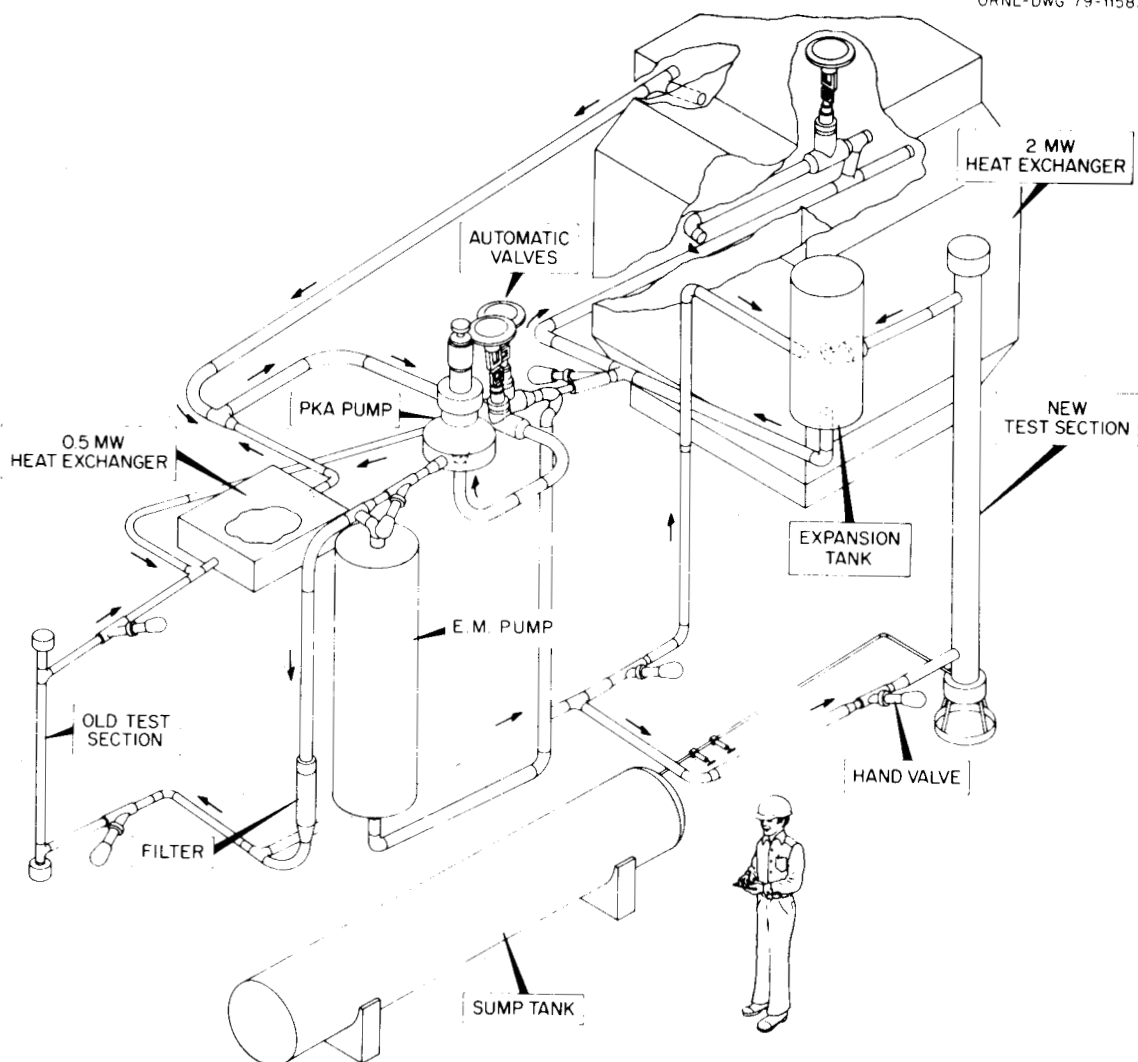


Fig. 1.37. Isometric drawing of THORS facility for Bundle 9 flow transient and boiling tests.

A bypass line with a 13-mm (1/2-in.) flowmeter has been added at the test section inlet to permit more accurate measurement of lower test section inlet flows. With the bypass line in operation, the 89-mm (3.5-in.) flowmeter will be valved out of the system.

An additional manually operated damper has been added to the 2-MW heat exchanger outlet air duct to aid in finer control of cooling air flow under natural convection conditions. The hydraulic operator for the vanes in the inlet air duct has been replaced with an electric drive unit to enable more precise positioning.

The system has been charged with sodium, and a preliminary shakedown has begun. The EM pump acceptance tests were completed during this initial shakedown, and the pump flow and head proved to be more than adequate for the facility requirements. Bundle 9 Phase 2 testing will begin following this checkout.

1.3 Reports and Major Correspondence Issued

THORS Bundle 9 Phase 1 Data Transmittal (to WARD).

J. F. Dearing, *Analysis of Steady-State Data from a 19-Pin Internally Guard Heated Simulated LMFBR Fuel Assembly (THORS Bundle 3C) Using the COBRA and SABRE Subchannel Analysis Codes*, ORNL/TM-6963, February 1980.

R. J. Ribando, "Comparison of Numerical Results with Experimental Data for Single-Phase Natural Convection in an Experimental Sodium Loop," Specialists' Meeting on Decay Heat Removal and Natural Convection in FBRs, Upton, Long Island, NY, Feb. 28-29, 1980.

M. H. Fontana, Letter to D. E. Ferguson, FRSTMC, "THORS SHRS Test Program - Options," February 20, 1980.

1.4 Important Meetings

THORS staff members attended a FRSTMC Topical Meeting on Shutdown Heat Removal Systems held at ORNL on January 15, 1980.

Breeder Reactor Safety Program principal investigators met with Charles Larson (GE) Jan. 17, 1980, in preparation for his assignment as U.S. LMFBR Representative to Japan.

P. W. Garrison and G. A. Klein attended the Specialists' Meeting on Decay Heat Removal and Natural Convection in FBRs, Upton, Long Island, NY, Feb. 28-29, 1980.

R. H. Morris attended a Measurement Systems Dynamics Short Course, Phoenix, Ariz., Mar. 17-21, 1980.

References

1. M. H. Fontana and J. L. Wantland, *LMFBR Safety and Core Systems Programs Progress Report for January-March 1977*, ORNL/TM-5940.
2. R. J. Ribando et al., *Sodium Boiling in a Full-Length 19-Pin Simulated Fuel Assembly (THORS Bundle 6A)*, ORNL/TM-6553, January 1979.
3. J. L. Wantland et al., "Sodium Boiling Incoherence in a 19-Pin Wire-Wrapped Bundle," *Proceedings of the International Meeting on Fast Reactor Safety, August 19-23, 1979*, Seattle, Wash., vol. IV, p. 1678.
4. D. S. Rowe, *COBRA III-C: A Digital Computer Program for Steady State and Transient Thermal-Hydraulic Analysis of Rod Bundle Nuclear Fuel Elements*, BNWL-1965, Battelle Northwest Laboratories, Richland, Wash., 1973.
5. M. H. Fontana, *ORNL Breeder Reactor Safety - LOA 2, 3, 4 and 5 Quart. Technical Prog. Rep. for January-March 1979*, ORNL/TM-6947.
6. J. D. Macdougall, *SABRE 2: A Computer Program for the Calculation of Transient Three Dimensional Flows in Rod Clusters*, AEEW-R1104, United Kingdom Atomic Energy Authority, July 1978.
7. F. E. Dunn, personal communication to G. A. Klein, ORNL, September 1978; Subject: Multiple-Pin Model Used in SAS3D for P-2 Analysis.
8. J. F. Dearing, personal communication to G. A. Klein, Mar. 4, 1980; Subject: Pretest Analysis of Test 202, THORS Bundle 9 Phase 2 Test Plan.
9. M. H. Fontana and J. L. Wantland, *ORNL Breeder Reactor Safety Quart. Technical Prog. Rep. July-September 1979*, ORNL/TM-7229.
10. R. Potter, *SABRE 1 - A Computer Program for the Calculation of Three-Dimensional Flows in Rod Clusters*, AEEW-R1057, United Kingdom Atomic Energy Authority, February 1979.
11. M. H. Fontana and J. L. Wantland, *ORNL Breeder Reactor Safety Quart. Technical Prog. Rep. October-December 1979*, ORNL/TM-7301.
12. M. H. Fontana, *LMFBR Safety and Core Systems Prog. Rep. April-June 1976*, ORNL/TM-5699.
13. M. H. Fontana and J. L. Wantland, *Breeder Reactor Safety and Core Systems Programs Prog. Rep. January-March 1978*, ORNL/TM-6439.
14. M. H. Fontana and J. L. Wantland, *Breeder Reactor Safety and Core Systems Programs Prog. Rep. July-September 1978*, ORNL/TM-6698.



ORNL/TM-7348
Part 2
Dist. Category UC-79,
-79e, -79p

ORNL BREEDER REACTOR SAFETY — LOA 3
QUARTERLY TECHNICAL PROGRESS REPORT
FOR JANUARY—MARCH 1980

M. H. Fontana G. F. Flanagan

AG 10 20 41 3

Task 02 — ORNL LOA 3 Tasks: Analytical
Models for Energetics Accommodation

OBJECTIVE

To develop and validate the technology base for analytical tools required to achieve LOA 3 goals for capabilities to predict the probability of containment-damaging energetics from postulated core meltdown accidents through the use of generalized perturbation methods for assessment of safety calculation sensitivity to input parameters and through analysis of disrupted NRC criticals using transport and diffusion methods.

Any further distribution of this report is the responsibility of the recipient of the data.
The information contained herein is preliminary and tentative and is subject to change without notice.
This report is the property of the Department of Energy.

NOTICE: This document is an internal report of the Breeder Reactor Program and is preliminary and tentative. It is subject to change without notice and therefore does not represent a final report.

Prepared by the
OAK RIDGE NATIONAL LABORATORY
Oak Ridge, Tennessee 37830
operated by
UNION CARBIDE CORPORATION
for the
DEPARTMENT OF ENERGY



ORNL BREEDER REACTOR SAFETY — LOA 3
QUARTERLY TECHNICAL PROGRESS REPORT
FOR JANUARY—MARCH 1980

ABSTRACT

Final work on an adjoint code for the single-phase portion of MELT is complete, and documentation is near completion.

2. TASK 02 — ORNL LOA 3 TASKS: ANALYTICAL MODELS
FOR ENERGETICS ACCOMMODATION

G. F. Flanagan C. V. Parks
P. J. Maudlin

The purposes of this project are to develop and to validate the technology base of analytical tools required to achieve LOA-3 goals for predicting the probability of containment-damaging energetics from postulated core meltdown accidents through the use of generalized perturbation methods for assessing safety calculation sensitivities to input parameters.

During January, the final discrepancies between the adjoint sensitivity coefficients and the forward perturbed coefficients were resolved. These discrepancies arose from an inadequate handling of the pressure coupling that exists between the reactor channels in loop flow. Proper handling of this coupling in MELTADJ resulted in a channel coupling in the adjoint hydraulics. All sensitivity coefficients for the power trace sample problem now show two-digit agreement with those obtained from perturbing the forward code. A summary which presents the adjoint coupled thermal-hydraulic equations and the sensitivity coefficients for the power trace problem has been submitted for the ANS meeting in Las Vegas.

During validation of the coupled neutronic/thermal-hydraulic problem, a change in the module used for solving the adjoint point kinetics equations became necessary. The QXCHIP module being used was having numerical problems caused by the time-dependent source term. A standard ordinary differential equation solver that uses Gear's method has now been incorporated into MELTADJ and has presented no numerical problems.

Work is near completion on two journal articles that will thoroughly describe the MELT adjoint work and its significance in heat transfer and reactor analysis. One paper, to be submitted to *Nuclear Technology*, describes the work with MELT. The other paper, to be submitted to the ASME *Journal of Heat Transfer*, provides an adjoint sensitivity theory for the general three-dimensional, time-dependent, nonlinear thermal-hydraulic equations.

Work with the adjoint steady-state portion of MELT has also been completed, and documentation is being written.



ORNL BREEDER REACTOR SAFETY — LOA 4
QUARTERLY TECHNICAL PROGRESS REPORT
FOR JANUARY—MARCH 1980

ABSTRACT

Additional experimental data were obtained for the oxidation behavior of alternate advanced FBR fuels. Finely powdered (Th,U)C and UC ignited spontaneously on exposure to air, but ThC did not. Negligible entrainment of solid oxidation products in the combustion gases occurred for the experimental conditions used. A mass spectrometer for combustion-gas analysis was received. Preparations were completed for publication of a report on the environmental effects of tritium releases. A progress report reviewing accomplishments on a subcontract during FY 1979 on modeling release of radioactivity from a thorium ore pile was received from Colorado State University.

3. TASK 03 — ORNL LOA 4 TASKS: ENVIRONMENTAL
ASSESSMENT OF ALTERNATE FBR FUELS

V. J. Tennery	H. R. Meyer
E. S. Bomar	P. S. Rohwer
R. G. Donnelly	J. E. Till

Experiments to determine the oxidation characteristics of the ThC-based FBR fuels were nearly completed during this quarter. Samples weighing ~40 mg were oxidized in two temperature modes, isothermally and at a constant heating rate, while the sample mass was measured (thermogravimetric analysis). A second series of samples weighing ~2 g each was oxidized in a small tube furnace while being heated at essentially a constant heating rate. Information sought in these experiments included (1) oxidation rate as a function of temperature, composition of the atmosphere, and sample particle size; (2) products of oxidation; (3) susceptibility of the fuel to spontaneous ignition; and (4) extent of particle entrainment in the exhaust gases. In addition to the alternate FBR fuels ThC and (Th,U)C, samples of UC were also oxidized for comparison.

A graphic analysis of the data obtained from the thermogravimetric analysis experiments shows that the time-dependence of the fraction of sample oxidized is best described by a model in which the kinetics are

controlled by nucleating and growth of the oxidation product on the original fuel. Further data from some additional experiments were required to complete the analyses, and these experiments are being completed. Afterward, the activation energy for the oxidation process for each fuel will be obtained.

Additional experiments with 2-g samples of UC and ThC showed little difference in the behavior of -325 mesh powders on exposure to air as compared with 21% O₂-Ar. Uranium carbide and (Th,U)C ignite spontaneously on exposure to either of these atmospheres, whereas the ThC must be heated to nearly 250°C before ignition occurs.

Attempts to recover information about the amount of entrained particles from the oxidation process by means of slides taken from the cascade impactor were unsuccessful. Reproducible weights could not be obtained with a microbalance because of nonreproducible residual electrostatic charge on the glass slides. Alpha spectrometry was used as an alternative method of analyzing the deposits on several slides removed from the impactor. Less than 1 µg of thorium or 1 µg of uranium was carried over and deposited on individual slides at a gas flow rate of 0.017 liter/s through the oxidation furnace. This is the limiting flow rate through the impactor for a furnace atmosphere pressure of 0.101 MPa. Deposits on filter papers positioned below the last stage of the impactor also contained ~1 µg of thorium or uranium.

The long-delayed mass spectrometer, which was purchased for use in measuring the real-time composition of gaseous fuel combustion products resulting from oxidation of the advanced FBR fuels, was received in February. However, prior to shipment, the digital-display mass identifier module had malfunctioned and had been removed for repair. The repaired module was received March 24. Checkout of the spectrometer by the manufacturer's representative, to ensure that it meets specifications, must be completed before the instrument can be placed in service.

A major effort this quarter was applied to final preparation for publication of the report entitled *Tritium - Analysis of Key Environmental and Dosimetric Questions*, by J. E. Till et al., ORNL/TM-6990. Review comments have been addressed. The report will be published in April 1980.

Several papers were submitted for oral presentation or publication.

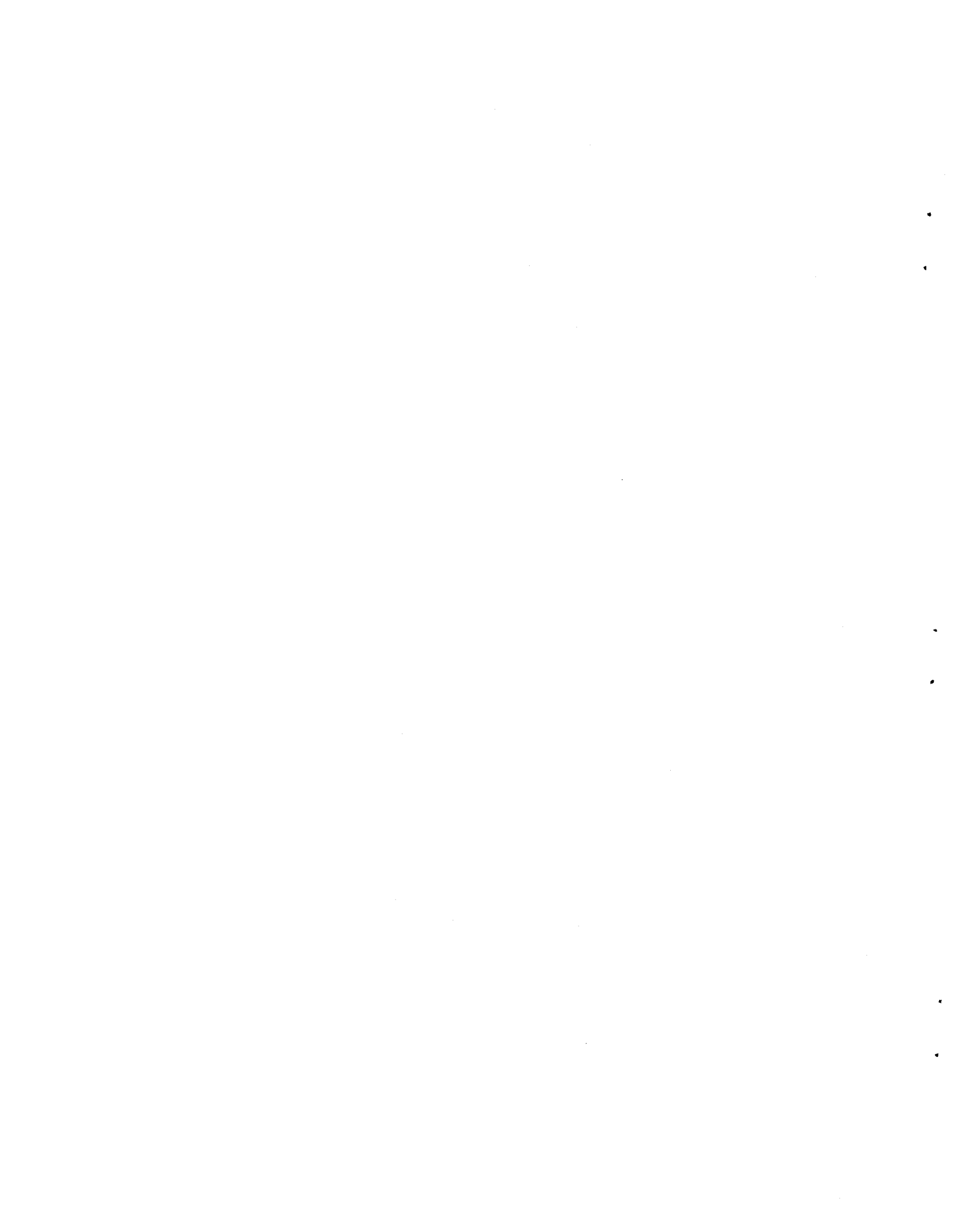
1. An abstract of a paper entitled "Tritium - Potential Impacts of Nuclear Fuel Cycle Releases," by H. R. Meyer, J. E. Till, and E. T. Etnier, was accepted for presentation at the 25th Annual Health Physics Society Meeting in Seattle, July 20-25, 1980.
2. An abstract of a paper entitled "Updating of Tritium Quality Factor, The Argument for Conservatism," by J. E. Till, E. L. Etnier, and H. R. Meyer, was accepted for presentation at the ANS Topical Meeting, Dayton, Ohio, Apr. 25-May 1, 1980. A longer version of this paper will appear in the Proceedings of the Meeting.
3. A paper entitled "Estimation of Dose to Man from Environmental Tritium," by P. S. Rohwer and E. T. Etnier, was also accepted for presentation and publication at the ANS Topical Meeting.
4. A paper entitled "A Review of Methodologies for Calculating Doses from Environmental Releases of Tritium," by J. E. Till, E. L. Etnier, and H. R. Meyer, has been written for submission to the journal *Nuclear Safety*.
5. A paper entitled "Significance of Incorporating Age-Dependent Data into Population Dose Estimates," by E. T. Etnier and J. E. Till, was published in the December 1979 issue of the journal *Health Physics*.
6. A paper entitled "Reevaluation of the Dose Equivalent per Unit Intake of ^{232}Th ," by H. R. Meyer and D. E. Dunning, was published in the October issue of the journal *Health Physics*.
7. A paper entitled "Environmental Impact of Radioactive Releases from Recycle of Thorium-Based Fuel Using Current Containment Technology" was presented by V. J. Tennery on Mar. 17, 1980, at the Second US DOE Environmental Control Symposium, Reston, Va. It will be published in the proceedings of this symposium.

An analysis is being made of the adaptability of the AIRDOS-EPA atmospheric transport code to calculating doses that would result from LOA-4 transient releases.

A progress report was received covering the period from May 1 to Sept. 30, 1979, for the subcontract work at Colorado State University to

model release of radioactivity from a thorium ore pile. The report, entitled "Gaseous and Particulate Source Terms for a Thorium Ore Pile," was prepared by W. J. Smith, F. W. Wicker, and J. H. Smith, Department of Radiology and Radiation Biology.

A review of LOA-4 (4.2 Attenuation in the Environment) work at ORNL was presented at ORNL on Jan. 16, 1980, to the Fast Breeder Reactor Safety Technology Management Center Staff.



ORNL BREEDER REACTOR SAFETY — LOA 4
QUARTERLY TECHNICAL PROGRESS REPORT
FOR JANUARY—MARCH 1980

ABSTRACT

An evaluation of the variability of three biological factors involved in determining the dose per unit intake of ingested ^{131}I has been performed for several age categories using Monte Carlo techniques.

4. TASK 04 — ORNL LOA 4 TASKS: MODEL EVALUATION OF
BREEDER REACTOR RADIOACTIVITY RELEASES

R. O. Chester C. W. Miller

4.1 Comprehensive Testing of Selected Models

4.1.1 Particle-in-cell model

One of the models selected for further examination in the project is the PIC numerical method for estimating atmospheric dispersion of aerosols. This is a three-dimensional dispersion technique in which Lagrangian "particles" or "parcels" are used to represent an ensemble of real particles or a quantity of some substance. Because PIC models are generally very complex and require large amounts of input data, computer space, and computer time, they are not likely to come into wide use for routine assessment purposes in the near future. However, PIC models may prove useful for special conditions such as low wind speed conditions, complex terrain, and plumes involving complex chemical interactions like sodium aerosols in air. We will attempt in this project to delineate more specifically the applications for which the PIC technique is appropriate.

A computer code, NEXUS, is being developed to implement the PIC model at ORNL. This development is necessary because no nonproprietary PIC code exists that can be readily implemented on the ORNL computing system. This code will be used in an attempt to simulate the results of the sodium aerosol release tests conducted at INEL by NOAA and AI.

4.1.2 Hanford-67 data comparisons

Work is continuing on a comparative analysis of Hanford-67 atmospheric dispersion data for releases of fluorescein particles from a height of 56 m and values of the normalized, ground-level, centerline air concentration calculated by the computer code DWNWND. Comparisons are being made for predictions based on two different sets of Gaussian plume dispersion parameters, the PG set and BNL set. Comparisons are also being made for two different methods of estimating atmospheric stability, one based on the vertical temperature gradient $\Delta T/\Delta Z$ and one based on the standard deviation of the wind direction near the point of release σ_θ . Ratios of predicted air concentration to observed air concentration have been calculated for each of these comparisons. Median values of this ratio as a function of downwind distance are shown in Table 4.1. In general, all methods tend to underpredict near the source and to overpredict farther from the source. The PG values, however, tend to approach the desired value of 1 sooner and to overpredict thereafter less than the BNL

Table 4.1. Median values of the ratio predicted air concentration to observed air concentration for two methods of estimating atmospheric stability and two sets of dispersion parameters

Downwind distance (m)	Pasquill-Gifford parameters		Brookhaven parameters	
	$\frac{\Delta T}{\Delta Z}$	σ_θ	$\frac{\Delta T}{\Delta Z}$	σ_θ
400	4.0E-07 ^a	1.2E-04	1.2E-33	3.4E-23
800	1.2E-02	9.0E-02	1.9E-12	3.4E-09
1,200	1.2E-01	3.6E-01	8.2E-07	4.5E-05
1,600	3.6E-01	6.9E-01	1.7E-04	2.2E-03
2,200	1.2	1.5	1.4E-02	3.9E-02
3,200	1.5	1.5	1.8E-01	2.7E-01
5,000	4.5	3.3	2.4	1.9
7,000	3.9	2.5	3.9	2.3
12,800	7.3	4.2	10.7	6.5
Overall	0.139	0.365	4.6E-07	3.7E-05

^a4.0E-07 = 4×10^{-7} .

values for the same method of determining stability. Also, the σ_θ method of determining stability seems to perform better overall than does the $\Delta T/\Delta Z$ method.

4.1.3 Report ORNL-5573

Comments were received by telephone from George Sherwood, DOE, concerning his review of ORNL-5573, *The Evaluation of Models Used for the Assessment of Radionuclide Releases to the Environment, a Summary of Documentation for the Period of April 1976 through July 1979*. These comments have been incorporated into the manuscript, and it has been sent to Laboratory Records for final review and printing.

4.2 Recommendations of Models and Parameters Best Suited to Breeder Reactor Assessments

Report ORNL-5529, *Recommendations Concerning Models and Parameters Best Suited to Breeder Reactor Environmental Radiological Assessments*, was reviewed within the Health and Safety Research Division, and copies were sent to George Sherwood, DOE, and Jack Van der Hoven, NOAA, for their review. Their comments were received by telephone and are currently being incorporated into the manuscript before the report is printed.

4.3 Evaluation of Uncertainties Associated with Computational Models

4.3.1 Atmospheric dispersion parameters

Two critical parameters in the Gaussian plume atmospheric dispersion model are the crosswind and vertical standard deviations of the concentrations in the plume, σ_y and σ_z , respectively. The computer program TEDPED has been used to perform a statistical analysis of a limited number of values of σ_y and σ_z , based on short-term (≤ 30 min) air concentration measurements taken at Karlsruhe, Federal Republic of Germany. The probability distributions associated with these parameters were assumed to be lognormal. A summary of results of the statistical analysis for the σ_z values considered in this study is shown in Table 4.2. A range of values,

Table 4.2. Summary of a statistical analysis of selected σ_z values for HTO released from a height of 100 m at Karlsruhe, Federal Republic of Germany

Stability category	Downwind distance (m)	Number of values	Logarithms		Range of measured values (m)	Ratio $\left(\frac{\text{High value}}{\text{Low value}}\right)$
			Mean	Standard deviation		
A	300	4	4.21	0.25	46-99	2.2
	500	4	4.91	0.23	107-200	1.9
	1000	4	5.87	0.36	188-520	2.8
B	500	6	4.07	0.11	52-69	1.3
	1000	6	5.04	0.46	79-276	3.5
	2000	3	6.72	0.18	617-969	1.6
C	700	11	5.07	1.01	44-1533	35
	1000	11	5.23	1.11	52-2077	40
	2000	24	5.54	1.02	59-3749	64
D	700	7	4.98	0.57	66-268	4.1
	1000	7	4.79	0.10	105-141	1.3
	1500	12	5.10	0.69	59-499	8.5

rather than a single value, is associated with each stability category and downwind distance. The ratio of high to low values for each combination is most often near 2 or less. For all three distances in stability category C, however, this ratio is over 10 in value. Also, any separation of the σ_z values on the basis of stability category is not large for the downwind distances considered here. The ranges of the values at one downwind distance common to all stability categories, 1000 m, overlap between categories. The mean values of the logarithms at this 1000-m distance also do not uniformly decrease in the progression from A stability to D stability. These findings indicate that it is possible to have some of the same values of σ_z in all four stability categories represented. Similar results were found for the σ_y analysis.

4.3.2 Dose due to ^{131}I

Uncertainty is present in estimates of dose because of a number of factors, including variability in human physiological and metabolic characteristics. The importance of the variability in human-related characteristics has been reemphasized by a recent study in which the variability

in those parameters contributed most to the overall imprecision in dose to infants. To substantiate this result, an evaluation of variability of the three principal biological factors (thyroid mass, thyroid uptake, and biological half-life) on determining the dose per unit intake of ingested ^{131}I has been performed for several age categories. Resulting imprecision in predicted thyroid dose was estimated using Monte Carlo techniques.

The best estimates of the distributions for the principal parameters involved were made for adults. There is sufficient evidence that all these parameters resemble a lognormal distribution with truncations at a certain minimum/maximum level. The resulting imprecision in dose per unit intake for ingestion is given in Fig. 4.1, which represents the frequency distribution of dose for an adult. The 95th and 99th percentiles of the distribution, respectively, are ~ 2.2 and ~ 3.2 times the mean value (\bar{x}). Similar values were observed for other age groups and are consistent with previous attempts to quantify the imprecision in dose.

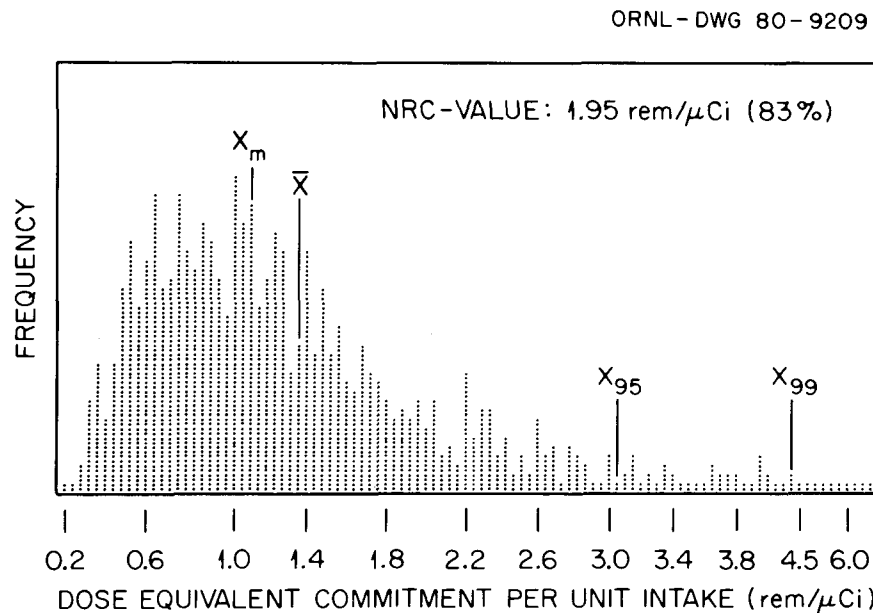


Fig. 4.1. Thyroid dose commitment per unit intake of ingested ^{131}I for adults.

4.4 Meetings

On Jan. 16, 1980, P. S. Rohwer, R. O. Chester, J. T. Holdeman, and C. W. Miller participated in the Fast Reactor Safety Technology Management Center Environmental Attenuation Topical Meeting at ORNL.

C. W. Miller attended the Second Joint Conference on Applications of Air Pollution Meteorology, Mar. 24-27, 1980, in New Orleans, La. He presented a paper coauthored with C. A. Little and S. J. Cotter entitled "Comparison of Observed and Predicted Normalized Air Concentrations for 56-M Releases of Fluorescein Particles."

ORNL/TM-7348
Part 5
Dist. Category UC-79,
-79e, -79p

ORNL BREEDER REACTOR SAFETY — LOA SUPPORT
QUARTERLY TECHNICAL PROGRESS REPORT
FOR JANUARY—MARCH 1980

M. H. Fontana W. B. Cottrell
 J. R. Buchanan

AG 10 20 41 5

Task 05 — ORNL LOA Support and Integration: NSIC

OBJECTIVE

To disseminate safety information on the breeder and other reactor programs to the nuclear community through reports and the bimonthly publication, *Nuclear Safety*, and to individuals through SDI, searches, and consultation. (NOTE: DOE pays for only 15% of the work described.)

[REDACTED]

Any further distribution of this report is the responsibility of the data
producer. This report is prepared for the U.S. Government and is
not to be distributed outside the Government. The U.S. Government
owns all rights in this report. The U.S. Government is authorized to
reproduce and distribute reprints for Government purposes not with-
standing any copyright notation that may appear hereon. This report
was prepared for the U.S. Department of Energy.

[REDACTED]

No part of this document is to be distributed outside the Government
without the prior written approval of the U.S. Department of Energy.
This report contains information that is tentative and preliminary. It is
subject to change without notice. Therefore, it is not to be used as a
basis for any action.

Prepared by the
OAK RIDGE NATIONAL LABORATORY
Oak Ridge, Tennessee 37830
operated by
UNION CARBIDE CORPORATION
for the
DEPARTMENT OF ENERGY



ORNL BREEDER REACTOR SAFETY — LOA SUPPORT
QUARTERLY TECHNICAL PROGRESS REPORT
FOR JANUARY—MARCH 1980

5. TASK 05 — ORNL LOA SUPPORT AND INTEGRATION:
NUCLEAR SAFETY INFORMATION CENTER

W. B. Cottrell J. R. Buchanan

In 1963, the NSIC was established by the USAEC as a focal point for collecting, analyzing, and disseminating information for the benefit of the nuclear community. It aids those concerned with analysis, design, and operation of nuclear facilities by providing and/or identifying relevant information on their nuclear safety problems. This may be done directly (as through special searches, SDI, and consultation) or indirectly (as through the publication of reports, bibliographies, and the technical progress review, *Nuclear Safety*). In addition, the center's staff participates in various special studies and evaluations. The NSIC is jointly sponsored by NRC and DOE.

The capabilities of NSIC's technical staff are augmented by a computer file that contains 100-word abstracts and complete bibliographic data on over 150,000 nuclear safety documents and is increasing at the rate of 12,000 documents per year. Pertinent abstracts are readily retrievable from the computer to meet a number of requirements. These files are frequently queried for retrospective bibliographies to aid the staff in answering technical inquiries. The files are also used extensively during preparation of NSIC reports and review articles for the bimonthly journal, *Nuclear Safety*. A routine form of reference output from the storage files is a biweekly SDI program that selects references according to individual user requirements. NSIC's computerized capability has been extended by including the NSIC file on the DOE-RECON system, where it may be accessed by the RECON network.

Principal activities of the Center from Jan. 1 to Mar. 31, 1980, are summarized. Since mid-1975 the Center has operated under the DOE Information Center Pricing Policy, which was implemented on July 1, 1975, for certain NSIC services and was subsequently extended to apply to SDI (with biweekly mailings). This experience is reported, as well as the more

customary Center activities, including the preparation of reports and the journal.

5.1 Routine Services

During the months of January, February, and March 1980, the staff of NSIC (1) entered 2821 documents, (2) responded to 198 inquiries (of which 142 involved technical staff), (3) made 54 computer searches (of which 8 were for paying customers), (4) provided SDI to 396 subscribers (including 47 paying subscribers), (5) received 26 visitors, (6) attended 13 meetings, and (7) issued 2 reports. The DOE report on use of the data bases on the RECON system for the period Feb. 4, 1980, to Feb. 29, 1980, is presented in Table 5.1. The NSIC is the fifth most widely used of the data bases on RECON.

In accordance with the DOE Information Center Pricing Policy, which has been applicable to NSIC, those organizations or persons other than

Table 5.1. RECON data base activity from Feb. 4 to Feb. 29, 1980 (17 operating days)

Data base identification	Data base	Supporting installation	Number of sessions	Number of expands	Citations printed
EDB	DOE Energy Database	TIC	3115	4544	128,981
NSA	Nuclear Science Abstracts	TIC	528	985	7,947
WRA	Water Resources Abstracts	WRSIC	291	1012	18,576
EMI	Environmental Mutagens Information	EMIC	193	288	9,156
NSC	Nuclear Safety Information Center	NSIC	148	298	12,223
RIP	Energy Research in Progress	DOE	148	226	1,037
GAP	General and Practical Information	DOE	124	170	972
FED	Federal Energy Data Index	DOE/EIA	99	159	1,367
ESI	Environmental Science Index	EIC	93	149	618
ETI	Environmental Teratology	ETIC	89	99	2,129
EIA	Energy Information Abstracts	EIC	81	110	497
WRE	Water Resource Research	WRSIC	44	107	1,502
EIS	Epidemiology Information System	TIRC	37	38	42
ERG	Enhanced Oil and Gas Recovery	BERC	28	35	313
API	American Petroleum Data Base	API	27	47	1,528
RSI	Radiation Shielding Information	RSIC	24	16	1,056
PRD	Power Reactor Dockets	TIC/NRC	23	16	827
CIM	Central Inventory of Models	DOE	22	36	9
NBI	National Biomonitoring Inventory	NBIC	19	13	
NRC	National Referral Center	LC	19	43	
NES	National Energy Software	NESC	18	11	95
NER	National Energy Referral	EIC	15	16	
TUL	Tulsa Data Base	U. Tulsa	15	42	240
NSR	Nuclear Structure Reference	NDP	11	16	53
RSC	Radiation Shielding Codes	RSIC	9	10	69
ARF	Agent Registry File	EMIC/ETIC	7	3	

sponsors and their direct subcontractors must pay for the services they receive. As noted previously, NSIC performed 8 paid searches during the quarter and at the end of the quarter had 47 paid SDI subscriptions. However, these funds are not received by us but in accordance with DOE policy are collected by the National Technical Information Service — serving as our billing agent — and then credited to the DOE General Fund.

5.2 ORNL-NSIC Reports

Work was concluded, continued, or initiated on several reports as follows:

ORNL/NUREG/NSIC-160, *Annotated Bibliography on Safeguards Against Proliferation of Nuclear Materials* (in preparation).

ORNL/NUREG/NSIC-161, *Nuclear Power and Radiation in Perspective* (in preparation).

ORNL/NUREG/NSIC-166, *Breeder Reactor Safety — Review of Current Issues and Bibliography of 1978 Literature* (January 1980).

ORNL/NUREG/NSIC-167, *Role of Probability in Risk and Safety Analysis* (in preparation).

ORNL/NUREG/NSIC-168, *Annotated Bibliography on the Transportation and Handling of Radioactive Materials* (in preparation).

ORNL/NUREG/NSIC-169, *Bibliography of Reports on Research Sponsored by the NRC Office of Nuclear Regulatory Research* (issued).

ORNL/NUREG/NSIC-172, *Annotated Bibliography on Fires and Fire Protection in Nuclear Facilities* (in preparation).

ORNL/NUREG/NSIC-175, *Index to Nuclear Safety, Vol. 11 through Vol. 20* (in preparation).

ORNL/NUREG/NSIC-176, *Description of Selected Incidents Which Have Occurred in Nuclear Facilities* (in preparation).

ORNL/NUREG/NSIC-178, *Summary and Bibliography of Safety-Related Events at Boiling Water Nuclear Power Plants as Reported in 1979* (in preparation).

ORNL/NUREG/NSIC-179, *Summary and Bibliography of Safety-Related Events at Pressurized Water Nuclear Power Plants as Reported in 1979* (in preparation).

5.3 Journal of Nuclear Safety

Preparation and review of material for the technical progress review, *Nuclear Safety*, continued apace with the requirements of its bi-monthly publication schedule. All technical articles for *Nuclear Safety* 21(4) were completed and mailed to NRC, DOE, and TIC on March 21. The "current events" material (covering events which occurred in January and February) for *Nuclear Safety* 21(3) was completed by March 17 (except for data on operating power reactors that were not yet available from NRC). Most technical articles for *Nuclear Safety* 21(5) have been received and are in various stages of preparation. Final copies of *Nuclear Safety* 21(2) were received from the printer on March 19. The regular bimonthly *Nuclear Safety* staff meetings were held February 6 and March 26. Minutes of those meetings and tentative outlines for the next several issues of *Nuclear Safety* were received and distributed shortly after both meetings.

ORNL/TM-7348
Part 6
Dist. Category UC-79,
-79e, -79p

ORNL BREEDER REACTOR SAFETY — LOA SUPPORT
QUARTERLY TECHNICAL PROGRESS REPORT
FOR JANUARY—MARCH 1980

M. H. Fontana G. F. Flanagan

AG 10 20 41 5

Task 06 — ORNL LOA Support and Integration: Breeder
Reactor Reliability Data Analysis Center

OBJECTIVE

To define, develop, and maintain a central reliability data
analysis center for use in dissemination of reliability
data in support of safety programs.

Any further dissemination of the data
contained herein is to be made only
by the Breeder Reactor Reliability
Data Analysis Center, Department of Energy.

This document is a technical report of the Breeder Reactor
Program and contains information of a preliminary
nature and therefore does not constitute a
final report.

Prepared by the
OAK RIDGE NATIONAL LABORATORY
Oak Ridge, Tennessee 37830
operated by
UNION CARBIDE CORPORATION
for the
DEPARTMENT OF ENERGY

ORNL BREEDER REACTOR SAFETY — LOA SUPPORT
 QUARTERLY TECHNICAL PROGRESS REPORT
 FOR JANUARY—MARCH 1980

ABSTRACT

Continued progress on development of a centralized data base and supporting organization for collection, analysis, and dissemination of breeder component reliability data is reported. Historic engineering and event data are the primary emphasis of data collection at EBR-II. Engineering data collection efforts at FFTF have been initiated through HEDL's FFTF Plant Utilization Program, and data tapes have been received by CREDO.

6. TASK 06 — ORNL LOA SUPPORT AND INTEGRATION: BREEDER
 REACTOR RELIABILITY DATA ANALYSIS CENTER

G. F. Flanagan P. M. Haas
 G. W. Cunningham S. D. Hudson
 N. M. Greene H. E. Knee
 J. J. Manning

6.1 Initial Data Collection and Evaluation

Engineering data collection, review, and transcription to CREDO format were completed for seven systems at EBR-II:

1. primary sodium storage and purification system,
2. secondary sodium storage and purification system,
3. secondary sodium vent system,
4. secondary sodium monitoring system,
5. primary cold trap NaK cooling system,
6. secondary Dowtherm cooling system,
7. secondary sodium components evaluation system.

Detailed EBR II cycling histories for the first five years of the facility's operation were gathered, and historic event data collection was initiated for the following systems: (1) primary reactor heat transport, (2) sodium pressure relief, and (3) secondary sodium storage and processing.

A study of EBR-II's unscheduled outages was initiated. Data on unscheduled outages is being collected and categorized according to cause, total downtime, and other factors in order to identify generic and specific reasons for the apparent increase in EBR-II's availability with increased operating experience.

Data collection at FFTF was initiated on the primary heat transfer system. Approximately 25% of all components have been "pedigreed" in this system. A subcontract to HEDL's FFTF Plant Utilization Program was initiated to provide assistance to CREDO in collecting FFTF data. Computer tapes for the trace heater engineering index and for the instrument calibration and maintenance system data were requested through the Plant Utilization Program. The latter tape has been received and is being transferred to IBM format. The trace heater tape has not yet been received; however, programming has been initiated for converting data from both tapes into CREDO format.

6.2 Development of the Data Base Management System

The DBMS event, engineering, and operating files were restructured into ADSEP form. Restructuring these files provided a more efficient means of storing the data as well as accommodating changes in the CREDO input forms. Modification of the failure rate program to accept these newly structured files was initiated.

6.3 Interface and Coordination

The proposed collection of engineering data at FFTF through its Plant Utilization Program was accepted. J. Ziff will be coordinating all CREDO requests for data and background material, making contact with appropriate HEDL and FFTF Project Office personnel as necessary.

Two data requests were received by CREDO. Failure data for intermediate heat exchangers and data on ball-type check valves were compiled, and informal reports were made to the requesting parties.

Preliminary plans were made for the Second Annual Steering Committee Meeting to be held at ORNL. A tentative date of June 4, 1980, was set.

6.4 Reports and Major Correspondence Issued

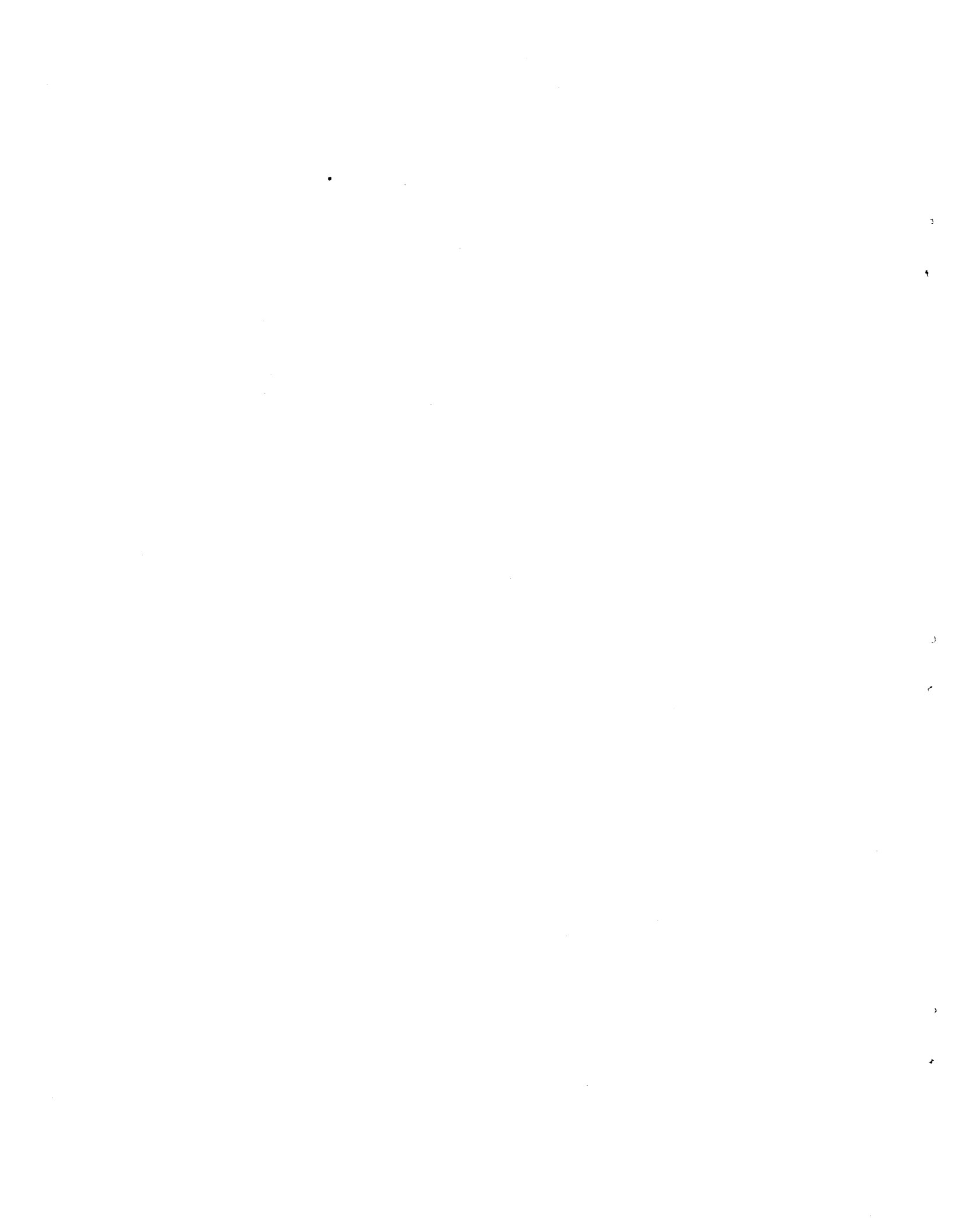
A paper by CREDO staff members entitled "The Development of the Centralized Reliability Data Organization" was accepted for presentation at the Joint Conference: Sixth Advances in Reliability Technology Symposium and at the Third European Reliability Data Bank Seminar to be held at the University of Bradford, Bradford, United Kingdom, on April 8 through 11.

6.5 Important Meetings

Two CREDO staff members met with Eric Green of the National Centre of Systems Reliability (United Kingdom) during his visit to this country in January. Interaction with foreign data banks was discussed, and several suggestions were made by Mr. Green for possible contacts, which will be made during a proposed trip to the United Kingdom in April.

A member of the CREDO staff met with Charles Larson (GE) to discuss the CREDO effort. A presentation of CREDO history, development, and current status was made in preparation for his assignment as U.S. LMFBR Program Representative to Japan.

The FRSTMC review of CREDO was held in Chicago on March 10. Progress to date, milestones, funding, and future plans were the major topics discussed.





ORNL BREEDER REACTOR SAFETY — LOA SUPPORT
QUARTERLY TECHNICAL PROGRESS REPORT
FOR JANUARY—MARCH 1980

ABSTRACT

Work continued on entering NSMH update information into SACRD. The SACRD mailing list has been reviewed and updated. Software has been completed which makes possible remote display plots.

7. TASK 07 — ORNL SUPPORT AND INTEGRATION: CENTRAL
DATA BASE FOR BREEDER REACTOR SAFETY CODES

G. F. Flanagan F. M. Forsberg
J. W. Arwood N. M. Greene
 G. B. Raiford

Work continues on entering NSMH update information into SACRD. The NSMH update package No. 19 was received late in the quarter just as package No. 18 had been finished. Programs were written to take the new saturated sodium properties data, received last quarter from ANL, from magnetic tape in preparation for entry into the data base. Minor problems have delayed this work until contacts can be made with appropriate ANL personnel. A special interactive program was written for use with the new inhalation uptake fraction file entered into SACRD last quarter.

The SACRD mailing list has been extensively reviewed, and an updated listing has been prepared.

Software has been completed to make possible remote display of plots on a Tektronix terminal.

A variation of the normal SACRD data editing program, which requires a separate request for every single property to be edited, was prepared to allow global requests to be made by data file. Output from this program is sorted according to material, property, and version.

Several examples of uncertainty data were prepared for entry into SACRD; these examples illustrate the variety of formats encountered in the data sources of SACRD data.

Files are being prepared to augment the present dosimetry data files. These new files will identify the sources of these data and will also be used to mark any corrections and/or modifications to the files, and they will be accessible with the interactive software used with the dosimetry data.

Internal Distribution

- | | | | |
|--------|----------------------|--------|---------------------------------|
| 1. | A. H. Anderson | 45. | R. E. MacPherson |
| 2. | S. I. Auerbach | 46. | F. C. Maienschein |
| 3. | M. Bender | 47. | J. J. Manning |
| 4. | E. S. Bomar | 48. | P. J. Maudlin |
| 5. | R. S. Booth | 49. | H. R. Meyer |
| 6. | J. R. Buchanan | 50. | R. W. McCulloch |
| 7. | R. G. Chenoweth, Jr. | 51. | C. W. Miller |
| 8. | R. O. Chester | 52. | B. H. Montgomery |
| 9. | N. E. Clapp | 53. | R. H. Morris |
| 10. | J. T. Cockburn | 54. | F. R. Mynatt |
| 11. | C. W. Collins | 55. | F. H. Neill |
| 12. | W. B. Cottrell | 56. | W. R. Nelson |
| 13. | G. W. Cunningham | 57. | L. C. Oakes |
| 14. | J. F. Dearing | 58. | E. M. Oblow |
| 15. | R. G. Donnelly | 59. | C. V. Parks |
| 16. | H. K. Falkenberry | 60. | P. Patriarca |
| 17. | G. F. Flanagan | 61-62. | J. L. Rich |
| 18-22. | M. H. Fontana | 63. | P. S. Rohwer |
| 23. | P. W. Garrison | 64. | S. D. Rose |
| 24. | U. Gat | 65. | M. W. Rosenthal |
| 25. | P. A. Gnat | 66. | R. L. Rudman |
| 26. | N. M. Greene | 67. | J. P. Sanders |
| 27. | A. G. Grindell | 68. | D. L. Shaeffer |
| 28. | P. M. Haas | 69. | M. J. Skinner |
| 29. | K. Haga | 70. | I. Spiewak |
| 30. | T. J. Hannatty | 71. | R. D. Stulting |
| 31. | W. O. Harms | 72. | V. J. Tennery |
| 32. | F. O. Hoffman | 73. | D. G. Thomas |
| 33. | H. W. Hoffman | 74. | J. E. Till |
| 34. | S. D. Hudson | 75. | E. T. Tomlinson |
| 35. | A. F. Johnson | 76. | H. E. Trammell |
| 36. | J. E. Jones, Jr. | 77. | D. B. Trauger |
| 37. | P. R. Kasten | 78-82. | J. L. Wantland |
| 38. | S. V. Kaye | 83. | J. R. Weir |
| 39. | G. A. Klein | 84. | G. D. Whitman |
| 40. | H. E. Knee | 85. | Central Research Library |
| 41. | T. S. Kress | 86. | Y-12 Document Reference Section |
| 42. | A. E. Levin | 87-88. | Laboratory Records Department |
| 43. | L. F. Lischer | 89. | Laboratory Records (RC) |
| 44. | C. A. Little | | |

External Distribution

90. Assistant Administrator for Nuclear Energy, DOE, Washington, DC 20545
91. Director, Division of Reactor Research and Technology, DOE, Washington, DC 20545
92. Director, Division of Nuclear Power Development, DOE, Washington, DC 20545
93. Chief, Safety and Physics Branch, Division of Reactor Research and Technology, DOE, Washington, DC 20545
94. Chief, Safety Section, Division of Reactor Research and Technology, DOE, Washington, DC 20545
95. Office of Assistant Manager for Energy Research and Development, DOE, ORO, Oak Ridge, TN 37830
96. Deputy Assistant Manager for Energy Research and Development, DOE, ORO, Oak Ridge, TN 37830
97. Director, Nuclear Research and Development Division, DOE, ORO, Oak Ridge, TN 37830
98. Director, Fast Safety Technology Management Center, Argonne National Laboratory, 9700 S. Cass Ave., Argonne, IL 60439
- 99-277. For distribution as shown in DOE/TIC-4500 under categories UC-79, -79e, -79p